Thermal dynamics of one-dimensional quantum systems

by

Filippo Bovo

A thesis submitted to
The University of Birmingham
for the degree of
DOCTOR OF PHILOSOPHY

Theoretical Physics Group
School of Physics and Astronomy
The University of Birmingham

August 2015

UNIVERSITY OF BIRMINGHAM

University of Birmingham Research Archive

e-theses repository

Abstract

In this work we examine the dynamics of one-dimensional systems. We present a continuum approach to the construction of the non-equilibrium Keldysh functional integral and derive a relation between the classical and quantum fields of the Keldysh formalism and the occupation of a state. Using the Keldysh formalism, we give a self-contained presentation of bosonization and refermionisation of fermionic and bosonic interacting particles. We derive the first two non-linear corrections to linear bosonization due to the fermionic spectrum curvature using the functional integral formalism. Using the previous results, we study the thermal dynamics of one-dimensional systems. We consider both the phonons, coming from bosonization, and fermionic quasiparticles, coming from refermionisation, in a single theory. Having them in a single theory is justified by a scale separation between them. Studying the dynamical structure factor we find three regimes. From higher to lower energies we have a ballistic and a collisional regimes of fermionic quasiparticles and a hydrodynamical regime of non-linear phonons. The phase field of the non-linear bosons satisfies the Kardar-Parisi-Zhang equation, thereby linking the dynamics of one-dimensional quantum systems to the universality class of surface growth. The time-scale separating the phononic and fermionic quasiparticle regimes is very long for up-to-date experiments, meaning that the ballistic regime of fermionic quasiparticles is the only one likely to be observed. Since this approach has a limited range of validity for weakly interacting bosons, we derive their dynamical structure factor using a semiclassical approach.

Acknowledgements

This work would not have been possible without the constant support of my supervisor, Dr. Dimitri M. Gangardt. He has always been kind and helpful and I enjoyed all the many afternoons full of discussions that we had in these four years. I thank Prof. Igor V. Lerner, Dr. Martin W. Long, Prof. Mike Gunn and Dr. Rob A. Smith for their help in various situations. Rephrasing a quote from The Big Bang Theory: "What is the most important thing in science?...Money.", I acknowledge the financial support of the University of Birmingham. Of course, a PhD would not be a good one without the company of good friends. I enjoyed a lot fun times Arvid J. Kingl and Max Arzamasovs. With these two friends I shared most of my adventures in Birmingham. In the physics department I met a lot of super friendly people with whom I enjoyed many laughs. There is Max Jones and his subtle humour, Matt Robson and his witty puns, Matt Hunt and his attitude and angelic voice, Greg Oliver and his extravagance and dexterity, Andy Cave and his cocky funny attitude, Andy Latief and his contagious laugh, Austin Tomlinson and his happy presence and beatboxing skills, Jon Watkins and his vigorous office entrances and contagious smile, Richard Mason and his relaxing attitude, Amy Briffa and her playfulness, Kevin Ralley and the philosophical debates and Alexey Galda for the many table tennis and squash matches. I thank all my friends in Birmingham and Italy for all the good times I shared with them. In particular, I thank Francesca Ronconi with whom I shared a great part of my life and many of its happiest moments. A special thank goes to my parents and brother for their immense support during these four years. They were more than two thousands kilometres away but their presence could not have been closer.

This thesis is dedicated to my parents and my brother.

Publications

[1] M. Arzamasovs, F. Bovo, and D. M. Gangardt. Kinetics of mobile impurities and correlation functions in one-dimensional superfluids at finite temperature. *Physical Review Letters*, 112(17):170602, 2014.

[2] F. Bovo. Continuum Approach to Non-equilibrium Quantum Functional Integral. *arXiv:1502.07630*, 2015. (To be published.)

[3] F. Bovo, and D. M. Gangardt. Thermal dynamics of weakly interacting bosons. (To be published.)

[4] F. Bovo. Nonlinear Bosonization and (naive) Refermionisation within the Keldysh Technique. (To be published.)

Contents

List of Figures

Introduction

Quantum systems in one dimension are appealing for two main reasons: they exhibit high correlations and are more likely to be exactly solvable, lending themselves to a better conceptual understanding [1]. The first breakthrough to the understanding of one-dimensional systems came in 1950 due to Tomonaga [2]. Tomonaga showed that by linearising the spectrum of one-dimensional interacting fermions, the fermionic system could be mapped into a system of non-interacting quantised density waves or phonons. The interesting aspect of this approach is that the fermionic kinetic and interaction terms are both mapped into phononic quadratic terms. Unaware of Tomonaga's work, in 1963 Luttinger rediscovered the mapping between fermions and phonons and attempted to evaluate the distribution function of the interacting fermions [3], later clarified by Mattis and Lieb in 1965 [4]. The second breakthrough came in 1985, when Haldane connected the Tomonaga-Luttinger model to the low energy excitations of one-dimensional interacting bosonic and fermionic particles [5, 6], opening the road to the study of one-dimensional quantum systems at low temperatures. The phenomenology behind the success of the phononic description for one-dimensional systems relies on this fact: particles moving in one dimension cannot avoid each other as would be possible in higher dimensions. As a consequence, any amount of interaction between bosonic or fermionic particles leads to a "domino effect" where a particle pushes the next one in line in a sequence that leads to a density wave.

After these theoretical discoveries, the interest in one-dimensional quantum systems was fostered by the advances in experimental techniques [7]. The mainstream experimental

exploration of one-dimensional systems began in the 90s with the advent of nanowires [8]. Nanowires are hollow tubes whose diameter is comparable to the wavelength of an electron and, as a consequence, the motion of electrons is confined along the one-dimensional direction of the tube. Among the quantum wires, the most famous are carbon nanotubes, that, despite being known since the 50s, become popular in 1991 [9]. Meanwhile, the quantum Hall effect was discovered in 1980 and its connection to one-dimensional quantum mechanics was pioneered by Wen ten years later [10]. The quantum Hall effect is observed in two-dimensional conductors at low temperatures immersed in a magnetic field perpendicular to the surface. This leads to a quantisation of the Hall conductance and the appearance of chiral edge states, one-dimensional states that move in only one direction along the edge of the two-dimensional conductor. More recently cold atoms provided a new platform for the experimental study of quantum systems [11, 12]. The experimental control over cold atoms, such as their confinement or their interactions, opened new avenues for the study of one-dimensional systems of both bosonic and fermionic particles. In these experiments, a cloud of atoms is confined in two transverse directions, leaving the atoms free to move only in the longitudinal direction.

Experiments in cold atoms allow the study of the dynamics of one-dimensional quantum systems using techniques such as the Bragg spectroscopy [7, 11]. On the theoretical side, the dynamics of quantum systems is best studied using the Keldysh technique for non-equilibrium systems [13]. This is the subject of the first chapter. We start with the derivation of the Keldysh technique for the quantum field theory description of systems out of equilibrium. Despite various approaches having simplified the derivation of the Keldysh technique over the years, they all relied on the discretisation of the time axis for operations within the functional integral formalism [13]. In this work we present a novel derivation of the Keldysh formalism that employs a continuous approach, leading to a better insight on the role of the non-equilibrium fields. This continuous approach is the first original contribution of this work.[1]

---

[1] See Ref. [2] in the Publications section at the beginning of this thesis.

Within the non-equilibrium functional integral developed in chapter one, we proceed to the study of one-dimensional quantum systems. As we saw before, particles in one-dimension cannot avoid each other. This implies that a local perturbation propagates further than in higher dimensions, leading to correlations over a longer range. This characteristic manifests itself in the signature behaviour of one-dimensional quantum systems at zero temperatures: power-law correlation functions [1]. Despite one-dimensional systems not exhibiting long-range order due to the Mermin-Wagner theorem, the propagation of perturbations for very long distances generate a power-law behaviour known as quasi-long range order. In comparison, in higher dimensions, local perturbations propagate in more directions, weakening the more they travel and generating correlation functions with exponential decay [14]. The power-law behaviour of one-dimensional systems is a consequence of the low-energy physics being dominated by phonons described by a Gaussian model or equivalently by a massless bosonic theory. Phonons are fairly successful at describing low energy properties, becoming the favourite tool to study static or equilibrium properties of one-dimensional quantum systems [1]. However, they are not sufficient for a proper description of dynamical or non-equilibrium properties: phonons are often necessary but only combined with additional degrees of freedom describing higher-energy excitations [7]. Despite these additions, phonons still sit atop the throne of the static and zero-temperature dynamics of one-dimensional quantum systems.

As part of the original contributions to this work, in the second chapter we develop a self-contained pedagogical presentation of the theory of phonons and higher excitations within the functional integral framework.[2] We derive the Tomonaga-Luttinger liquid model of linear phonons starting from interacting fermionic and bosonic particles, a procedure know as bosonization [1, 15]. In addition, we derive the lowest non-linear correction to the linear model related to the spectrum curvature. Finally, using the relation between non-linear phonons and interacting fermions we derive a theory of effective fermionic quasiparticles, a procedure known as refermionisation [7]. In this way we build a map

---

[2]See Ref. [4] in the Publications section at the beginning of this thesis.

between the bosonic and fermionic particles and effective bosonic and fermionic excitations, that is, phonons and fermionic quasiparticles. Such a map is derived using the Keldysh formalism of non-equilibrium quantum field theory. The second original contribution to the second chapter is the calculation of non-linear corrections to the non-interacting phononic theory using the functional integral formalism. Using the operator formalism with the assumption that excitations are created over the ground state of the system, it was shown that a single non-linear correction appears [5]; however, it can be shown that there is an infinite series of such corrections [16]. In Appendix B, we derive the first two non-linear corrections in the small momentum asymptotic limit and use these results to check a more naive approach employed in the second chapter for the derivation of the first correction within the non-equilibrium functional integral. We conclude the chapter with a paradox that arises in the thermal dynamics of one-dimensional systems: while the descriptions of the dynamics using non-linear phonons or fermionic quasiparticles are equivalent at zero temperature, at finite temperatures they lead to different results, in contrast to the mapping equivalence derived in the chapter. The solution of this paradox is one of the topics of the third chapter.

Starting from the non-equilibrium framework developed in the second chapter, in the third chapter we shed light on the thermal dynamics of one-dimensional quantum systems. The dynamics of one-dimensional quantum gases has been studied for more than three decades. The studies developed mainly around the quantum dynamics, leaving the thermal effects an open investigation [7]. The dynamics at zero temperature is well captured by phonons, characterising low energies, coupled to a single mobile impurity, characterising higher energies. Power-laws characterise the dynamics of one-dimensional quantum systems, but in a different way from the static case. While in the static case power-laws are associated to long-distance correlation functions, in the dynamical case they are associated to power-law singularities at the energy and momentum of the prevailing excitations. As a consequence, the zero temperature dynamics of one-dimensional systems is permeated by dynamical exponents characterising the singularities. When the temperature

4

is increased, thermal fluctuations smooth out the singularities, leading to bell-shaped distributions centred around the prevailing excitations. Then, the quantity of interest moves from the dynamical exponent to the width and height of the bell-shaped distributions.

The study of the thermal dynamics of one-dimensional quantum systems in the third chapter represents the main original contribution to this work, part of which has been published.[3] As we explained above, phonons are sufficient to describe most of the static properties of one-dimensional systems as they are the lowest-energy excitations. When moving to the zero-temperature dynamics, the addition a single mobile impurity coupled to phonons is necessary to account for higher energies. Finite temperatures require an additional extension: instead of a single mobile impurity, we will need a thermodynamical number of them. Using this model of phonons coupled to mobile impurities, we study the dynamics using the dynamical structure factor, giving the probability per unit time to excite a density fluctuation by an external source field, a quantity experimentally accessible through Bragg spectroscopy [7]. Using the dynamical structure factor we solve the paradox of one-dimensional thermal dynamics that arises in the second chapter. This in turn leads to a characterisation of the thermal dynamics in terms of different regimes. One of these regimes falls into a well known universality class of classical dynamical systems, thereby bridging a new gap with the dynamics of one-dimensional quantum systems. However, the most important result is that phonons hardly participate in the thermal dynamics of one-dimensional quantum system, leaving the throne to another kind of excitation.

---

[3]See Ref. [1] in the Publications section at the beginning of this thesis.

Chapter 1

Non-equilibrium quantum field theory
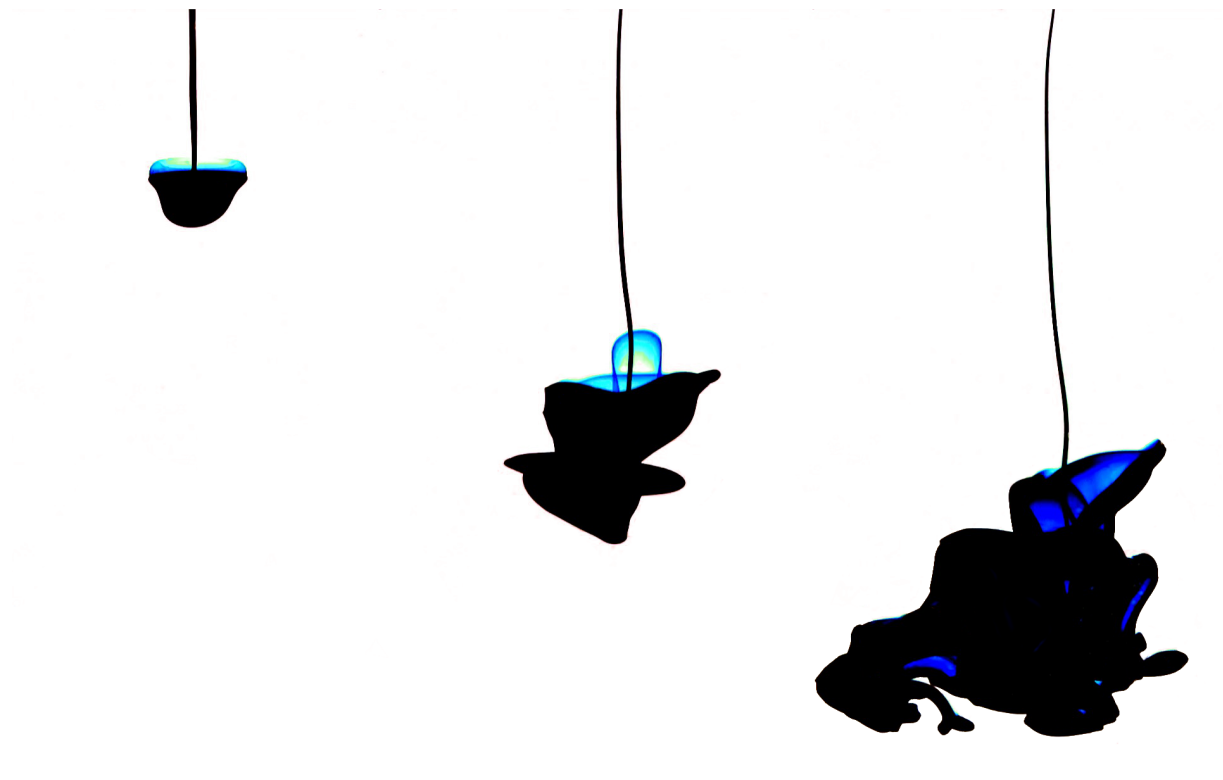
Ink drop falling in water.

An ink drop falls in a glass of water under the action of gravity. Initially, the ink molecules are just below the surface of water, with momenta pointing downwards. As the ink falls down, some of the ink molecules collide with the water molecules and change their momenta. The number of ink molecules with momenta pointing downwards decreases and number of molecules with different momenta increases. If the ink has the same density of water, it diffuses into the water until it is homogeneously spread in an equilibrium state and the number of molecules with momenta pointing downwards is the same as in every other direction. This example encompasses some of the main features of non-equilibrium quantum field theory: the time evolution of the average number of particles with certain momenta, diffusion and equilibration. As we will see in this chapter, the average number of particles is particularly important as it is directly related to the Green's function of non-equilibrium systems. Also, the Green's function contains information on the fluctuations that lead to diffusion and on the energy dissipation that leads to equilibration.

Non-equilibrium quantum field theory has its foundations on the closed time contour, the third in Fig. 1.1. The contour, introduced by Schwinger [17, 18], is used to evaluate expectation values and replaces the real time axis of the equilibrium theory. The contour was developed in statistical quantum mechanics by Kadanoff and Baym [19] and its formulation was made simpler and more transparent by Keldysh [20]. Keldysh's formulation is even more transparent in its functional integral analogue, developed by Kamenev [21]. This formulation, used also in Refs. [13, 14], accounts for the statistical distribution as an off-diagonal component of the inverse Green's function in the discrete time representation. The Green's function is calculated by matrix inversion and the continuum limit is eventually taken. Instead, in this work we adopt a continuum approach: we derive the functional integral by accounting for the statistical distribution through the boundary conditions

and evaluate the Green's function as a solution of a differential equation with boundary conditions derived from those of the functional integral.

The continuum approach developed in this chapter is part of the original contribution of this thesis (see Ref. [2] in the Publication section at the beginning of this thesis). We start by reviewing the close time contour and the difference between equilibrium and non-equilibrium quantum field theory. We use the contour to develop a quantum functional integral formulation, starting from single-level non-interacting bosons and fermions and extending the results to many levels and interactions.

1.1   From equilibrium to non-equilibrium

Beginning from the familiar equilibrium quantum field theory, in this section, we discuss its limitations and set the ground for developing non-equilibrium quantum field theory. We start from a general interacting and time-dependent system described by the many-body distribution operator $\hat{\rho}(t)$ at time t. The distribution $\hat{\rho}(t)$ evolves in time according to the von Neumann equation,

$$\partial_t \hat{\rho}(t) = -\mathrm{i}\left[\hat{H}(t), \hat{\rho}(t)\right],\tag{1.1}$$

where $\hat{H}(t)$ is the Hamiltonian of the system. Eq. (1.1) is solved by,

$$\hat{\rho}(t) = \hat{\mathcal{U}}(t, -\infty)\,\hat{\rho}\,\hat{\mathcal{U}}(-\infty, t),\tag{1.2}$$

where $\hat{\rho}$ is the initial condition in the distant past, $t \to -\infty$,

$$\hat{\mathcal{U}}(t_b, t_a) = \mathbb{T}e^{-\mathrm{i}\int_{t_a}^{t_b}\mathrm{d}t\hat{H}(t)}\tag{1.3}$$

is the time-evolution operator from time t_a to time t_b and $\mathbb{T}$ is the time-order operator.

The distribution $\hat{\rho}(t)$ is used to calculate the expectation values of observables. The
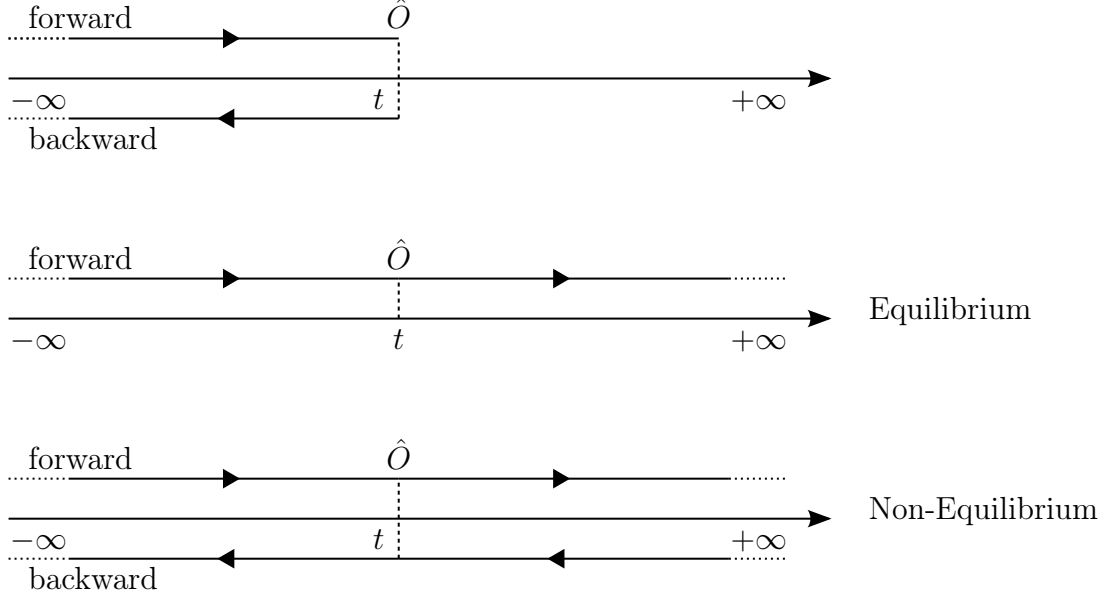
Figure 1.1: Time contours.

expectation value of an observable, $\hat{\mathcal{O}}$, at time t is,

$$\langle \hat{\mathcal{O}} \rangle(t) \equiv \frac{\mathrm{Tr}\left[\hat{\mathcal{O}}\hat{\rho}(t)\right]}{\mathrm{Tr}\left[\hat{\rho}(t)\right]} = \frac{\mathrm{Tr}\left[\hat{\mathcal{U}}(-\infty,t)\hat{\mathcal{O}}\hat{\mathcal{U}}(t,-\infty)\hat{\rho}\right]}{\mathrm{Tr}\left[\hat{\rho}\right]}, \qquad (1.4)$$

where Tr denotes the trace over the many-body Hilbert space. In the second equality we used the periodicity of the trace and, in the denominator, the Hermiticity of the time-evolution operator, $\left[\hat{\mathcal{U}}(t_b, t_a)\right]^\dagger = \hat{\mathcal{U}}(t_a, t_b)$. In Eq. (1.4), the denominator is just a normalisation. The meaningful part is the numerator and, with the help of Fig. 1.1-top, we interpret the expectation value (1.4) by reading the numerator from right to left: from the distant past the system evolves until time t, the observable $\hat{\mathcal{O}}$ is evaluated and the system evolves back to the distant past.

The expectation value (1.4) simplifies for an equilibrium system. Consider a system that is non-interacting in the distant past and, as the time passes, interactions are switched on. If the average is on the ground state of the system, the simplification is based on the Gell-Mann and Low theorem, which tells intuitively that, if interactions are switched on slowly enough, the system has time to adapt to the change and remains in its evolving ground state, that is, in *equilibrium* (see e.g., Ref. [22]). This is an example of *adiabatic*

10

process, that is, a process that does not change the occupation of evolving states. Here comes the trick: the Gell-Mann and Low theorem applied to a system that is in the ground state, $|0\rangle$, in the distant past and evolves adiabatically to the state $\hat{\mathcal{U}}(+\infty, -\infty)|0\rangle$ in the distant future tells that the two states are the same representation of the system, that is, they can only differ by a phase factor [23],

$$\hat{\mathcal{U}}(+\infty, -\infty)|0\rangle = e^{ia}|0\rangle \ , \ a \in \mathbb{R} \, . \tag{1.5}$$

This is the identity that allows the simplification in the equilibrium case. Indeed, the expectation value can be rewritten as

$$\begin{aligned}
\langle \hat{\mathcal{O}} \rangle(t) &= \langle 0|\hat{\mathcal{U}}(-\infty, t)\hat{\mathcal{O}}\hat{\mathcal{U}}(t, -\infty)|0\rangle \\
&= \langle 0|\hat{\mathcal{U}}(-\infty, +\infty)\hat{\mathcal{U}}(+\infty, t)\hat{\mathcal{O}}\hat{\mathcal{U}}(t, -\infty)|0\rangle \\
&= \frac{\langle 0|\hat{\mathcal{U}}(+\infty, t)\hat{\mathcal{O}}\hat{\mathcal{U}}(t, -\infty)|0\rangle}{\langle 0|\hat{\mathcal{U}}(+\infty, -\infty)|0\rangle} \, ,
\end{aligned} \tag{1.6}$$

where in the second line we used the composition rule of the evolution operator,

$$\hat{\mathcal{U}}(t_c, t_b)\hat{\mathcal{U}}(t_b, t_a) = \hat{\mathcal{U}}(t_c, t_a) \, , \tag{1.7}$$

and in the last line we used Eq. (1.5) together with $e^{ia} = \langle 0|\hat{\mathcal{U}}(+\infty, -\infty)|0\rangle$, obtained by applying $\langle 0|$ to the left of Eq. (1.5). With the help of Fig. 1.1-middle, we interpret the equilibrium expectation value (1.6) by reading the numerator from right to left: from the distant past the system evolves until time t, the observable $\hat{\mathcal{O}}$ is evaluated and the system evolves to the distant future. So, in equilibrium we drop the complication of evolving back in time, however, at the price of a non-trivial denominator, $\langle 0|\hat{\mathcal{U}}(+\infty, -\infty)|0\rangle$.

A similar result holds if we consider a system in thermal equilibrium at temperature T, where the distribution is $\hat{\rho}(t) = e^{-\hat{H}(t)/T}$. In thermal equilibrium, expectation values are commonly calculated using the Matsubara formalism (see e.g., Refs. [14]), which is based on the fact that the distribution can be rewritten as an evolution operator with

imaginary time, $-i/T$. Using this analogy, expectation values are calculated using a forward evolution in imaginary time, $\tau = it$ and, eventually, analytically continued to the real time, t.

We have just seen one example of adiabatic process, in which interactions are slowly switched on and off. Another common example is the presence of time dependent external potentials. When these potentials change in time slowly enough they are adiabatic. However, external potential that change quickly enough can push a system into a non-equilibrium state. The simplest of these potentials are periodic potentials that keep the system in an non-equilibrium state or impulses that instantaneously push the system into a non-equilibrium state. For example, the ink dropped in water can be thought as the instantaneous release of an external potential that confines the ink in a small region of water.

In a non-equilibrium situation, the presence of non-adiabatic potentials lifts the validity of the equilibrium simplifications made above: at zero temperature, for example, the system is not guaranteed to remain in the same evolving state, which means that, even if interactions are switched on and off slowly, identity (1.5) cannot be used anymore. In a similar way, the Matsubara formalism loses its validity as it only applies to systems in thermal equilibrium. So, we need to step back to the general form of expectation value (1.4), where the system evolves forward until time t and backward again. It is convenient to extend the evolution to the distant future and back again to the distant past by using the composition rule (1.7) in Eq. (1.4),

$$\langle \hat{\mathcal{O}} \rangle(t) \equiv \frac{\text{Tr}\left[\hat{\mathcal{U}}\left(-\infty, +\infty\right) \hat{\mathcal{U}}(+\infty, t) \hat{\mathcal{O}} \hat{\mathcal{U}}(t, -\infty) \hat{\rho} \right]}{\text{Tr}\left[\hat{\rho} \right]}. \tag{1.8}$$

As before, we read the numerator from right to left: from the distant past the system evolves until time t, the observable $\hat{\mathcal{O}}$ is evaluated, the system evolves to the distant future and back again to the distant past. This is represented in Fig. 1.1-bottom and is called *closed time contour*. The close time contour is at the base of non-equilibrium quantum

field theory. This contour is the combination of two time branches, forward and backward, instead of the single forward branch in the equilibrium case. In the next section, we will manipulate the closed time contour to describe non-equilibrium systems using a single forward branch.

1.2   Functional Integral

In this section, we derive the non-equilibrium functional integral on the closed time contour to evaluate expectation value (1.8). For notation clarity we restrict the time interval between an initial time t_i and a final time t_f. The starting point is the partition function along the closed time contour,

$$Z[u] = \frac{\text{Tr}\left[\hat{\mathcal{U}}_{u^-}\left(t_i, t_f\right) \hat{\mathcal{U}}_{u^+}\left(t_f, t_i\right) \hat{\rho}\right]}{\text{Tr}\left[\hat{\rho}\right]} \, , \tag{1.9}$$

where $\hat{\rho}$ is the initial distribution, $\hat{\mathcal{U}}_u(t_b, t_a) = \mathbb{T} e^{-\mathrm{i}\int_{t_a}^{t_b} \mathrm{d}t \hat{H}_u(t)}$ ($\hbar = 1$) is the time-evolution operators dependent on $u^{\pm}(t)$, two external sources coupled to the system. The operators $\hat{\mathcal{U}}_{u^+}\left(t_f, t_i\right)$ and $\hat{\mathcal{U}}_{u^-}\left(t_i, t_f\right)$ are referred to as forward and backward time-evolution operators [13]. The external sources $u^{\pm}(t)$ are like external potentials coupled to the system and are used to generate correlation functions of the quantity coupled to them. Unlike external potentials, in order to generate correlation functions they need to be different in forward and backward time-evolution operators. Indeed, if they are the same, $u^+(t) = u^-(t)$, then $\hat{\mathcal{U}}_{u^+}\left(t_i, t_f\right) \hat{\mathcal{U}}_{u^-}\left(t_f, t_i\right) = 1$ and,

$$Z[u]_{u^+=u^-} = 1 \, . \tag{1.10}$$

For this reason, the external sources are kept different during the calculation of correlation functions and set equal to an external potential, $u^+(t) = u^-(t) = u(t)$, at the end of the calculation.

We start by constructing the functional integral representation of Z for a non-interacting

13

single-level system of energy ε populated by bosons or fermions. The Hamiltonian is,

$$\hat{H}_{u^\pm}(t) = (\varepsilon + u^\pm(t))\hat{a}^\dagger\hat{a} = E^\pm(t)\hat{a}^\dagger\hat{a}\,, \tag{1.11}$$

where $\hat{a}$ and $\hat{a}^\dagger$ are bosonic or fermionic creation and annihilation operators, satisfying the canonical commutation relation $[\hat{a}, \hat{a}^\dagger]_+ = 1$ for bosons or anti-commutation relation $[\hat{a}, \hat{a}^\dagger]_- = 1$ for fermions and $u^\pm(t)$ are external sources coupled to the number operator, $\hat{a}^\dagger\hat{a}$. To derive the functional integral representation of the partition function, we consider the coherent states of bosons and fermions, ϕ and $\bar{\phi}$, respectively associated to $\hat{a}$ and $\hat{a}^\dagger$ through the relations $\hat{a}|\phi\rangle = \phi|\phi\rangle$ and $\langle\phi|\hat{a}^\dagger = \bar{\phi}\langle\phi|$, where ϕ and $\bar{\phi}$ are complex numbers for bosons or Grassmann number for fermions. Inserting the resolution of identity of coherent states between the three operators in the numerator of Eq. (1.9) and using the coherent state representation of the trace, the partition function becomes,

$$\begin{aligned}
Z[u] = \frac{1}{\text{Tr}\,[\hat{\rho}]} \int \mathrm{d}\big[\bar{\phi}_i^-, \phi_i^-\big]\mathrm{d}\big[\bar{\phi}_i^+, \phi_i^+\big]\mathrm{d}\big[\bar{\phi}_f, \phi_f\big]\, e^{-\bar{\phi}_i^+\phi_i^+}\langle\phi_i^+|\hat{\rho}|\zeta\phi_i^-\rangle\times \\
e^{-\bar{\phi}_i^-\phi_i^-}\langle\phi_i^-|\hat{\mathcal{U}}_{u^-}(t_i, t_f)|\phi_f\rangle\, e^{-\bar{\phi}_f\phi_f}\langle\phi_f|\hat{\mathcal{U}}_{u^+}(t_f, t_i)|\phi_i^+\rangle\,,
\end{aligned} \tag{1.12}$$

where $\mathrm{d}\big[\bar{\phi}, \phi\big] = \mathrm{d}(\text{Re}\phi)\,\mathrm{d}(\text{Im}\phi)/\pi$, $\zeta = +1$ for bosons and $\mathrm{d}\big[\bar{\phi}, \phi\big] = \mathrm{d}\bar{\phi}\,\mathrm{d}\phi$, $\zeta = -1$ for fermions. We used the superscript $+$ and $-$ for initial states acting respectively on forward and backward time-evolution operators. As opposed to the initial states, $|\phi_i^+\rangle$ and $|\phi_i^-\rangle$, the final state, $|\phi_f\rangle$, acts on both forward and backward time-evolution operators.

The partition function assumes a simpler form for initial states defined by the distribution,

$$\hat{\rho} = \rho^{\hat{b}^\dagger\hat{b}}\,, \quad \rho = \frac{\bar{n}}{1 + \zeta\bar{n}}, \tag{1.13}$$

where $\bar{n}$ is the average occupation of the level,

$$\bar{n} = \langle\hat{a}^\dagger\hat{a}\rangle_\rho = \frac{\text{Tr}\,[\hat{a}^\dagger\hat{a}\hat{\rho}]}{\text{Tr}\,[\hat{\rho}]}\,, \tag{1.14}$$

Here, $\bar{n} \geq 0$ for bosons and $0 \leq \bar{n} \leq 1$ for fermions. An example of a state described by

distribution (1.13) is the thermal state of a non-interacting system, where $\bar{n} = (e^{\frac{\varepsilon-\mu}{T}} - \zeta)^{-1}$, $\rho = e^{-\frac{\varepsilon-\mu}{T}}$ is the Boltzmann factor, T is the temperature and μ is the chemical potential. Using distribution (1.13) and the identity $\langle\phi|\rho^{\hat{b}^\dagger\hat{b}}|\phi'\rangle = e^{\rho\bar{\phi}\phi'}$ [13], the integrand in the first line of Eq. (1.12) becomes $e^{-|\phi_i^+|^2}\langle\phi_i^+|\hat{\rho}|\zeta\phi_i^-\rangle = e^{-\bar{\phi}_i^+(\phi_i^+ - \zeta\rho\phi_i^-)}$ and integration over $\bar{\phi}_i^+$ enforces the constraint $\phi_i^+ = \zeta\rho\phi_i^-$. Integration over ϕ_i^+ in partition function (1.12) leads to,

$$
\begin{aligned}
Z[u] =& (1 - \zeta\rho)^\zeta \int \mathrm{d}\big[\bar{\phi}_i, \phi_i\big]\mathrm{d}\big[\bar{\phi}_f, \phi_f\big] \\
&\times e^{-\bar{\phi}_i\phi_i}\langle\phi_i|\hat{\mathcal{U}}_{u^-}(t_i, t_f)|\phi_f\rangle e^{-\bar{\phi}_f\phi_f}\langle\phi_f|\hat{\mathcal{U}}_{u^+}(t_f, t_i)|\zeta\rho\phi_i\rangle,
\end{aligned}
\tag{1.15}
$$

where we remove the label $-$ from the initial state. The pre-factor of the integral is the normalisation of the partition function, $\mathrm{Tr}\,[\hat{\rho}] = (1 - \zeta\rho)^{-\zeta}$. We express the expectation value of the time-evolution operator in the functional integral form,

$$
e^{-\bar{\phi}_b\phi_b}\langle\phi_b|\hat{\mathcal{U}}_u(t_b, t_a)|\phi_a\rangle = \int_{\phi(t_a)=\phi_a}^{\substack{\phi(t_b)=\phi_b \\ \bar{\phi}(t_b)=\bar{\phi}_b}} \mathcal{D}\big[\bar{\phi}, \phi\big]e^{i\int_{t_a}^{t_b}\mathrm{d}t\,\bar{\phi}(t)(i\partial_t - E(t))\phi(t)},
$$

Here, the functional integral measure and the action in the exponent are defined by splitting the time interval $t_b - t_a$ in N smaller intervals $\delta t = (t_b - t_a)/N$ and taking the symbolical limit,

$$
\begin{aligned}
\mathcal{D}\big[\bar{\phi}, \phi\big] &= \lim_{N\to\infty}\prod_{n=1}^{N-1}\mathrm{d}\big[\bar{\phi}_n, \phi_n\big], \\
\int_{t_a}^{t_b}\mathrm{d}t\,\bar{\phi}(t)\,(i\partial_t - \varepsilon)\,\phi(t) &= \lim_{N\to\infty}\sum_{n=1}^{N}\delta t\left[i\bar{\phi}_n\frac{\phi_n - \phi_{n-1}}{\delta t} - E_n\bar{\phi}_n\phi_{n-1}\right],
\end{aligned}
\tag{1.16}
$$

where $\phi_0 = \phi_a$, $\phi_N = \phi_b$ and $E_n = \varepsilon + u(t_i + n\delta t)$. Integrating over initial and final fields, we arrive at,

$$
\begin{aligned}
Z[u] =& (1 - \zeta\rho)^\zeta \int_{\phi^+(t_i)=\zeta\rho\phi^-(t_i)}^{\phi^-(t_f)=\phi^+(t_f)} \mathcal{D}\big[\bar{\phi}^+, \phi^+\big]\mathcal{D}\big[\bar{\phi}^-, \phi^-\big] \\
&\times e^{i\int_{t_i}^{t_f}\mathrm{d}t\,\big[\bar{\phi}^+(t)\big(i\partial_t - E^+(t)\big)\phi^+(t) - \bar{\phi}^-(t)\big(i\partial_t - E^-(t)\big)\phi^-(t)\big]},
\end{aligned}
\tag{1.17}
$$

where $+$ and $-$ fields are associated to forward and backward time-evolutions and the minus sign in front of the second term in the exponent comes from the inversion of the integration limits. The integration measure has been redefined to contain the additional integration over the initial and final variables, ϕ_0^-, $\bar{\phi}_0^-$ and ϕ_N^+, $\bar{\phi}_N^+$, which are $\phi^-(t_i)$, $\bar{\phi}^-(t_i)$ and $\phi^+(t_f)$, $\bar{\phi}^+(t_f)$ in continuum notation. This partition function is the sum over all the possible configurations of $+$ and $-$ fields, related only through the boundary conditions at initial and final times, with a weight that depends on the difference of their actions. The stationary configurations satisfy $\phi^+(t) = \phi^-(t)$ and $\bar{\phi}^+(t) = \bar{\phi}^-(t)$. These configurations are the most important as, among individual ones, they carry most of the weight of the partition function[1]. As a consequence, the quantity $\phi^+(t) - \phi^-(t)$ measures how far away configurations are from the most important ones.

1.3 Bosons

The goal of the remaining derivation is the evaluation of the Green's function. The procedure is different for bosons and fermions and we start from bosons. In analogy to equilibrium quantum field theory [14], we associate stationary configurations, $\phi^+(t) = \phi^-(t)$ and $\bar{\phi}^+(t) = \bar{\phi}^-(t)$, to classical ones. Motivated by this identification and following Ref. [13], we define a classical field, $\phi^{\mathrm{cl}}(t)$, and a quantum field, $\phi^{\mathrm{q}}(t)$, as,

$$
\begin{cases}
\phi^{\mathrm{cl}}(t) & = \frac{1}{\sqrt{2}} \left(\phi^+(t) + \phi^-(t) \right) \\
\phi^{\mathrm{q}}(t) & = \frac{1}{\sqrt{2}} \left(\phi^+(t) - \phi^-(t) \right) ,
\end{cases}
\tag{1.18}
$$

and the same for the complex conjugates. This transformation is known as Keldysh rotation [20, 13]. In terms of these new fields, classical configurations are characterised by $\phi^{\mathrm{q}}(t) = 0$ and, as we will see soon, $\phi^{\mathrm{cl}}(t)$ satisfies the classical equations of motion. Moreover, the quantum field $\phi^{\mathrm{q}}(t)$ measures how far away configurations are from classical

---

[1]We note that configurations satisfying $\phi^+ = -\phi^-$ and $\bar{\phi}^+ = -\bar{\phi}^-$ are stationary, as well. However, contrary to the previous ones, they may not be stationary for an interacting system [13].

ones. In terms of classical and quantum fields, the partition function becomes,

$$Z[u] = \frac{1}{1+\bar{n}} \int_{\phi^{\mathrm{q}}(t_i)=-\frac{\phi^{\mathrm{cl}}(t_i)}{1+2\bar{n}}}^{\phi^{\mathrm{q}}(t_f)=0} \mathcal{D}[\bar{\phi}^{\mathrm{cl}},\phi^{\mathrm{cl}}]\mathcal{D}[\bar{\phi}^{\mathrm{q}},\phi^{\mathrm{q}}] e^{i \int_{t_i}^{t_f} \mathrm{d}t\, \bar{\phi}^{\alpha}(t)\left\{[G_{\bar{n}}^{-1}]^{\alpha\beta}(t)-u^{\mathrm{q}}(t)\delta^{\alpha\beta}\right\}\phi^{\beta}(t)}, \quad (1.19)$$

where $\alpha,\beta = \mathrm{cl},\mathrm{q}$, $u^{\mathrm{cl},\mathrm{q}}(t) = (u^{+}(t) \pm u^{-}(t))/2$ and we use the conventional sum over repeated indices. The inverse Green's function is,

$$\left[G_{\bar{n}}^{-1}\right]^{\alpha\beta}(t) = \begin{pmatrix} 0 & i\partial_t - E(t) \\ i\partial_t - E(t) & 0 \end{pmatrix}_{\bar{n}}. \quad (1.20)$$

where we redefined $E(t) = \varepsilon - u^{\mathrm{cl}}(t)$. The inverse Green's function depends on the initial average occupation, $\bar{n}$, because, by construction, it is an operator whose domain is the set of fields, $\phi^{\alpha}(t)$, that satisfy the boundary conditions in Eq. (1.19) and the initial boundary condition depends on $\bar{n}$. Integration over the quantum fields, $\phi^{\mathrm{q}}(t)$ and $\bar{\phi}^{\mathrm{q}}(t)$, enforces the classical equations of motion, $(i\partial_t - \varepsilon - u^{\mathrm{cl}}(t))\phi^{\mathrm{cl}}(t) = 0$ and $(-i\partial_t - \varepsilon - u^{\mathrm{cl}}(t))\bar{\phi}^{\mathrm{cl}}(t) = 0$. This fact originally motivated the name "classical field" [13].

It is worth to pause for a moment and discuss the initial boundary condition in partition function (1.19). This condition relates the values of the initial classical and quantum variables, $\phi^{\mathrm{cl}}(t_i)$ and $\phi^{\mathrm{q}}(t_i)$, and the initial occupation number, $\bar{n}$. Taking the modulus, the equation reads,

$$|\phi^{\mathrm{q}}(t_i)| = \frac{1}{1+2\bar{n}}|\phi^{\mathrm{cl}}(t_i)|. \quad (1.21)$$

Since for bosons $\bar{n} \geq 0$, for a fixed $\phi^{\mathrm{cl}}(t_i)$ the quantum variable is initially bounded, $0 \leq |\phi^{\mathrm{q}}(t_i)| \leq |\phi^{\mathrm{cl}}(t_i)|$ (A more restrictive condition applies to the final state, $\phi^{\mathrm{q}}(t_f) = 0$). When $\bar{n} \ll 1$, the level occupation is microscopic and $\phi^{\mathrm{q}}(t_i) \approx \phi^{\mathrm{cl}}(t_i)$. Instead, when $\bar{n} \gg 1$, the level occupation becomes macroscopic and $|\phi^{\mathrm{q}}(t_i)| \ll |\phi^{\mathrm{cl}}(t_f)|$. This, as expected [14], means that the larger the initial occupation of the level, the closer the initial state of the system is to a classical one. These results are summarised in Fig. 1.2.

We proceed and calculate the Green's function, $G^{\alpha\beta}(t,t') = -\mathrm{i}\langle\phi^{\alpha}(t)\bar{\phi}^{\beta}(t')\rangle$, which
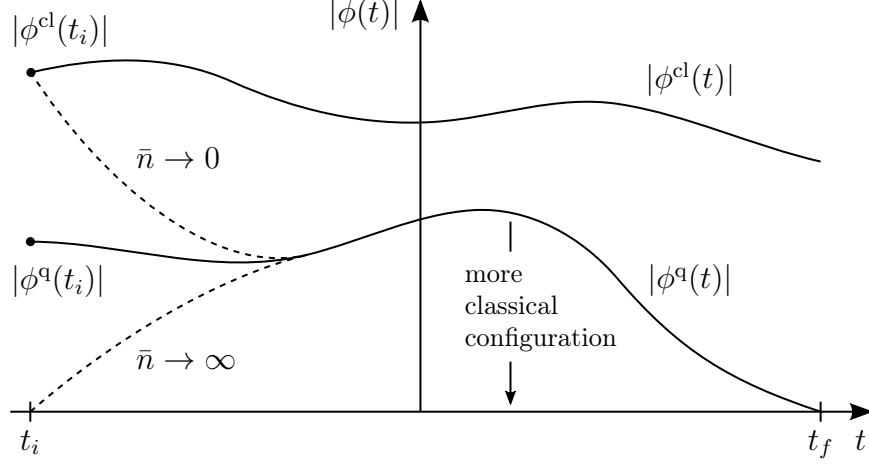
Figure 1.2: Example of a configuration of the modulus of quantum and classical fields, $|\phi^{\mathrm{cl}}(t)|$ and $|\phi^{\mathrm{q}}(t)|$. The smaller $|\phi^{\mathrm{q}}(t)|$ the closer is the configuration to a classical one. At the final time, $t = t_f$, $|\phi^{\mathrm{q}}(t_f)| = 0$. Instead, at $t = t_i$, the initial value of the quantum field, $|\phi^{\mathrm{q}}(t_i)|$, is related to the initial value of the classical field, $|\phi^{\mathrm{cl}}(t_i)|$, through Eq. (1.21). For a fixed value of $|\phi^{\mathrm{cl}}(t_i)|$, $|\phi^{\mathrm{q}}(t_i)| \to |\phi^{\mathrm{cl}}(t_i)|$ for $\bar{n} \to 0$ and $|\phi^{\mathrm{q}}(t_i)| \to 0$ for $\bar{n} \to \infty$.

satisfies the differential equation,

$$
\begin{pmatrix} 0 & i\partial_t - E(t) \\ i\partial_t - E(t) & 0 \end{pmatrix}_{\bar{n}} \begin{pmatrix} G^{\mathrm{clcl}}(t,t') & G^{\mathrm{clq}}(t,t') \\ G^{\mathrm{qcl}}(t,t') & G^{\mathrm{qq}}(t,t') \end{pmatrix} = \begin{pmatrix} \delta(t-t') & 0 \\ 0 & \delta(t-t') \end{pmatrix} ,
$$

where we used the matrix representation (1.20) of the inverse Green's function. The general solution of this equation is,

$$
G^{\alpha\beta}(t,t') = -\mathrm{i}e^{\mathrm{i}\int_t^{t'} \mathrm{d}t\, E(t)} \begin{pmatrix} a & (b+1)\,\theta\,(t-t') + b\theta\,(t'-t) \\ (c+1)\,\theta\,(t-t') + c\theta\,(t'-t) & d \end{pmatrix}.
$$
(1.22)

The constants a, b, c and d are fixed by the boundary conditions in (1.19). For this, we multiply each boundary condition of the partition function (1.19) by $\phi^\alpha(t')$, take the average and use the definition of Green's function, $G^{\alpha\beta}(t,t') = -\mathrm{i}\langle \phi^\alpha(t)\bar{\phi}^\beta(t')\rangle$, to obtain the boundary conditions of the Green's function,

$$
G^{\mathrm{q}\alpha}(t_f, t') = 0 ,
$$
$$
G^{\mathrm{cl}\alpha}(t_i, t') = -(1+2\bar{n})G^{\mathrm{q}\alpha}(t_i, t') ,
$$
(1.23)

18

for $\alpha = \mathrm{cl}, \mathrm{q}$. The first boundary condition fixes the constants of $G^{\mathrm{q}\alpha}(t, t')$ to $c = -1$ for $\alpha = \mathrm{cl}$ and $d = 0$ for $\alpha = \mathrm{q}$, where we used the fact that the first and second theta functions in $G^{\mathrm{qcl}}(t_f, t')$ are respectively equal to 1 and 0 for $t_i < t' < t_f$.[2] Using $G^{\mathrm{q}\alpha}(t_i, t')$ in the second boundary condition, the constants of $G^{\mathrm{cl}\alpha}(t, t')$ are fixed to $a = 1 + 2\bar{n}$ for $\alpha = \mathrm{cl}$ and $b = 0$ for $\alpha = \mathrm{q}$. Substituting these values in Eq. (1.22), the Green's function becomes,

$$G^{\alpha\beta}(t, t') = \begin{pmatrix} G^{\mathrm{K}}(t, t') & G^{\mathrm{R}}(t, t') \\ G^{\mathrm{A}}(t, t') & 0 \end{pmatrix}, \tag{1.24}$$

where,

$$G^{\mathrm{R}}(t, t') = -\mathrm{i}\theta(t - t') \, e^{\mathrm{i}\int_t^{t'} \mathrm{d}t \, E(t)},$$

$$G^{\mathrm{A}}(t, t') = \mathrm{i}\theta(t' - t) \, e^{\mathrm{i}\int_t^{t'} \mathrm{d}t \, E(t)}, \tag{1.25}$$

$$G^{\mathrm{K}}(t, t') = -\mathrm{i}(1 + 2\bar{n}) \, e^{\mathrm{i}\int_t^{t'} \mathrm{d}t \, E(t)}.$$

The first two Green's functions in Eq. (1.25) are respectively retarded and advanced Green's functions and, as in the equilibrium case, they only carry information on the spectrum. Retarded and advanced Green's functions are still undefined at equal times because the theta function, $\theta(t)$, needs to be regularised at $t = 0$. Since at equal times there is no dependence on the external source $u^{\mathrm{cl}}(t)$, we can set it equal to zero. First, using the Fourier transform, $G^{R,A}(\omega) = (\omega - \varepsilon + \mathrm{i}0^{\pm})^{-1}$, we have,

$$G^{\mathrm{R}}(t, t) - G^{\mathrm{A}}(t, t) = \int \frac{\mathrm{d}\omega}{2\pi} \left[G^{\mathrm{R}}(\omega) - G^{\mathrm{A}}(\omega) \right] = -\mathrm{i}.$$

Second, $\langle \phi^{\mathrm{cl}}(t)\bar{\phi}^{\mathrm{q}}(t') \rangle = -\langle \phi^{\mathrm{q}}(t')\bar{\phi}^{\mathrm{cl}}(t) \rangle^{\dagger}$ leads to $G^{\mathrm{R}}(t, t') = \left[G^{\mathrm{A}}(t, t') \right]^{\dagger}$, where $\dagger$ denotes complex conjugation and time transposition. It follows that the regularisation is $\theta(t = 0) = 1/2$. In particular, this leads to the useful identity,

$$G^{\mathrm{R}}(t, t) + G^{\mathrm{A}}(t, t) = 0.$$

---

[2]To fix the constants we did not consider $t' = t_i, t_f$ because this would lead to equal time Green's functions and the theta functions in $G^{\mathrm{qcl}}(t, t')$ and $G^{\mathrm{clq}}(t, t')$ have not been regularised at equal times, $t = t'$, yet.

Unlike retarded and advanced Green's functions, $G^{\mathrm{K}}(t,t')$, known as *Keldysh* Green's function, is characteristic of non-equilibrium quantum field theory. The Keldysh Green's function contains information about the distribution function through the average particle number $\bar{n}$ and is at the heart of non-equilibrium phenomena as it describes how the average particle number changes in time. The Keldysh Green's function is anti-hermitian, $G^{\mathrm{K}}(t,t') = -\left[G^{\mathrm{K}}(t,t')\right]^{\dagger}$, and is related to retarded and advanced ones through the relation,

$$G^{\mathrm{K}}(t,t') = F\left[G^{\mathrm{R}}(t,t') - G^{\mathrm{A}}(t,t')\right], F \equiv 1 + 2\bar{n}. \tag{1.26}$$

Eq. (1.26) is known as *Fluctuation-Dissipation theorem* as it relates the fluctuations of the classical field, $\langle \phi^{\mathrm{cl}}(t)\bar{\phi}^{\mathrm{cl}}(t')\rangle = \mathrm{i}G^{\mathrm{K}}(t,t')$, to its dissipation time through $G^{\mathrm{R}}(t,t') - G^{\mathrm{A}}(t,t')$. This will be clear in chapter 3 where fluctuations and dissipation will be derived explicitly. In thermal equilibrium, $\bar{n} = (e^{\frac{\varepsilon-\mu}{T}} - 1)^{-1}$ and,

$$F = \coth\left(\frac{\varepsilon - \mu}{2T}\right). \tag{1.27}$$

Now that the Green's function is known, we integrate over the bosonic fields in (1.19) to obtain the generating function of particle number correlation functions,

$$
\begin{aligned}
Z[u] &= \frac{1}{1+\bar{n}} \frac{1}{\det\left[-\mathrm{i}G_{\bar{n}}^{-1} + \mathrm{i}u^{\mathrm{q}}\right]} \\
&= \frac{1}{1+\bar{n}} \frac{1}{\det\left[-\mathrm{i}G_{\bar{n}}^{-1}\right]} \frac{1}{\det\left[1 - G \circ u^{\mathrm{q}}\right]} \\
&= e^{-\mathrm{Tr}\log[1 - G \circ u^{\mathrm{q}}]},
\end{aligned}
\tag{1.28}
$$

where $\circ$ denotes sum over indices and time convolution and we omitted time and indices. In the last line we used the identity,

$$\det\left[-\mathrm{i}G_{\bar{n}}^{-1}\right] = \frac{1}{1+\bar{n}},$$

derived by applying identity (1.10) for $u^{\mathrm{q}}(t) = u^{+}(t) - u^{-}(t) = 0$ to the first line. Deriving

(1.28) by $u^{\mathrm{q}}(t)$ we generate correlation functions of the particle number. First, using Eq. (1.19), we note that,

$$\left.\frac{\delta Z[u]}{\delta u^{\mathrm{q}}(t)}\right|_{u^{\mathrm{q}}=0} = \langle \bar{\phi}^{\mathrm{cl}}(t)\phi^{\mathrm{cl}}(t) + \bar{\phi}^{\mathrm{q}}(t)\phi^{\mathrm{q}}(t)\rangle = \langle \bar{\phi}^{+}(t)\phi^{+}(t) + \bar{\phi}^{-}(t)\phi^{-}(t)\rangle .$$

The last line in the operator formalism corresponds to,

$$\langle \bar{\phi}^{+}(t)\phi^{+}(t) + \bar{\phi}^{-}(t)\phi^{-}(t)\rangle = \langle \hat{a}^{\dagger}(t)\hat{a}(t) + \hat{a}(t)\hat{a}^{\dagger}(t)\rangle = \langle 1 + 2\hat{a}^{\dagger}(t)\hat{a}(t)\rangle .$$

In the second equality, the order of creation and annihilation operators at equal times is different in forward and backward branches (see Eq. (1.16)). Defining,

$$\hat{F}(t) = 1 + 2\hat{a}^{\dagger}(t)\hat{a}(t) , \tag{1.29}$$

and using the generating function (1.28), by successive derivations over $u^{\mathrm{q}}(t)$ we have [13],

$$\langle \hat{F}(t)^{n}\rangle = \left.\frac{\delta^{n} Z[u]}{\delta\left[u^{\mathrm{q}}(t)\right]^{n}}\right|_{u^{\mathrm{q}}=0} = \begin{cases} F & n = 1 \\ F^{2} - 1 & n = 2 \\ 2F(F^{2} - 1) & n = 3 \\ \dots \end{cases}$$

1.4 Fermions

The derivation is different for fermions, since they do not have a classical analogue. Instead of classical and quantum, we use the labels 1 and 2 through the transformation [24, 13],

$$\begin{cases} \phi_{1}(t) &= \frac{1}{\sqrt{2}}\left(\phi^{+}(t) + \phi^{-}(t)\right) \\ \phi_{2}(t) &= \frac{1}{\sqrt{2}}\left(\phi^{+}(t) - \phi^{-}(t)\right) , \end{cases} \qquad \begin{cases} \bar{\phi}_{1}(t) &= \frac{1}{\sqrt{2}}\left(\bar{\phi}^{+}(t) - \bar{\phi}^{-}(t)\right) \\ \bar{\phi}_{2}(t) &= \frac{1}{\sqrt{2}}\left(\bar{\phi}^{+}(t) + \bar{\phi}^{-}(t)\right) . \end{cases}$$

In these new variables, the partition function reads,

$$
Z[u] = (1 - \bar{n}) \int_{\phi_1(t_i) = -(1-2\bar{n})\phi_2(t_i)}^{\phi_2(t_f) = 0} \mathcal{D}\big[\bar{\phi}_1, \phi_1\big] \mathcal{D}\big[\bar{\phi}_2, \phi_2\big] e^{i \int_{t_i}^{t_f} dt \, \bar{\phi}_a(t) \left\{ [G_{\bar{n}}^{-1}]^{ab}(t) - u^q(t)\sigma_1^{ab} \right\} \phi_b(t)} ,
$$

(1.30)

where $a, b = 1, 2$, σ_1^{ab} is the first Pauli matrix and the inverse Green's function is,

$$
\big[G_{\bar{n}}^{-1} \big]^{ab}(t) = \begin{pmatrix} i\partial_t - E(t) & 0 \\ 0 & i\partial_t - E(t) \end{pmatrix}_{\bar{n}} .
$$

(1.31)

Again, we redefined $E(t) = \varepsilon - u^{\mathrm{cl}}(t)$. The Green's function, $G^{ab}(t, t') = -i\langle \phi_a(t)\bar{\phi}_b(t') \rangle$, satisfies the differential equation,

$$
\begin{pmatrix} i\partial_t - E(t) & 0 \\ 0 & i\partial_t - E(t) \end{pmatrix}_{\bar{n}} \begin{pmatrix} G^{11}(t, t') & G^{12}(t, t') \\ G^{21}(t, t') & G^{22}(t, t') \end{pmatrix} = \begin{pmatrix} \delta(t - t') & 0 \\ 0 & \delta(t - t') \end{pmatrix} ,
$$

for which the general solution is,

$$
G^{ab}(t, t') = -i e^{i \int_t^{t'} dt \, E(t)} \begin{pmatrix} (a+1)\, \theta\, (t - t') + a\theta\, (t' - t) & b \\ c & (d+1)\, \theta\, (t - t') + d\theta\, (t' - t) \end{pmatrix} ,
$$

(1.32)

We fix the constants a, b, c and d using the boundary conditions of the Green's function,

$$
G^{2a}(t_f, t') = 0 ,
$$

$$
G^{1a}(t_i, t') = -(1 - 2\bar{n})G^{2a}(t_i, t') .
$$

(1.33)

obtained from the partition function (1.30) in the same way we did for bosons. The boundary conditions at $t = t_f$ fix $c = 0$ and $d = -1$ and the ones at $t = t_i$ fix $a = 0$ and $b = 1 - 2\bar{n}$. Substituting these values in Eq. (1.32), the Green's function becomes,

$$
G^{ab}(t, t') = \begin{pmatrix} G^{\mathrm{R}}(t, t') & G^{\mathrm{K}}(t, t') \\ 0 & G^{\mathrm{A}}(t, t') \end{pmatrix} ,
$$

(1.34)

where,

$$G^{\mathrm{R}}(t, t') = -\mathrm{i}\theta\left(t - t'\right) e^{\mathrm{i} \int_t^{t'} \mathrm{d}t\, E(t)} ,$$

$$G^{\mathrm{A}}(t, t') = \mathrm{i}\theta\left(t' - t\right) e^{\mathrm{i} \int_t^{t'} \mathrm{d}t\, E(t)} , \tag{1.35}$$

$$G^{\mathrm{K}}(t, t') = -\mathrm{i}\left(1 - 2\bar{n}\right) e^{\mathrm{i} \int_t^{t'} \mathrm{d}t\, E(t)} .$$

As in the bosonic case, we have retarded, advanced and Keldysh Green's function. The regularisation of the theta functions is the same as for bosons. The only difference between Eqs. (1.25) and (1.35) is the minus sign in front of $\bar{n}$ in the Keldysh Green's function. The fluctuation-dissipation theorem (1.26) holds with,

$$F = 1 - 2\bar{n} .$$

In thermal equilibrium, $\bar{n} = (e^{\frac{\varepsilon - \mu}{T}} + 1)^{-1}$ and,

$$F = \tanh\left(\frac{\varepsilon - \mu}{2T}\right) .$$

By integrating over the fermionic fields in (1.30), we obtain the generating function of particle number correlation functions,

$$
\begin{aligned}
Z[u] &= (1 - \bar{n}) \det\left[-\mathrm{i}G_{\bar{n}}^{-1} + \mathrm{i}u^{\mathrm{q}}\sigma_1\right] \\
&= (1 - \bar{n}) \det\left[-\mathrm{i}G_{\bar{n}}^{-1}\right] \det\left[1 - G_{\bar{n}}\sigma_1 \circ u^{\mathrm{q}}\right] \\
&= e^{\mathrm{Tr}\log[1 - G_{\bar{n}}\sigma_1 \circ u^{\mathrm{q}}]} .
\end{aligned}
\tag{1.36}
$$

In the last line we used the identity,

$$\det\left[-\mathrm{i}G_{\bar{n}}^{-1}\right] = \frac{1}{1 - \bar{n}} ,$$

derived by applying identity (1.10) for $u^{\mathrm{q}}(t) = u^+(t) - u^-(t) = 0$ to the first line.

1.5 Many levels

In the previous pages we derived the Green's function for systems with a single level. In this section, we extend the results to systems with many levels. In a system with many levels, for every level i, we consider the annihilation and creation operators $\hat{a}_i$ and $\hat{a}_i^\dagger$, satisfying commutation or anti-commutation relations $[\hat{a}_i, \hat{a}_j^\dagger]_\pm = \delta_{ij}$. The single-level non-interacting Hamiltonian $\hat{H} = \varepsilon \hat{a}^\dagger \hat{a}$, is replaced by $\hat{H} = \hat{a}_i^\dagger \varepsilon_{ij} \hat{a}_j$ where, ε_{ij}, is a Hermitian matrix and the average particle number, $\bar{n}$, is replaced by the one-body density matrix $\bar{n}_{ij} = \langle \hat{a}_i^\dagger \hat{a}_j \rangle$, a Hermitian matrix, as well. For clarity, we employ the bold notation for vectors, $\hat{\boldsymbol{a}} = (\dots, \hat{a}_{i-1}, \hat{a}_i, \hat{a}_{i+1}, \dots)$, and matrices, $\boldsymbol{\varepsilon}$ and $\bar{\boldsymbol{n}}$. To proceed, we diagonalise the density matrix through a unitary transformation, so that the initial distribution $\hat{\rho}$ is the product of single-level distributions (1.13), derive the partition function and transform back to the original density matrix. Associating the coherent states vectors $\boldsymbol{\phi}$ and $\bar{\boldsymbol{\phi}}$ to the operators $\hat{\boldsymbol{a}}$ and $\hat{\boldsymbol{a}}^\dagger$, the partition function of bosons and fermions are respectively (1.19) and (1.30) with bold notation and boundary conditions given by,

$$\begin{cases} \boldsymbol{\phi}^{\mathrm{q}}(t_f) = 0 \\ \boldsymbol{\phi}^{\mathrm{q}}(t_i) = -(\boldsymbol{I} + 2\bar{\boldsymbol{n}}^{\mathrm{T}})^{-1}\boldsymbol{\phi}^{\mathrm{cl}}(t_i) \,, \end{cases} \tag{1.37}$$

and,

$$\begin{cases} \boldsymbol{\phi}_2(t_f) = 0 \\ \boldsymbol{\phi}_1(t_i) = -(\boldsymbol{I} - 2\bar{\boldsymbol{n}}^{\mathrm{T}})\boldsymbol{\phi}_2(t_i) \,, \end{cases} \tag{1.38}$$

where $\boldsymbol{I}$ is the identity matrix over the many level indices and T denotes transposition. The procedure to calculate the Green's function is the same as before with the difference that the columns on which we apply the boundary conditions are over the many-level indices, as well. The Green's function are identical in form to (1.24) for bosons and (1.34)

for fermions, but now each component is a matrix over the many-level indices given by,

$$\boldsymbol{G}^R(t,t') = -\mathrm{i}\theta\left(t-t'\right)e^{-\mathrm{i}\varepsilon(t-t')},$$

$$\boldsymbol{G}^A(t,t') = \mathrm{i}\theta\left(t'-t\right)e^{-\mathrm{i}\varepsilon(t-t')},$$

$$\boldsymbol{G}^K(t,t') = -\mathrm{i}e^{-\mathrm{i}\varepsilon(t-t_i)}\left(\boldsymbol{I}+2\zeta\bar{\boldsymbol{n}}^{\mathrm{T}}\right)e^{\mathrm{i}\varepsilon(t'-t_i)}.$$

The transposition of the many-body density matrix is due to the fact that the order of creation and annihilation operator in the definitions of Green's function and one-body density matrix are exchanged.

In the usual case of momentum indices, k, of a system with diagonal energy matrix, $\varepsilon_k\delta_{kk'}$, and diagonal one-body density matrix, $\bar{n}_k\delta_{kk'}$, boundary conditions (1.37) and (1.38) simplify to,

$$\begin{cases} \phi_k^{\mathrm{q}}(t_f) = 0 \\ \phi_k^{\mathrm{q}}(t_i) = -\frac{\phi_k^{\mathrm{cl}}(t_i)}{1+2\bar{n}_k}, \end{cases} \qquad (1.39)$$

and,

$$\begin{cases} \phi_{2,k}(t_f) = 0 \\ \phi_{1,k}(t_i) = -(1-2\bar{n}_k)\phi_{2,k}(t_i), \end{cases} \qquad (1.40)$$

for each k. Retarded, advanced and Keldysh Green's functions are diagonal in the momentum indices, with diagonal elements given by,

$$G_k^R(t,t') = -\mathrm{i}\theta\left(t-t'\right)e^{-\mathrm{i}\varepsilon_k(t-t')},$$

$$G_k^A(t,t') = \mathrm{i}\theta\left(t'-t\right)e^{-\mathrm{i}\varepsilon_k(t-t')},$$

$$G_k^K(t,t') = -\mathrm{i}\left(1+2\zeta\bar{n}_k\right)e^{-\mathrm{i}\varepsilon_k(t-t')}.$$

for each k.

1.6 Interactions

In the previous sections we saw the derivation of the non-equilibrium functional integral for non-interacting fermions and bosons. In this section, we introduce interactions, studying a single-level bosonic system. Hamiltonian (1.11) now becomes,

$$\hat{H}_{u^\pm}(t) = E^\pm(t)\hat{a}^\dagger\hat{a} + H_{\text{int}}(\hat{a}^\dagger, \hat{a}),$$

where $H_{\text{int}}(\hat{a}^\dagger, \hat{a})$ is the interaction part, containing terms of higher order than quadratic in $\hat{a}$ and $\hat{a}^\dagger$. In $H_{\text{int}}(\hat{a}^\dagger, \hat{a})$, $\hat{a}$ and $\hat{a}^\dagger$ are normal ordered. If, as in the previous case, we consider a system that is described by the average number $\bar{n} = \langle \hat{a}^\dagger \hat{a} \rangle$ at time t_i, then the partition function (1.17) is modified by interactions as,

$$
\begin{aligned}
Z[u] =& (1-\rho) \int_{\phi^+(t_i)=\rho\phi^-(t_i)}^{\phi^-(t_f)=\phi^+(t_f)} \mathcal{D}[\bar{\phi}^+, \phi^+]\mathcal{D}[\bar{\phi}^-, \phi^-] \\
& \times e^{i\int_{t_i}^{t_f} dt\left[\bar{\phi}^+(t)\left(i\partial_t - E^+(t)\right)\phi^+(t) - \bar{\phi}^-(t)\left(i\partial_t - E^-(t)\right)\phi^-(t)\right]} \\
& \times e^{-i\int_{t_i}^{t_f} dt\left[H_{\text{int}}(\bar{\phi}^+(t), \phi^+(t)) - H_{\text{int}}(\bar{\phi}^-(t), \phi^-(t))\right]},
\end{aligned}
\tag{1.41}
$$

that is, by the additional third line. Applying the Keldysh rotation (1.18), the partition function reads,

$$
\begin{aligned}
Z[u] =& \frac{1}{1+\bar{n}} \int_{\phi^q(t_i)=-\frac{\phi^{cl}(t_i)}{1+2\bar{n}}}^{\phi^q(t_f)=0} \mathcal{D}[\bar{\phi}^{cl}, \phi^{cl}]\mathcal{D}[\bar{\phi}^q, \phi^q] \\
& \times e^{i\int_{t_i}^{t_f} dt\, \bar{\phi}^\alpha(t)\left\{\left[G_{\bar{n}}^{-1}\right]^{\alpha\beta}(t) - u^q(t)\delta^{\alpha\beta}\right\}\phi^\beta(t) - i\int_{t_i}^{t_f} dt\, H'_{\text{int}}(\bar{\phi}^\alpha(t), \phi^\alpha(t))},
\end{aligned}
\tag{1.42}
$$

where,

$$H'_{\text{int}}(\bar{\phi}^\alpha(t), \phi^\alpha(t)) = H_{\text{int}}\left(\frac{\bar{\phi}^{cl}(t)+\bar{\phi}^q(t)}{\sqrt{2}}, \frac{\phi^{cl}(t)+\phi^q(t)}{\sqrt{2}}\right) - H_{\text{int}}\left(\frac{\bar{\phi}^{cl}(t)-\bar{\phi}^q(t)}{\sqrt{2}}, \frac{\phi^{cl}(t)-\phi^q(t)}{\sqrt{2}}\right).$$

Since the interaction is odd in the quantum fields, that is, $H'_{\text{int}} \to -H'_{\text{int}}$ for $\bar{\phi}^q(t) \to -\bar{\phi}^q(t)$ and $\phi^q(t) \to -\phi^q(t)$, it follows that H'_{int} contains only odd powers of the quantum field. In particular, there is no term with only classical fields. If we expand the exponential of

the interaction term in power series, then the Wick's theorem follows immediately from the Gaussian form of the non-interacting term. Therefore, the treatment of interactions in non-equilibrium is analogous to the equilibrium case, with a different interaction term and the two additional classical and quantum indices.

Using the Wick's theorem, in the same way of equilibrium quantum field theory, we have the Dyson equation for the Green's function [13],

$$(G_{\bar{n}}^{-1} - \Sigma) \circ G = 1 \,, \tag{1.43}$$

where time and matrix indices have been omitted and,

$$\Sigma = \begin{pmatrix} 0 & \Sigma^{\mathrm{A}} \\ \Sigma^{\mathrm{R}} & \Sigma^{\mathrm{K}} \end{pmatrix} \,,$$

is the self-energy. We set $u^q(t) = 0$ since we just need the Green's function, not higher correlations. Retarded, advanced and Keldysh components of the self-energy satisfy the same properties of the respective components of the Green's function. Using expression (1.20) for the inverse Green's function $G_{\bar{n}}^{-1}$, the Dyson equation (1.43) leads to the three equations,

$$\left(\mathrm{i}\partial_t - \varepsilon - u^{\mathrm{cl}}(t) - \Sigma^{\mathrm{R}}\right) \circ G^{\mathrm{R}}(t, t') = \delta(t - t') \,,$$
$$\left(\mathrm{i}\partial_t - \varepsilon - u^{\mathrm{cl}}(t) - \Sigma^{\mathrm{A}}\right) \circ G^{\mathrm{A}}(t, t') = \delta(t - t') \,, \tag{1.44}$$
$$\left(\mathrm{i}\partial_t - \varepsilon - u^{\mathrm{cl}}(t) - \Sigma^{\mathrm{R}}\right) \circ G^{\mathrm{K}}(t, t') = \Sigma^{\mathrm{K}} \circ G^{\mathrm{A}}(t, t') \,.$$

The first two equations are the usual equations for retarded and advanced Green's functions in equilibrium quantum field theory. Instead, the third equation is characteristic of non-equilibrium quantum field theory. To get a clearer form of the equation, we parametrise the Keldysh Green's function as,

$$G^{\mathrm{K}}(t, t') = G^{\mathrm{R}} \circ F(t, t') - F \circ G^{\mathrm{A}}(t, t') \,, \tag{1.45}$$

where $F(t,t')$ is a Hermitian function. Substituting this parametrisation into the third equation in (1.44), multiplying it from the right by $\left(\mathrm{i}\partial_t - \varepsilon - u^{\mathrm{cl}}(t) - \Sigma^{\mathrm{A}}\right)$ and using the first two equations in (1.44) we arrive to,

$$- \left[\left(\mathrm{i}\partial_t - \varepsilon - u^{\mathrm{cl}}(t)\right) \,\overset{\circ}{,}\, F\right](t,t') = \Sigma^{\mathrm{K}}(t,t') - \left(\Sigma^{\mathrm{R}} \circ F - F \circ \Sigma^{\mathrm{A}}\right)(t,t')\,. \tag{1.46}$$

Here $[\,\overset{\circ}{,}\,]$ denotes commutation and convolution. It can be shown that F correspond to the average of,

$$\hat{F}(t,t') = 1 + 2\hat{a}^{\dagger}(t')\hat{a}(t)\,.$$

This is the interacting analogue of Eq. (1.29) for different times, t and t'. Equation (1.46) is known as *kinetic equation* as for $t = t'$ it describes the time evolution of the average number of particles $\langle \hat{a}^{\dagger}(t)\hat{a}(t)\rangle$. The left hand side of Eq. (1.46) is the *kinetic term* and the right hand side is the *collision integral*. In equilibrium, the kinetic term is zero, leading to the equilibrium identity,

$$\Sigma^{\mathrm{K}}(t,t') = \Sigma^{\mathrm{R}} \circ F(t,t') - F \circ \Sigma^{\mathrm{A}}(t,t')\,, \tag{1.47}$$

having the same structure of the Green's function, Eq. (1.45). Moreover, when there is no interaction F reduces to Eq. (1.27).

The results just derived apply to an initial distribution characterised only by the average particle number. However, a more common situation is represented by the thermal distribution of an interacting system,

$$\hat{\rho} = e^{-\mathrm{i}\hat{H}/T}\,, \tag{1.48}$$

for which the average particle number is not enough to characterise it, due to the interaction terms contained in the Hamiltonian. This initial distribution is complicated in the present form. To simplify it, we follow Keldysh's trick [20]: we express the interacting distribution at time $t = t_i$ in terms of a non-interacting one in the distant past, $t \to -\infty$. For this, we

consider a system that evolves up to time $t = t_i$ with Hamiltonian,

$$\hat{H}(t) = \varepsilon \hat{a}^\dagger \hat{a} + e^{-\delta(t-t_i)} H_{\text{int}}(\hat{a}^\dagger, \hat{a}) , \qquad (1.49)$$

where $\delta \to 0^+$ and there are no external sources nor external potentials. This Hamiltonian describes the adiabatic switching on of interactions discussed in section 1.1. The adiabatic character comes from the slow increase in time of the interaction term through the prefactor $e^{-\delta(t-t_i)}$ with $\delta \to 0^+$. Using (1.48) and (1.49), in the distant past the distribution is non interacting,

$$\hat{\rho}(-\infty) = e^{-i\varepsilon \hat{a}^\dagger \hat{a}/T} = \rho^{\hat{a}^\dagger \hat{a}} , \quad \rho = e^{-i\frac{\varepsilon}{T}} ,$$

and at $t = t_i$ we have again the interacting distribution. It can be shown that the distribution in the distant past is related to the distribution at time t_i by [20],

$$\hat{\rho}(t_i) = e^{\frac{F}{T}} \hat{\mathcal{U}}(t_i, -\infty) \hat{\rho}(-\infty) \hat{\mathcal{U}}(-\infty, t_i) , \qquad (1.50)$$

where F is a constant representing the free energy in the distant past. Using this relation, we rewrite the partition function (1.9) as,

$$
\begin{aligned}
Z[u] &= \frac{\text{Tr}\left[\hat{\mathcal{U}}_{u^-}(t_i, t_f)\hat{\mathcal{U}}_{u^+}(t_f, t_i)\, e^{\frac{F}{T}}\hat{\mathcal{U}}(t_i, -\infty)\hat{\rho}(-\infty)\hat{\mathcal{U}}(-\infty, t_i)\right]}{\text{Tr}\left[e^{\frac{F}{T}}\hat{\mathcal{U}}(t_i, -\infty)\hat{\rho}(-\infty)\hat{\mathcal{U}}(-\infty, t_i)\right]} \\
&= \frac{\text{Tr}\left[\hat{\mathcal{U}}(-\infty, t_i)\hat{\mathcal{U}}_{u^-}(t_i, t_f)\hat{\mathcal{U}}_{u^+}(t_f, t_i)\hat{\mathcal{U}}(t_i, -\infty)\rho^{\hat{a}^\dagger \hat{a}}\right]}{\text{Tr}\left[\rho^{\hat{a}^\dagger \hat{a}}\right]} \\
&= \frac{\text{Tr}\left[\hat{\mathcal{U}}'_{u^-}(-\infty, t_f)\hat{\mathcal{U}}'_{u^+}(t_f, -\infty)\, \rho^{\hat{a}^\dagger \hat{a}}\right]}{\text{Tr}\left[\rho^{\hat{a}^\dagger \hat{a}}\right]} ,
\end{aligned}
$$

where in the second line we used the periodicity of the trace and in the third line we

defined the evolution operator $\hat{\mathcal{U}}'_u(t, -\infty)$ using Eq. (1.3) with Hamiltonian,

$$\hat{H}(t) = \begin{cases} \varepsilon \hat{a}^\dagger \hat{a} + e^{-\delta(t-t_i)} H_{\text{int}}(\hat{a}^\dagger, \hat{a}) & t \leq t_i \\ (\varepsilon + u^\pm(t)) \hat{a}^\dagger \hat{a} + H_{\text{int}}(\hat{a}^\dagger, \hat{a}) & t > t_i. \end{cases}$$

Since the time t_i can be chosen arbitrarily as long as it is finite, it is always possible to choose it far enough in the past from the time of any correlation functions that one wants to calculate. So, for every practical proposes we can neglect the switching on of interactions and we end up with the partition function (1.42) with $t_i \to -\infty$. It is also convenient to let $t_f \to \infty$. Analogous derivations hold for fermions and many-level systems. In conclusion, we can treat initial thermal distributions of an interacting systems by considering the respective non-interacting distributions in the distant past.

In this chapter we saw how to derive the non-equilibrium functional integral for bosons and fermions by accounting for the initial distribution through the boundary conditions of the functional integral and without resorting to a discrete representation to find the Green's function. Using this approach, not only is the derivation shorter and simpler than the discrete approach but highlights the properties of the classical configurations. Indeed, we showed how a state with a smaller quantum field is more classical and we connected the classical field, the quantum field and the occupation of a state in a single equation. The equation shows that for a higher occupation of a state, the amplitude of the quantum field is smaller, corresponding to a more classical state. Moreover, within this approach it is easy to extend the procedure to many-level systems with non-diagonal density matrices. The approach can be applied to the study of the quench dynamics using free effective theories, such as the Luttinger liquid model or linear optics models, by accounting for the state before the quench through the boundary conditions of the functional integral.

Chapter 2

One-dimensional systems

In one dimension, systems of bosonic and fermionic particles behave differently than in higher dimensions, as particles constrained to move on a line cannot avoid each other. As a consequence, fermions, even in absence of interactions, cannot go past each other because of the Pauli exclusion principle and, similarly, for bosons with local repulsive interactions [1, 6]. These systems are dominated by collisions and, for times longer than the time between two consecutive collisions, are in a *hydrodynamic* regime. Since longer times translate into lower energies, at *low enough energies* we expect these systems to be described by the hydrodynamic Hamiltonian of a liquid [25],

$$\hat{H} = \int \mathrm{d}x \left[\frac{1}{2} m \hat{n}(x) \hat{v}(x)^2 + e_0[\hat{n}] - \mu \hat{n}(x) \right] ,$$

where $\hat{n}(x)$ and $\hat{v}(x)$ are the density and velocity operators of the liquid, m is the mass contained in a unit volume of liquid, $e_0[\hat{n}]$ is the ground state energy per unit length and μ is the chemical potential. The first and second terms in the square brackets are respectively the kinetic and internal energies of the liquid.

The ground state of the liquid corresponds to $\hat{v} = 0$ and $\hat{n} = n$, where n is the constant homogeneous density determined by $e_0'[n] = \mu$ and the prime symbol, $'$, denotes derivative with respect to the argument. The low energy physics is associated with small variations of velocity, $\hat{v}$, and density, $\hat{\rho}$, over the ground state values, $\hat{v} = 0$ and $\hat{n} = n$. Expressing

the density as $\hat{n} = n + \hat{\rho}$, the Hamiltonian becomes,

$$\hat{H} = \int dx \left[\frac{1}{2} m(n + \hat{\rho})\hat{v}^2 + e_0(n + \hat{\rho}) - \mu(n + \hat{\rho}) \right],$$

and expanding over the small variations, $\hat{\rho}$ and $\hat{v}$, we have,

$$\hat{H} \approx L\left[e_0(n) - \mu n\right] + \int dx \left[\frac{1}{2}\left(mn\hat{v}^2 + \frac{1}{\kappa n^2}\hat{\rho}^2 \right) + \frac{m}{2}\hat{\rho}\hat{v}^2 + \frac{\alpha}{6}\hat{\rho}^3 \right], \qquad (2.1)$$

where $\kappa = 1/n^2 e_0''[n]$ is the compressibility of the liquid [26], $\alpha = e_0'''[n]$ and we neglected higher order terms. It is common to express the hydrodynamic Hamiltonian in terms of the phase fields $\theta(x,t)$ and $\phi(x,t)$, related to density and velocity as [5, 6, 1, 7],[1]

$$\hat{\rho}(x,t) = \frac{1}{\pi}\partial_x\hat{\theta}(x,t),$$
$$\hat{v}(x,t) = \frac{1}{m}\partial_x\hat{\phi}(x,t). \qquad (2.2)$$

Substituting Eqs. (2.2) in Hamiltonian (2.1) we obtain,

$$\hat{H} = L\left[e_0(n) - \mu n\right]$$
$$+ \int dx \left[\frac{c}{2\pi}\left(K(\partial_x\hat{\phi})^2 + \frac{1}{K}(\partial_x\hat{\theta})^2 \right) + \frac{1}{2\pi m}\partial_x\hat{\theta}(\partial_x\hat{\phi})^2 + \frac{\alpha}{6\pi^3}(\partial_x\hat{\theta})^3 \right], \qquad (2.3)$$

where we defined the *speed of sound, c*, and the *Luttinger parameter, K*, as [1],

$$c = \frac{1}{\sqrt{\kappa m n}},$$
$$\frac{K}{\pi} = \sqrt{\frac{\kappa n^3}{m}}. \qquad (2.4)$$

The quadratic part of Eq. (2.3), the term in parenthesis, is the *Tomonaga-Luttinger liquid* Hamiltonian describing linear waves in one dimension [1, 2, 3, 5, 6]. The cubic terms are the non-linear part of the Hamiltonian and they will be useful to the dynamics of one-dimensional systems, as will be shown at the end of this chapter and in the following

---

[1]Here we follow the convention of Refs. [5, 6]. The convention of Refs. [1, 7] is obtained by the substitutions $\phi \to \theta$ and $\theta \to -\phi$ in our equations.
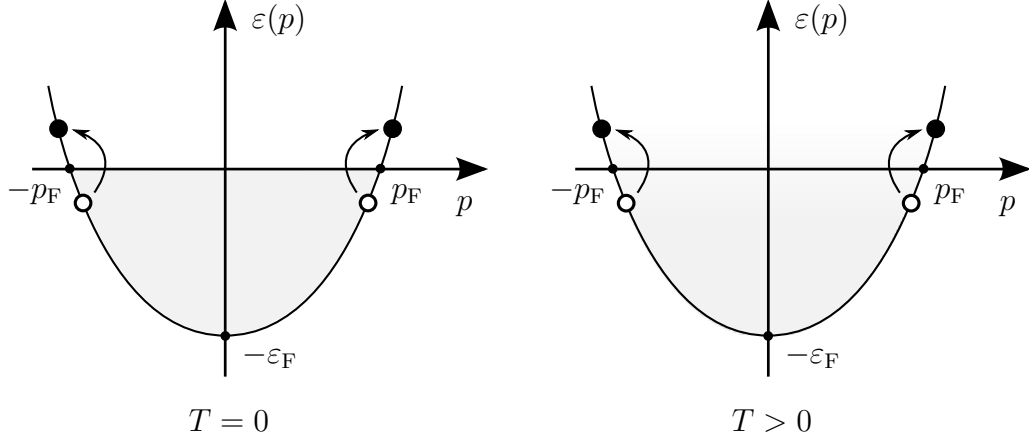
Figure 2.1: Occupation of states for free fermions at zero temperature, $T = 0$, and finite temperature, $T > 0$. The Fermi sea is represented by the grey regions and the Fermi surface is constituted by two separate points, $p = \pm p_F$. The temperature leads to a smearing of the average occupation of states around the Fermi surface. The circles and arrows represent particle-hole excitations.

one. In this chapter, we will see how the low energy physics of bosons and fermions with local repulsive interactions in one dimension is described by hydrodynamics Hamiltonian (2.3) and how to map it into an effective theory of free fermionic quasiparticles.

The first original part of the chapter is a self-contained and coherent derivation of hydrodynamics and fermionic quasiparticles using the Keldysh functional integral. The second original part, together with Appendix B, is the derivation of non-linear terms of the hydrodynamic theory within the functional integral formalism.

2.1 Fermion hydrodynamics

In this section we derive the hydrodynamic theory for interacting fermions. Since hydrodynamics is a theory of low energy excitations, it is instructive to study the low energy excitations of free fermions at zero and finite temperatures. At zero temperature, $T = 0$, fermions occupy all the states below the Fermi surface, as shown in Fig. 2.1-left. The Fermi surface in one dimension is constituted by two separate points in momentum space, $p = \pm p_F$, a central fact for one dimensional hydrodynamics, as we will see soon. Fermions inside the Fermi sea, the grey region in Fig. 2.1-left, are frozen due to the Pauli exclusion

principle. However, they can jump across the Fermi points to the unfilled region above, as shown by the the circles and arrows in Fig. 2.1-left. This process is referred to as *particle-hole excitation*. The hight of the jump is the energy of the excitation and it becomes clear that low energy particle-hole excitations are fermions just below a Fermi point jumping slightly above it. Then, low energy particle-hole excitations must be centred around and be close to the Fermi points. At temperatures much smaller than the Fermi energy, $T \ll \varepsilon_{\mathrm{F}} = \frac{p_{\mathrm{F}}^2}{2m}$, where m is the mass of fermions, the average occupation of the states is smeared around the Fermi points, as shown in Fig. 2.1-right. However, the above argument still holds. Then, given that particle-hole excitations can be arbitrarily close to the Fermi surface, they constitute the lowest energy excitations of the system, suggesting that they could be good candidates for the hydrodynamical description.

To check this intuitive picture, it is useful to study the spectrum of particle-hole excitations. For the moment, we use the operator formalism of second quantisation, as it leads to a better insight. Although the particle-hole excitation spectrum of free fermions is known [7], it is useful to review its calculation in light of the results of the next chapter. We start from the zero temperature case and later extend the results to small temperatures. The spectrum of particle-hole excitations can be studied using the *dynamical structure factor*, that gives the probability per unit time to excite a density fluctuation of momentum q and energy ω by an external source. This quantity is accessible through Bragg spectroscopy [27] and was recently measured for an array of one-dimensional Bose gases [28]. The dynamical structure factor is defined as the Fourier transform of the density-density correlation [29, 7],

$$S(q,\omega) = \int_0^L dx \int_{-\infty}^{\infty} dt \, \langle \hat{n}(x,t)\hat{n}(0,0) \rangle \, e^{-iqx+i\omega t} \,, \tag{2.5}$$

where $\hat{n}(x,t)$ is the density operator, L is the system size and $\langle \ldots \rangle \equiv \langle 0| \ldots |0\rangle$ denotes the expectation value over the ground state, $|0\rangle$. Inserting the completeness relation $\sum_j |j\rangle\langle j| = 1$, where j labels the energy eigenstates, between the densities in Eq. (2.5),

we obtain,

$$S(q,\omega) = \int_0^L dx \int_{-\infty}^{\infty} dt \sum_j \langle 0|\hat{n}(x,t)|j\rangle\langle j|\hat{n}(0,0)|0\rangle e^{-iqx+i\omega t}\,.$$

Making the time dependence of the density explicit, $\hat{n}(x,t) = e^{i\hat{H}t}\hat{n}(x)e^{-i\hat{H}t}$, we have,

$$S(q,\omega) = \int_0^L dx \int_{-\infty}^{\infty} dt \sum_j e^{-i(E_j-E_0)t}\langle 0|\hat{n}(x)|j\rangle\langle j|\hat{n}(0)|0\rangle e^{-iqx+i\omega t}\,,$$

where E_j is the energy of the state $|j\rangle$ and E_0 is the energy of the ground state. Integrating over time we find,

$$S(q,\omega) = 2\pi \int_0^L dx \sum_j \langle 0|\hat{n}(x)|j\rangle\langle j|\hat{n}(0)|0\rangle e^{-iqx}\delta(\omega - E_j + E_0)\,.$$

In terms of the Fourier transform of the fermionic creation and annihilation operators of momentum k, $\hat{c}_k^\dagger$ and $\hat{c}_k$, the density reads $\hat{n}(x) = \frac{1}{L}\sum_q \hat{n}_q e^{iqx} = \frac{1}{L}\sum_{q,k} \hat{c}_{k-q}^\dagger \hat{c}_k e^{iqx}$ and the dynamical structure factor becomes,

$$S(q,\omega) = \frac{2\pi}{L} \sum_j \sum_{q',k,k'} \langle 0|\hat{c}_{k-q}^\dagger \hat{c}_k|j\rangle\langle j|\hat{c}_{k'-q'}^\dagger \hat{c}_{k'}|0\rangle\delta(\omega - E_j + E_0)\,. \qquad (2.6)$$

Here, $\hat{c}_{k+q}^\dagger \hat{c}_k|0\rangle$ is the ground state plus a particle excited from momentum k to momentum $k+q$, as pictured in Fig. 2.2, that is, a particle-hole excitation. Due to the orthogonality of these excited states, the only non-zero contribution comes from $|j\rangle = \hat{c}_{k+q}^\dagger \hat{c}_k|0\rangle = \hat{c}_{k'+q'}^\dagger \hat{c}_{k'}|0\rangle$, which also imposes $q = q'$ and $k = k'$. Then,

$$\begin{aligned} S(q,\omega) &= \frac{2\pi}{L} \sum_k \left|\langle 0|\hat{c}_k^\dagger \hat{c}_{k+q} \hat{c}_{k+q}^\dagger \hat{c}_k|0\rangle\right|^2 \delta\left(\omega - \frac{q(q+2k)}{2m}\right) \\ &\approx \frac{m}{q} \int dk \left|\langle 0|\hat{c}_k^\dagger \hat{c}_{k+q} \hat{c}_{k+q}^\dagger \hat{c}_k|0\rangle\right|^2 \delta\left(k - \frac{m\omega}{q} + \frac{q}{2}\right)\,, \end{aligned}$$

where we approximated the sum by the integral and we used the fact that the energy of
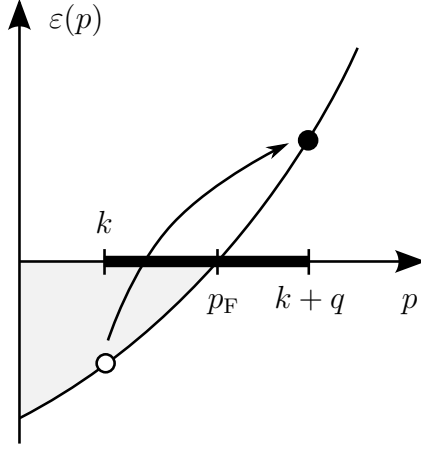
Figure 2.2: Particle-hole excitation close to the right Fermi point, p_F, given by a fermion with momentum k below the Fermi point excited to a state with momentum $k+q$ above the Fermi point. The momentum of the particle-hole excitation, q, is represented by the thick line. The dashed line is the linearisation of the spectrum around the Fermi point.

the ground state plus a particle excited from momentum k to momentum $k-q$ is,

$$E_j = E_0 + \frac{(k+q)^2}{2m} - \frac{k^2}{2m} = E_0 + \frac{q(q+2k)}{2m} .$$

In order for $c^\dagger_{k+q} c_k \left|0\right\rangle$ to be different from zero, because of the Pauli exclusion principle, c_k has to annihilate a particle inside the Fermi sea, that is, $|k| \leq k_\text{F}$, and $c^\dagger_{k+q}$ has to create a particle outside the Fermi sea, that is, $|k+q| > k_\text{F}$. In other words, in the case of the right Fermi point, p_F, the momentum q of the particle-hole excitation is represented by the thick line in Fig. 2.2 that can move left or right but has to be pinned to the Fermi point. Considering only positive q, for $q \leq 2k_\text{F}$ the restriction on k becomes $k_\text{F} - q < k \leq k_\text{F}$ and the result is symmetric for negative q. Finally, integrating over k we obtain,

$$S(q, \omega) = \frac{m}{q} \theta \left(\omega - \omega_-(q)\right) \theta \left(\omega_+(q) - \omega\right) ,$$
$$\omega_\pm(q) = v_\text{F} q \pm \frac{q^2}{2m} ,$$

(2.7)

where $v_\text{F} = p_\text{F}/m$ is the Fermi velocity. The dynamical structure factor at zero temperature
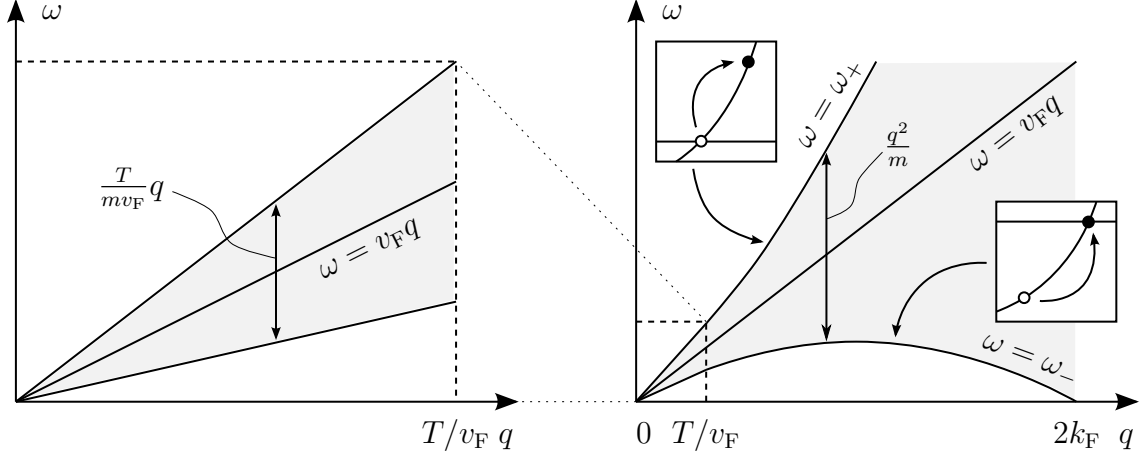
Figure 2.3: Dynamical structure factor, $S(q,\omega)$, of free fermions at a low temperature, $T \ll \varepsilon_{\mathrm{F}}$. For $q \gg T/v_{\mathrm{F}}$, $S(q,\omega)$ is given by the zero temperature result (2.7) and the grey colour represents the region where $S(q,\omega)$ is non-zero. The grey region is centred around $\omega = v_{\mathrm{F}}q$ and is bounded above and below by $\omega = \omega_+(q)$ and $\omega = \omega_-(q)$, the energies corresponding to the extremal particle-hole excitations shown in the insets. For $q \ll T/v_{\mathrm{F}}$, $S(q,\omega)$ is given by the small temperature result (2.8) and the grey colour represents qualitatively the width (2.9) of bell-shaped distribution centred around $\omega = v_{\mathrm{F}}q$. The small temperature result is magnified in the right picture.

as a function of ω is a box centred around $v_{\mathrm{F}}q$, of height m/q and width,

$$\delta\omega(q) = \omega_+(q) - \omega_-(q) = \frac{q^2}{m}.$$

Particle-hole excitations with momentum q and energy ω are present in the system where the dynamical structure factor is non-zero, that is, the grey region in Fig. 2.3-right (ignore $q \ll T/v_{\mathrm{F}}$ for the moment). For each momentum, the dynamical structure factor is bound in energy above and below. The upper bound, $\omega = \omega_+(q)$, corresponds to a particle picked from the Fermi surface, k_{F}, and moved to $k_{\mathrm{F}} + q$ and the lower bound, $\omega = \omega_-(q)$, corresponds to a particle picked from $k_{\mathrm{F}} - q$ and moved to the Fermi surface, k_{F}, as shown in the insets of Fig. 2.3-right. Higher and lower bounds correspond to the thick line pinned to the Fermi surface in Fig. 2.2 moved completely to the right or left. Moving the thick line from right to left creates all the intermediate particle-hole excitations between higher and lower bounds, the grey region in Fig. 2.3. The peculiarity of one-dimensional systems is the absence of low energy excitations away from $q = 0$ and $q = 2k_{\mathrm{F}}$. This absence is

37

related to the presence of the lower bound, which in turn is related to the Fermi surface in one dimension consisting just of two separate points. In higher dimensions, Fermi surfaces are continuous, for example, a circle in two dimensions, allowing one to play with angles to create excitations with arbitrary low energy for any momentum [1].

Now, we have a look at how the result is modified by temperature. At temperatures smaller than the Fermi energy, $T \ll \varepsilon_F$, the average over the ground state in Eq. (2.5) is replaced by the thermal average $\sum_i e^{-E_i/T} \langle i| \dots |i\rangle$, and for $q \ll T/v_F$ the dynamical structure factor becomes,[2]

$$
\begin{aligned}
S(q, \omega) &= \frac{m}{q} n_F \left(v_F \frac{2m(\omega - v_F q) - q^2}{2q} \right) n_F \left(v_F \frac{-2m(\omega - v_F q) - q^2}{2q} \right) \\
&\approx \frac{m}{4q} \frac{1}{\cosh^2 \left(\frac{m v_F}{2Tq} (\omega - v_F q) \right)} .
\end{aligned}
\tag{2.8}
$$

As a function of ω, the dynamical structure factor has the shape of a bell centred around $\omega = v_F q$, of height $m/4q$ and width linear in q,

$$
\delta\omega_T(q) \sim \frac{T}{m v_F} q
\tag{2.9}
$$

The width at finite temperatures is equal to the one at zero temperature with one power of q replaced by the thermal momentum, T/v_F. The width of the dynamical structure factor is represented by the grey region in Fig. 2.3-left. The thermal momentum scale, T/v_F, separates a thermal region for $q \ll T/v_F$ from a quantum region for $q \gg T/v_F$ as shown in 2.3-left. The important observation is that both at zero and finite temperature the widths $\delta\omega(q)$ and $\delta\omega_T(q)$ are small compared to the mean value $v_F q$ in the small momentum and small energy limits, $q \ll k_F$, $\omega \ll \varepsilon_F$ and $T \ll \varepsilon_F$. In turn, this means that in this limit excitations have approximately fixed velocity v_F, like the speed of sound, c, of hydrodynamic wave excitation in Eq. (2.4). In the next two subsections we will see how

---

[2]Note that to satisfy the f-sum rule, $\int d\omega\, \omega S(q,\omega) \propto q^2/2m$, (see e.g., Ref. [29]), one needs to consider the full expression, the first line of Eq. (2.8). This is because the full expression correctly accounts for the detailed balance at negative ω.

the physics of low energy excitations around the Fermi points leads to the hydrodynamic theory with speed of sound $c = v_{\mathrm{F}}$ for free fermions and a modified speed of sound in presence of interactions.

2.1.1 Bosonization

We are ready to derive the hydrodynamic theory for interacting fermions, a procedure known as *bosonization* [1, 7]. Bosonization of interacting fermions was first derived by Haldane using the operator formalism of second quantisation [5, 6]. Complementary to the operator approach, a functional integral approach was suggested in Ref. [30], elaborated in Ref. [31] and presented in a clear picture in Refs. [15, 32, 33]. This approach is known as *functional bosonization* and relies on the Hubbard-Stratonovich transformations. All these approaches are based on equilibrium physics and an extension to non-equilibrium was obtained in Ref. [34] using the Keldysh technique. An appealing aspect of bosonization is that the initial theory of interacting fermions is reformulated as a non-interacting theory that is completely solvable. However, the non-interacting theory is a low-energy approximation to which refinements can be added. One of such refinement is the inclusion of non-linear corrections. A non-linear correction was derived in Ref. [5] using the operator formalism and the assumption that the excitations of the system are created above the ground state. In this chapter we will derive the functional bosonization using the Keldysh technique and, in the spirit of Ref. [16], a double Hubbard-Stratonovich transformation approach, that results in a procedure a bit different from those mentioned above. The advantage of this procedure is that we are able to derive non-linear semiclassical corrections within the functional integral. The result is an infinite series of terms where higher non-linear terms are less important. We find that that the most important non-linear correction coincides with the one calculated in Ref. [5]. This correction is derived using the Keldysh formalism. However, due to the complication of the Keldysh indices and not to interrupt the flow of the chapter, we derive rigorously more terms using the Matsubara formalism in Appendix B.

Low-energy physics being restricted around the two Fermi points for free fermions is at the base of bosonization. The addition of *weak* local interactions between fermions smears the average occupation around the Fermi points, in addition to the smearing due to the temperature. However, the Fermi points, $\pm p_{\mathrm{F}}$, are not modified by the presence of interactions as a consequence of the Luttinger's theorem [35, 36, 37]. The Hamiltonian of a system of interacting fermionic particles is,

$$\hat{H} = \int \mathrm{d}x\, \hat{\psi}^{\dagger}(x) \left[-\frac{\partial_x^2}{2m} - \varepsilon_{\mathrm{F}} \right] \hat{\psi}(x) + \frac{1}{2} \int \mathrm{d}x \mathrm{d}x'\, : \hat{\psi}^{\dagger}(x)\hat{\psi}(x)V(x-x')\hat{\psi}^{\dagger}(x')\hat{\psi}(x') : ,$$
(2.10)

where $\hat{\psi}(x)$ is the fermionic field operator, m the mass of fermions, $V(x-x')$ a local density-density interaction and the colons denotes normal order of operators. In the functional integral representation, the partition function corresponding to Hamiltonian (2.10) is,

$$Z = \int \mathcal{D}[\bar{\psi}, \psi]\, e^{\mathrm{i} \int_{\rightleftarrows} \mathrm{d}t \left[\int \mathrm{d}x\, \bar{\psi}(x,t)\left(\mathrm{i}\partial_t + \frac{\partial_x^2}{2m} + \varepsilon_{\mathrm{F}} \right)\psi(x,t) - \frac{1}{2} \int \mathrm{d}x \mathrm{d}x'\, \bar{\psi}(x,t)\psi(x,t)V(x-x')\bar{\psi}(x',t)\psi(x',t) \right]},$$
(2.11)

where ψ and $\bar{\psi}$ are the Grassmann fields corresponding to $\hat{\psi}$ and $\hat{\psi}^{\dagger}$, $\rightleftarrows$ denotes the closed time contour introduced in the previous chapter (see Fig. 1.1-bottom) and the thermal distribution in the infinite past has an average occupation,

$$n(p) = \frac{1}{e^{\beta(\varepsilon(p)-\varepsilon_{\mathrm{F}})} + 1},$$
(2.12)

where $\varepsilon(p) = p^2/2m$ is the free fermionic spectrum. Here and in the following we include the normalisation factor of the partition function in the integration measure and use the fact that $Z = 1$ in absence of quantum sources (see Eq. (1.10)). Now, we use the fact that, at low energies, the physics is constrained around the Fermi points in order to simplify the interaction term in partition function (2.11), that in momentum space reads,

$$-\frac{1}{2} \int \mathrm{d}k \mathrm{d}k' \frac{\mathrm{d}q}{2\pi}\, V(q)\bar{\psi}(k-q,t)\psi(k,t)\bar{\psi}(k'+q,t)\psi(k',t)\,.$$
(2.13)
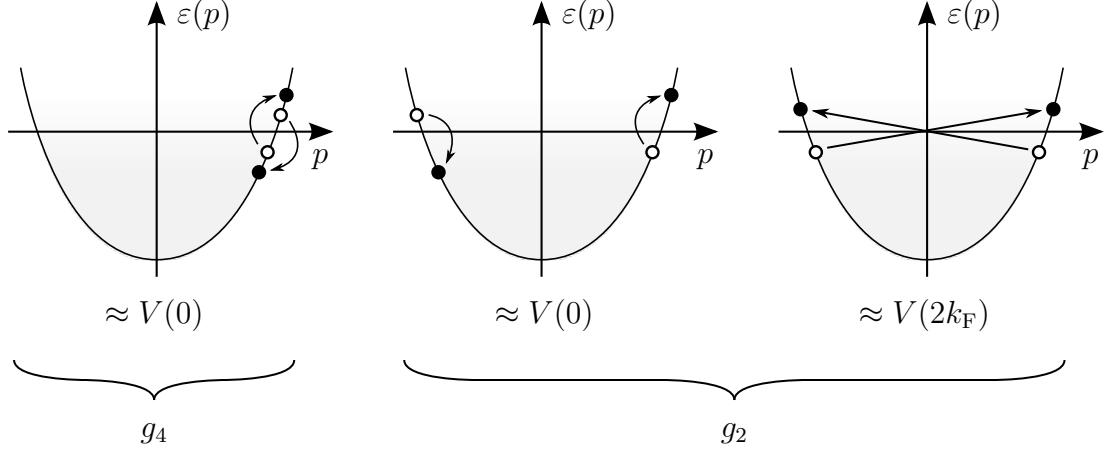
Figure 2.4: Relevant processes to the interaction term (2.13).

Here, quantities in real space and momentum space are related by,

$$V(q) = \int \mathrm{d}x\, V(x) e^{-iqx}\,,$$

$$\psi(k,t) = \int \mathrm{d}x\, \psi(x,t) e^{-ikx}\,,$$

where we considered a system of infinite length. The density-density interaction term (2.13) is represented by two particle-hole excitations: two particles with momentum k and k' are annihilated and two with momentum $k - q$ and $k' + q$ are created. At small energies, this leads to the three processes depicted in Fig. 2.4. All the three processes have small total momentum and energy; however, while single particle-hole excitations in the first two processes have small momenta, $q \approx 0$, the ones in the third process have large momenta, $q \approx \pm 2k_{\mathrm{F}}$, as particles move to opposite Fermi points. It is then convenient to split the fermion fields in the relevant parts, close to the Fermi points, and irrelevant ones, away from them,

$$
\begin{aligned}
\psi(x,t) &= \int \frac{\mathrm{d}k}{2\pi}\, \psi(k,t) e^{ikx} \\
&= e^{ik_{\mathrm{F}}x} \int_{-q_0/2}^{q_0/2} \frac{\mathrm{d}k}{2\pi}\, \psi(k_{\mathrm{F}} + k, t) e^{ikx} + e^{-ik_{\mathrm{F}}x} \int_{-q_0/2}^{q_0/2} \frac{\mathrm{d}k}{2\pi}\, \psi(-k_{\mathrm{F}} + k, t) e^{ikx} + \ldots \\
&= e^{ik_{\mathrm{F}}x} \psi_+(x,t) + e^{-ik_{\mathrm{F}}x} \psi_-(x,t) + \ldots\,,
\end{aligned}
$$

$$(2.14)$$

where we introduced the momentum cut-off q_0 around the Fermi points to delimit the relevant from the irrelevant parts, represented by the dots. Since ψ_+ and ψ_- are only constituted by positive or negative momenta, they move respectively to the right or to the left; for this reason we call them *right* and *left movers*. Substituting decomposition (2.14) into partition function (2.11) we have,

$$Z[u] = \int \mathcal{D}\big[\bar{\psi}_\pm, \psi_\pm\big] e^{i \int_{\rightleftarrows} dr\, \bar{\psi}_\eta(r) \big(G_\eta^{-1}(r) - u_\eta(r)\big) \psi_\eta(r)}$$
$$\times\, e^{-\frac{i}{2} \int_{\rightleftarrows} dr\, \bar{\psi}_\eta(r) \psi_\eta(r) g_{\eta\eta'} \bar{\psi}_{\eta'}(r) \psi_{\eta'}(r)} \,, \tag{2.15}$$

where $\eta = \pm 1$, $r = (x, t)$, $dr = dx dt$ and we defined the bare Green's functions,

$$G_\eta^{-1}(r) = i\partial_t + \eta i v_{\mathrm{F}} \partial_x + \frac{\partial_x^2}{2m} \,, \tag{2.16}$$

and the interaction matrix,

$$g_{\eta\eta'} = \begin{pmatrix} g_4 & g_2 \\ g_2 & g_4 \end{pmatrix} \,,$$

$$g_4 \approx V(0) \,,$$

$$g_2 \approx V(0) - V(2k_F) \,.$$

We also integrated over the fields far away from the Fermi points, represented by the dots in decomposition (2.14), as they contribute only through the quadratic free propagator to the normalisation of the partition function. We added external source fields, $u_+(r)$ and $u_-(r)$, coupled to the densities of right and left movers, $\bar{\psi}_+(r)\psi_+(r)$ and $\bar{\psi}_-(r)\psi_-(r)$, to keep track of what these quantities become after bosonization. Now, we decouple the interaction term using a Hubbard-Stratonovich transformation,

$$Z[u] = \int \mathcal{D}\varrho_\pm e^{\frac{i}{2} \int_{\rightleftarrows} dr\, \varrho_\eta g_{\eta\eta'}^{-1} \varrho_{\eta'}} Z_+[\varrho_+ + u_+] Z_-[\varrho_- + u_-] \,,$$

where,

$$Z_\eta[\varrho] = \int \mathcal{D}\big[\bar{\psi}_\eta, \psi_\eta\big] e^{i \int_{\rightleftarrows} dr\, \bar{\psi}_\eta \big(G_\eta^{-1} - \varrho\big) \psi_\eta} \,,$$

is the non-interacting part of the partition function. Here and in the following we often omit the r dependence of the fields. We make the shift $\varrho \to \varrho - u$ and the partition function becomes,

$$Z[u] = \int \mathcal{D}\varrho_{\pm} e^{\frac{i}{2} \int_{\rightleftarrows} dr\, (\varrho_{\eta} - u_{\eta}) g_{\eta\eta'}^{-1} (\varrho_{\eta'} - u_{\eta'})} Z_{+}[\varrho_{+}] Z_{-}[\varrho_{-}]. \tag{2.17}$$

The presence of the inverse interaction term is problematic when the interaction is zero, in the case of free fermions. To avoid this, in the spirit of Ref. [16], we make a second Hubbard-Stratonovich transformation,

$$Z[u] = \int \mathcal{D}\chi_{\pm} e^{i \int_{\rightleftarrows} dr \left[-\frac{1}{2} \chi'_{\eta} \frac{1}{(2\pi)^2} g_{\eta\eta'} \chi'_{\eta'} - \frac{1}{2\pi} \chi'_{\eta} u_{\eta} \right]} \tilde{Z}_{+}[\chi_{+}] \tilde{Z}_{-}[\chi_{-}], \tag{2.18}$$

where $\chi_{\pm}$ are called *right* and *left chiral fields*, prime denotes a position derivative, $\chi' = \partial_x \chi$, and $\tilde{Z}_{\eta}$ is the functional Fourier transform of Z_{η},

$$\tilde{Z}_{\eta}[\chi_{\eta}] = \int \mathcal{D}\varrho_{\eta} e^{i \int_{\rightleftarrows} dr\, \frac{1}{2\pi} \chi'_{\eta} \varrho_{\eta}} Z_{\eta}[\varrho_{\eta}].$$

The reason for having ∂_x acting on χ is that, as we will see in the next subsection, the final result will be local in position space.[3] After a Keldysh rotation, the partition function reads,

$$Z[u] = \int \mathcal{D}\chi_{\pm} e^{i \int dr \left[-\frac{1}{2} \chi'^{\alpha}_{\eta} \left(\frac{1}{2\pi^2} g_{\eta\eta'} \right) \chi'_{\eta'\alpha} - \frac{1}{\pi} \chi'^{\alpha}_{\eta} u_{\eta\alpha} \right]} \tilde{Z}_{+}[\chi_{+}] \tilde{Z}_{-}[\chi_{-}],$$

$$\tilde{Z}_{\eta}[\chi_{\eta}] = \int \mathcal{D}\varrho_{\eta} e^{i \int dr\, \frac{1}{\pi} \chi'^{\alpha}_{\eta} \varrho_{\eta\alpha}} Z_{\eta}[\varrho_{\eta}], \tag{2.19}$$

$$Z_{\eta}[\varrho_{\eta}] = \int \mathcal{D}\left[\bar{\psi}_{\eta}, \psi_{\eta} \right] e^{i \int_{-\infty}^{\infty} dr\, \bar{\psi}^a_{\eta} \left[\left[G_{\eta}^{-1} \right]^{ab} - \varrho^{ab}_{\eta} \right] \psi^b_{\eta}},$$

where $\left[G_{\eta}^{-1} \right]^{ab}(x,t) = \delta^{ab} G_{\eta}^{-1}(x,t)$ is the inverse Green's function and $\varrho^{ab}_{\eta} = \delta^{ab} \varrho^{cl}_{\eta} + \sigma^{ab}_1 \varrho^{q}_{\eta}$. For brevity, we omit the classical and quantum indices in the integration measure and we introduce the covariant-like notation $\varrho_{\alpha} = \sigma^{\alpha\beta}_1 \varrho^{\beta}$. The functional integrals in the first two lines do not have boundary conditions, while the one in the last line have boundary

---

[3]The derivative also contributes to the normalisation of the partition function, that we include in the integration measure.

conditions that in momentum space are given by Eqs. (1.40), that adapted to Eq. (2.19) read,

$$\begin{cases} \psi_\eta^2(p, t \to \infty) = 0 \\ \psi_\eta^1(p, t \to -\infty) = -(1 - 2n(p))\psi_\eta^2(p, t \to -\infty) \,, \end{cases}$$

with average occupation, $n(p)$, given by Eq. (2.12). To avoid loaded formulas, the boundary conditions are implied in the integration symbol. We evaluate $Z_\eta[\varrho_\eta]$ by integrating over right and left movers,

$$\begin{aligned} Z_\eta[\varrho_\eta] &= \frac{\det(-iG_\eta^{-1} + i\varrho_\eta)}{\det(-iG_\eta^{-1})} \\ &= e^{\mathrm{Tr}\log(-iG_\eta^{-1}+i\varrho_\eta) - \mathrm{Tr}\log(-iG_\eta^{-1})} \\ &= e^{\mathrm{Tr}\log(1 - G_\eta \circ \varrho_\eta)} \,, \end{aligned} \qquad (2.20)$$

where the compact notation means,

$$\varrho_\eta = \varrho_\eta^{ab}(r)\delta^2(r - r') \,,$$

$$G_\eta^{-1} = \left[G_\eta^{-1}\right]^{ab}(r)\delta^2(r - r') \,,$$

$$G_\eta = G_\eta^{ab}(r - r') \,.$$

Here G_η is the right or left movers Green's function and $\circ$ denotes convolution with respect to position and time. Substituting result (2.20) into the second line of Eq. (2.19), we have,

$$\tilde{Z}_\eta[\chi_\eta] = \int \mathcal{D}\varrho_\eta e^{i\int dr \frac{1}{\pi}\chi_\eta'^\alpha \varrho_{\eta\alpha} + \mathrm{Tr}\log(1 - G_\eta \circ \varrho_\eta)} \,. \qquad (2.21)$$

The trace of the logarithm can be expanded in the usual way [14], leading to the n-particle vertices for the field ϱ_η,

$$\begin{aligned} -\mathrm{Tr}\log(1 - G_\eta \circ \varrho_\eta) &= \mathrm{Tr}(G_\eta \circ \varrho_\eta) + \frac{1}{2}\mathrm{Tr}(G_\eta \circ \varrho_\eta \circ G_\eta \circ \varrho_\eta) + \dots \\ &= \sum_{n \geq 1} \frac{1}{n}\int dr_1 \dots dr_n\, \Gamma_{n\eta}^{\alpha_1 \dots \alpha_n}(r_1, \dots, r_n)\varrho_\eta^{\alpha_1}(r_1) \cdots \varrho_\eta^{\alpha_n}(r_n) \,. \end{aligned} \qquad (2.22)$$
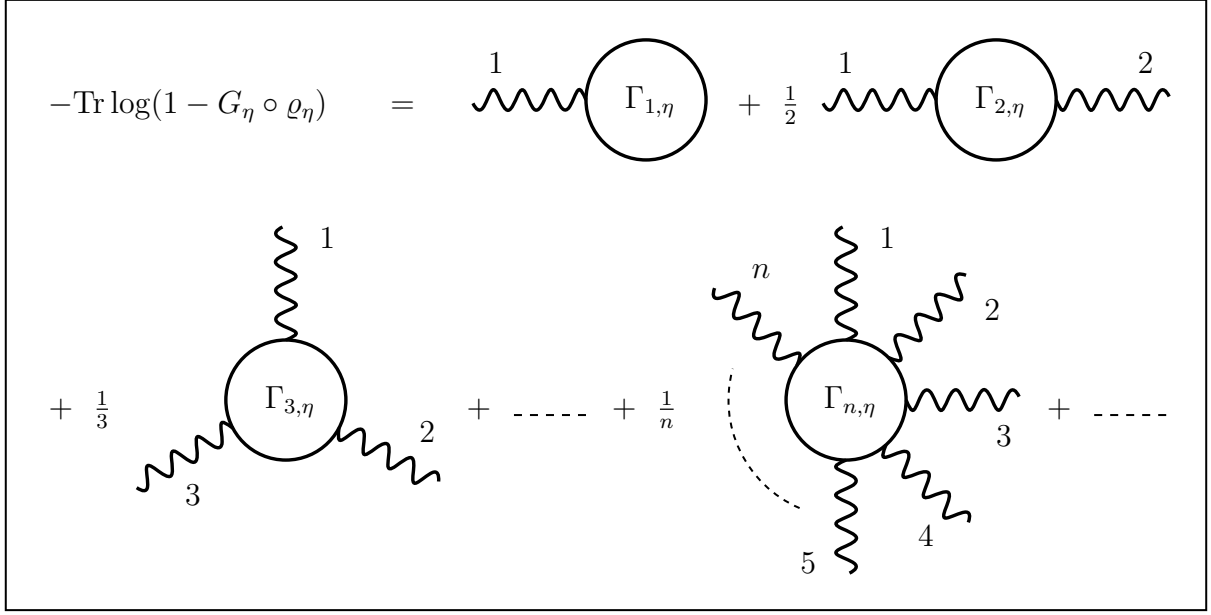
Figure 2.5: Diagrammatic representation of series (2.22). The wavy lines represent the fields ϱ_η's and the solid lines the fermionic Green's functions, G_η's. The fermionic loops $\Gamma_{n,\eta}$ are given by Eq. (2.23).

The interaction vertex is,

$$\Gamma_{n,\eta}^{\alpha_1\ldots\alpha_n}(r_1,\ldots,r_n) = \sigma_{\alpha_1}^{a_1,a_1'}G_\eta^{a_1'a_2}(r_1-r_2)\sigma_{\alpha_2}^{a_2,a_2'}G_\eta^{a_2'a_3}(r_2-r_3)\cdots\sigma_{\alpha_n}^{a_n,a_n'}G_\eta^{a_n'a_1}(r_n-r_1)\,,$$

$$(2.23)$$

where $\sigma_\alpha^{a,a'} = \delta_{\alpha,\mathrm{cl}}\delta^{aa'} + \delta_{\alpha,\mathrm{q}}\sigma_1^{aa'}$. Series (2.22) is represented by means of the Feynman diagrams in Fig. 2.5. The wavy lines represent the fields ϱ_η's and the solid lines the free fermion Green functions, G_η's. The first term of the series, known as tadpole diagram, is $\sim \int \mathrm{d}r \varrho_\eta^\mathrm{q}(r)$ and just contributes to the homogeneous density of the system. We omit it by measuring the density from its constant homogeneous value. The second term of the series, know as *polarisation* diagram, contributes to the free propagator of ϱ_η and is the leading contribution in the bosonization procedure. The rest of the terms, $n \geq 3$, are the non-linear diagrams, generating interactions between the fields ϱ_η's. Although the series of diagrams is infinite, in the limit of low energies non-linear corrections become smaller compared to the polarisation diagram, as we will see in the following. We proceed by considering the lowest approximation, that is, the polarisation diagram.
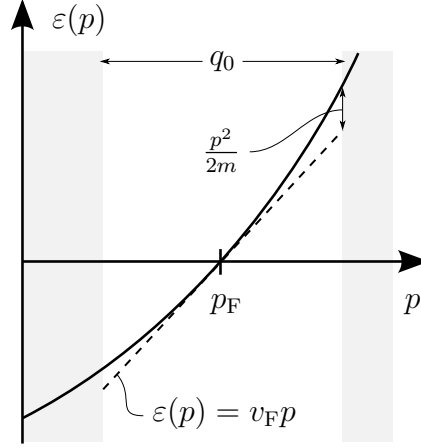
Figure 2.6: Linearisation of the spectrum, $\varepsilon(p) = v_{\mathrm{F}}p + p^2/2m$, around the right Fermi point. The dashed line represents the linearised spectrum, $\varepsilon(p) = v_{\mathrm{F}}p$, and q_0 is the cut-off introduced in the decomposition of the fermionic field into left and right movers, Eq. (2.14).

2.1.2 Linear spectrum

The lower the energy, the smaller the relevant region around the Fermi points. This means that we may choose a smaller cut-off, q_0. The spectrum with the cut-off around the right Fermi point is represented in Fig. 2.6. The dashed line in the figure represents the linearised spectrum around the right Fermi point and it is clear that the smaller the cut-off, the smaller the contribution of the curvature. Then, in the limit $q_0 \ll mv_{\mathrm{F}}$, in first approximation we may neglect the curvature. To do so, we consider the fermionic spectrum with momentum centred around the right or left Fermi points, $\pm p_{\mathrm{F}}$,

$$\varepsilon(p) = \frac{p^2}{2m} - \varepsilon_{\mathrm{F}} \longrightarrow \varepsilon_\eta(p) = \frac{(p - \eta p_{\mathrm{F}})^2}{2m} - \frac{p_{\mathrm{F}}^2}{2m} = \eta v_{\mathrm{F}}p + \frac{p^2}{2m}\,.$$

The linear approximation amounts to neglecting the quadratic term,

$$\varepsilon_\eta(p) \approx \eta v_{\mathrm{F}}p\,.$$

In the case of linear spectrum, Dzyaloshinski and Larkin proved that in equilibrium only the first two diagram in Fig. 2.5 are non-zero, that is, $\Gamma_{\eta,n} = 0$ for $n \geq 3$ in Eqs. (2.22) and (2.23) [38]. This statement goes by the name of the *Dzyaloshinski-Larkin theorem*

46

and we prove it in Appendix B within the Matsubara technique. In the non-equilibrium case, an infinite series of non-linear terms in the quantum field is present, leading to an expansion in noise cumulants [34]. However, we neglect these terms because, as we will see in the next chapter, we will just consider small deviations from equilibrium. Taking the linear spectrum approximation and using the Dzyaloshinski-Larkin theorem, Eq. (2.21) becomes,

$$\tilde{Z}_\eta[\chi_\eta] = \int \mathcal{D}\varrho_\eta e^{i\int dr \frac{1}{\pi}\chi'_{\eta\alpha}\varrho_\eta^\alpha - \frac{i}{2}\int drdr' \varrho_\eta^\alpha(r)\Pi_\eta^{\alpha\beta}(r-r')\varrho_\eta^\beta(r')}$$

$$= \frac{1}{\sqrt{\det i\Pi_\eta}} e^{i\int drdr' \frac{1}{2}\chi'_{\eta\alpha}(r)\frac{1}{\pi^2}[\Pi_\eta^{-1}]^{\alpha\beta}(r-r')\chi'_{\eta\beta}(r')},$$

where,

$$i\Pi_\eta^{\alpha\beta}(r) = \Gamma_{2,\eta}^{\alpha\beta}(r,-r) = \begin{pmatrix} 0 & i\Pi_\eta^A(r) \\ i\Pi_\eta^R(r) & i\Pi_\eta^K(r) \end{pmatrix}, \tag{2.24}$$

is the polarisation function of free fermions and,

$$i\Pi_\eta^R(x,t) = \left[i\Pi_\eta^A(-x,-t)\right]^*$$

$$= G_\eta^R(x,t)G_\eta^K(-x,-t) + G_\eta^K(x,t)G_\eta^A(-x,-t),$$

$$i\Pi_\eta^K(x,t) = G_\eta^K(x,t)G_\eta^K(-x,-t) + G_\eta^R(x,t)G_\eta^A(-x,-t) + G_\eta^A(x,t)G_\eta^R(-x,-t)$$

$$= G_\eta^K(x,t)G_\eta^K(-x,-t) - \left(G_\eta^R(x,t) - G_\eta^A(x,t)\right)\left(G_\eta^R(x,t) - G_\eta^A(x,t)\right),$$

where in the last line we used,

$$G_\eta^R(x,t)G_\eta^R(-x,-t) = 0,$$
$$G_\eta^A(x,t)G_\eta^A(-x,-t) = 0, \tag{2.25}$$

since their support is of null dimension. The polarisation function is easier to calculate in the Fourier representation,

$$\varrho_\eta^\alpha(x,t) = \int \frac{dq}{2\pi}\frac{d\omega}{2\pi}\varrho_\eta^\alpha(q,\omega)e^{iqx-i\omega t},$$

that gives,

$$\tilde{Z}_\eta[\chi_\eta] = \frac{1}{\sqrt{\det i\Pi_\eta}} e^{i\int \frac{d\omega}{2\pi}\frac{dq}{2\pi}\frac{1}{2}\bar{\chi}_{\eta\alpha}(q,\omega)\frac{q^2}{\pi^2}[\Pi_\eta^{-1}]^{\alpha\beta}(q,\omega)\chi_{\eta\beta}(q,\omega)} , \qquad (2.26)$$

where,

$$\begin{aligned}
\Pi_\eta^{\mathrm{R}}(q,\omega) &= \left[\Pi_\eta^{\mathrm{A}}(q,\omega)\right]^* \\
&= -i\int \frac{dk}{2\pi}\frac{d\varepsilon}{2\pi}\left[G_\eta^{\mathrm{R}}(k+q,\varepsilon+\omega)G_\eta^{\mathrm{K}}(k,\varepsilon) + G_\eta^{\mathrm{K}}(k+q,\varepsilon+\omega)G_\eta^{\mathrm{A}}(k,\varepsilon)\right] \\
&= i\int \frac{dk}{2\pi}\left(F(\varepsilon_\eta(k)) - F(\varepsilon_\eta(k+q))\right)\int \frac{d\varepsilon}{2\pi}G_\eta^{\mathrm{R}}(k+q,\varepsilon+\omega)G_\eta^{\mathrm{A}}(k,\varepsilon) , \\
\Pi_\eta^{\mathrm{K}}(q,\omega) &= -i\int \frac{dk}{2\pi}\frac{d\varepsilon}{2\pi}\left[G_\eta^{\mathrm{K}}(k+q,\varepsilon+\omega)G_\eta^{\mathrm{K}}(k,\varepsilon)\right. \\
&\qquad \left. - \left(G_\eta^{\mathrm{R}}(k+q,\varepsilon+\omega) - G_\eta^{\mathrm{A}}(k+q,\varepsilon+\omega)\right)\left(G_\eta^{\mathrm{R}}(k,\varepsilon) - G_\eta^{\mathrm{A}}(k,\varepsilon)\right)\right] \\
&= -i\int \frac{dk}{2\pi}\left(F(\varepsilon_\eta(k+q))F(\varepsilon_\eta(k)) - 1\right) \\
&\qquad \times \frac{d\varepsilon}{2\pi}\left(G_\eta^{\mathrm{R}}(k+q,\varepsilon+\omega) - G_\eta^{\mathrm{A}}(k+q,\varepsilon+\omega)\right)\left(G_\eta^{\mathrm{R}}(k,\varepsilon) - G_\eta^{\mathrm{A}}(k,\varepsilon)\right) .
\end{aligned}$$

Here we used the fluctuation-dissipation theorem to express the Keldysh component in terms of retarded and advanced ones,

$$\begin{aligned}
G_\eta^{\mathrm{K}}(k,\varepsilon) &= F(\varepsilon)\left(G_\eta^{\mathrm{R}}(k,\varepsilon) - G_\eta^{\mathrm{A}}(k,\varepsilon)\right) \\
&= F(\varepsilon_\eta(k))\left(G_\eta^{\mathrm{R}}(k,\varepsilon) - G_\eta^{\mathrm{A}}(k,\varepsilon)\right) .
\end{aligned}$$

We also used the fact that Eqs. (2.25) imply,

$$\begin{aligned}
\int \frac{d\varepsilon}{2\pi}G_\eta^{\mathrm{R}}(k+q,\varepsilon+\omega)G_\eta^{\mathrm{R}}(k,\varepsilon) &= 0 , \\
\int \frac{d\varepsilon}{2\pi}G_\eta^{\mathrm{A}}(k+q,\varepsilon+\omega)G_\eta^{\mathrm{A}}(k,\varepsilon) &= 0 .
\end{aligned}$$

Using the thermal equilibrium average occupation, $F(\varepsilon) = \tanh\left(\frac{\varepsilon}{2T}\right)$, and integrating over ε, the retarded component of the polarisation function becomes,

$$\begin{aligned}
\Pi_\eta^{\mathrm{R}}(q,\omega) &= \frac{1}{\omega - \eta cq + i0}\int \frac{dk}{2\pi}\left[\tanh\left(\eta\frac{v_{\mathrm{F}}k + v_{\mathrm{F}}q}{2T}\right) - \tanh\left(\eta\frac{v_{\mathrm{F}}k}{2T}\right)\right] \\
&= \frac{\eta}{\pi}\frac{q}{\omega - \eta cq + i0} ,
\end{aligned}$$

and the Keldysh component,

$$\Pi_\eta^{\mathrm{K}}(q,\omega) = -\mathrm{i}\delta(\omega - \eta v_{\mathrm{F}}q)\int \mathrm{d}k\left[1 - \tanh\left(\eta\frac{v_{\mathrm{F}}k + v_{\mathrm{F}}q}{2T}\right)\tanh\left(\eta\frac{v_{\mathrm{F}}k}{2T}\right)\right]$$

$$= -\mathrm{i}\delta(\omega - \eta v_{\mathrm{F}}q)\coth\left(\frac{cq}{2T}\right)\int \mathrm{d}k\left[\tanh\left(\frac{v_{\mathrm{F}}k + v_{\mathrm{F}}q}{2T}\right) - \tanh\left(\frac{v_{\mathrm{F}}k}{2T}\right)\right]$$

$$= -2\mathrm{i}q\coth\left(\frac{v_{\mathrm{F}}q}{2T}\right)\delta(\omega - \eta v_{\mathrm{F}}q)\,,$$

where in the second line we used the identity,

$$1 - \tanh(a)\tanh(b) = \coth\left(a - b\right)\left[\tanh(a) - \tanh(b)\right]\,. \tag{2.27}$$

Summarising, retarded, advanced and Keldysh Green's functions are,

$$\Pi_\eta^{\mathrm{R,A}}(q,\omega) = \frac{\eta}{\pi}\frac{q}{\omega - \eta v_{\mathrm{F}}q \pm \mathrm{i}0}\,,$$

$$\Pi_\eta^{\mathrm{K}}(q,\omega) = -2\mathrm{i}q\coth\left(\frac{v_{\mathrm{F}}q}{2T}\right)\delta(\omega - \eta v_{\mathrm{F}}q)\,,$$

$$= \coth\left(\frac{\omega}{2T}\right)\left(\Pi_\eta^{\mathrm{R}}(q,\omega) - \Pi_\eta^{\mathrm{A}}(q,\omega)\right)\,,$$

where the last identity is a statement of the fluctuation-dissipation theorem. Now that we know the explicit form of the polarisation function, Eq. (2.24), we can invert it and substitute it in Eq. (2.26). We invert it using the boundary conditions of the functional integral seen in Chap. 1 and write,

$$\left[\Pi_\eta^{-1}(q,\omega)\right]^{\alpha\beta} = \Pi_\eta^{-1}(q,\omega)\sigma_1^{\alpha\beta} = \eta\pi\frac{\omega - \eta v_{\mathrm{F}}q}{q}\sigma_1^{\alpha\beta}\,,$$

with boundary conditions,

$$\begin{cases} \chi_\eta^{\mathrm{q}}(q, t \to \infty) = 0\,, \\[2mm] \chi_\eta^{\mathrm{q}}(q, t \to -\infty) = -\frac{\chi_\eta^{\mathrm{cl}}(q, t \to -\infty)}{\coth(v_{\mathrm{F}}q/2T)}\,. \end{cases}$$

Note that these boundary conditions do not correspond to those of free fermions as here the mass curvature, m^{-1}, is not present. However, we may as well have started with fermions

that had no mass curvature, $m^{-1} \to 0$, in the infinite past and increased it adiabatically with time. Substituting the inverse Green's function in Eq. (2.26) we have,

$$\tilde{Z}_\eta[\chi_\eta] = \frac{1}{\sqrt{\det \mathrm{i}\Pi_\eta}} e^{\mathrm{i} \int \frac{d\omega}{2\pi} \frac{dq}{2\pi} \frac{1}{2} \bar{\chi}_\eta^\alpha(q,\omega) D_{0,\eta}^{-1}(q,\omega) \chi_{\eta\alpha}(q,\omega)} \,,$$

where we defined the propagator of the chiral fields without the contribution $\sim g_{\eta\eta'}$ from the density-density interactions of fermions (see first line of Eq. (2.19)) as,

$$D_{0,\eta}^{-1}(q,\omega) = \frac{q^2}{\pi^2} \Pi_\eta^{-1}(q,\omega) = \frac{\eta}{\pi} q(\omega - \eta v_\mathrm{F} q) \,.$$

Fourier transforming back to position and time, the partition function becomes,

$$Z_\eta[u] = \frac{1}{\sqrt{\det \mathrm{i}\Pi_\eta}} e^{\mathrm{i} \int dr \frac{1}{2} \chi_\eta^\alpha(r) D_{0,\eta}^{-1}(r) \chi_{\eta\alpha}(r)} \,, \tag{2.28}$$

where,

$$D_{0,\eta}^{-1}(r) = \frac{\eta}{\pi} \partial_x(\partial_t + \eta v_\mathrm{F} \partial_x) \,, \tag{2.29}$$

Finally, substituting Eqs. (2.28) into the first line in Eq. (2.19), we find the bosonized partition function of fermions with linear spectrum,

$$Z[u] = \int \mathcal{D}\chi_\pm e^{\mathrm{i} \int dr \left[\frac{1}{2} \chi_\eta^\alpha D_{\eta\eta'}^{-1} \chi_{\eta'\alpha} - \frac{1}{\pi} \chi_\eta'^\alpha u_{\eta\alpha}\right]} \,, \tag{2.30}$$

where the chiral fields propagator is,

$$D_{\eta\eta'}^{-1}(r) = \delta_{\eta\eta'} D_{0,\eta}^{-1}(r) + \frac{1}{\pi} \frac{g_{\eta\eta'}}{2\pi} \partial_x^2 \,. \tag{2.31}$$

The first thing that we note is that the exponent of partition function (2.30) is quadratic in $\chi_\pm$. As hinted at the beginning of the section, this is a major advantage of bosonization: we started with a system of interacting electrons and we ended up with a quadratic low-energy theory that allows for exact analytical results. Thanks to the external source

u_η we can relate the right and left chiral fields with right and left movers by comparing Eqs. (2.15) and (2.30), to obtain the correspondence,[4]

$$\bar{\psi}_\eta \psi_\eta \longleftrightarrow \frac{1}{2\pi} \partial_x \chi_\eta \,. \tag{2.32}$$

This means that $\frac{1}{2\pi} \partial_x \chi_\pm$ has the meaning of density of right and left movers. Partition function (2.30) is not the usual form found in literature [1]. The usual form corresponds to the expression in parenthesis of Eq. (2.3) and, to obtain it, we make the transformation,

$$\chi_\pm = \theta \pm \phi \,, \tag{2.33}$$

and find the Tomonaga-Luttinger liquid partition function,

$$Z[u] = \int \mathcal{D}\theta \mathcal{D}\phi\, e^{\mathrm{i} \int \mathrm{d}r \left[\begin{pmatrix} \theta^\alpha \\ \phi^\alpha \end{pmatrix}^{\mathrm{T}} \begin{pmatrix} \frac{c}{\pi K}\partial_x^2 & \frac{1}{\pi}\partial_t\partial_x \\ \frac{1}{\pi}\partial_t\partial_x & \frac{cK}{\pi}\partial_x^2 \end{pmatrix} \begin{pmatrix} \theta_\alpha \\ \phi_\alpha \end{pmatrix} - \begin{pmatrix} \frac{2}{\pi}\partial_x\theta^\alpha \\ \frac{2}{\pi}\partial_x\phi^\alpha \end{pmatrix} \begin{pmatrix} u_{\theta\alpha} \\ u_{\phi\alpha} \end{pmatrix} \right]} \tag{2.34}$$

where we defined,

$$\begin{aligned} c &= \sqrt{\left(v_{\mathrm{F}} + \frac{g_4}{2\pi}\right)^2 - \left(\frac{g_2}{2\pi}\right)^2} \,, \\ K &= \sqrt{\frac{v_{\mathrm{F}} + \frac{g_4}{2\pi} - \frac{g_2}{2\pi}}{v_{\mathrm{F}} + \frac{g_4}{2\pi} + \frac{g_2}{2\pi}}} \,, \end{aligned} \tag{2.35}$$

Note that $c \approx v_{\mathrm{F}}$ and $K \approx 1$ because the initial fermions are weakly interacting. We also defined the new source fields coupled to θ and ϕ in terms of the ones coupled to $\chi_\pm$ as,

$$u_{\theta,\phi} = \frac{u_+ \pm u_-}{2}$$

---

[4]Note that in this definition we dropped the Keldysh indices by writing the fields in the closed time contour of Fig. 1.1 in order to meet the standard definitions found in literature [5, 6, 1, 7]. We also removed a factor 2 multiplying $\partial_x \chi_\eta^\alpha / 2\pi$ that appears Keldysh formalism (See also Ref. [13]). We will refer again to this footnote, for example for the fields θ and ϕ.

Relation (2.32) is now updated to,[4]

$$\bar{\psi}_+\psi_+ + \bar{\psi}_-\psi_- \longleftrightarrow \frac{1}{\pi}\partial_x\theta \,.$$
$$\bar{\psi}_+\psi_+ - \bar{\psi}_-\psi_- \longleftrightarrow \frac{1}{\pi}\partial_x\phi \,. \qquad (2.36)$$

The first line is the sum of the densities of right and left movers. Remembering that we are measuring the non-homogeneous part of the density from its homogeneous part, the sum of the densities of right and left movers and, therefore, $\frac{1}{\pi}\partial_x\theta$ measures the density fluctuations (in the low energy limit). The term $\phi^\alpha\partial_t\left(\frac{1}{\pi}\partial_x\theta_\alpha\right)$ in partition function (2.34) is the term of the Legendre transform that relates the Lagrangian and the Hamiltonian, such as $p\dot{x}$ in $L = p\dot{x} - H$ in quantum mechanics. Then, in the same way p is conjugate to x, we deduce that ϕ is the phase conjugate to the density $\frac{1}{\pi}\partial_x\theta$. We conclude that we have obtained the hydrodynamic formalism given by the Luttinger liquid Hamiltonian, Eq. (2.3), without the non-linear corrections and the constant energy term.[5] Therefore, the the parameter c and K in Eq. (2.35) are the speed of sound and the Luttinger parameter. From the second line of Eq. (2.36) and Eq. (2.2) we also find that the low-energy velocity field in terms of right and left movers is $v = \frac{\pi}{m}(\bar{\psi}_+\psi_+ - \bar{\psi}_-\psi_-)$.

2.1.3   Non-linear corrections

In the last subsection we derived linear bosonization, corresponding to the first two diagrams of Fig. 2.5. The first diagram was omitted by measuring the density from its homogeneous value and the second diagram led to a quadratic low-energy theory of hydrodynamic excitations. As part of the original contributions of this work, in this sub-section we derive the first non-linear correction to linear bosonization, the three-leg diagram in Fig. 2.5, within the Keldysh functional integral. We show that perturbation theory in the spectrum curvature works well to derive the three-leg correction. We check this result using a more rigorous approach based on the Matsubara formalism, derived in

---

[5]For the comparison, note that there is an additional factor 2 multiplying the Lagrangian in the Keldysh formalism.

Appendix B, where we also derive the four-leg correction and formulate a conjecture for all other terms.

The non-linear part of series (2.22), given by the sum with $n \geq 3$, that we denote as $M_\eta[\varrho_\eta^\alpha]$, can be reformulated using the knowledge of the polarisation diagram. We split linear and non-linear parts of $\mathrm{Tr}\log(1 - G_\eta \circ \varrho_\eta)$ in (2.21),

$$\tilde{Z}_\eta[\chi_\eta] = \int \mathcal{D}\varrho_\eta e^{\mathrm{i}\int \mathrm{d}r\, \frac{1}{\pi}\chi_\eta'^\alpha \varrho_{\eta\alpha} - \frac{\mathrm{i}}{2}\int \mathrm{d}r\mathrm{d}r'\, \varrho_\eta^\alpha(r)\Pi_\eta^{\alpha\beta}(r-r')\varrho_\eta^\beta(r') - M_\eta[\varrho_\eta^\alpha]} .$$

We express the non-linear term, $M_\eta[\varrho_\eta^\alpha]$, in terms of the functional Fourier transform field, $\chi_\eta'^\alpha$, by substituting ϱ_η^α with $-\mathrm{i}\pi\frac{\delta}{\delta\chi_{\eta\alpha}'}$ and moving $M_\eta[-\mathrm{i}\pi\frac{\delta}{\delta\chi_{\eta\alpha}'}]$ in front of the integral,

$$\tilde{Z}_\eta[\chi_\eta] = e^{-M_\eta[-\mathrm{i}\pi\frac{\delta}{\delta\chi_\alpha'}]} \int \mathcal{D}\varrho_\eta e^{\mathrm{i}\int \mathrm{d}r\, \frac{1}{\pi}\chi_{\eta\alpha}'\varrho_\eta^\alpha - \frac{\mathrm{i}}{2}\int \mathrm{d}r\mathrm{d}r'\, \varrho_\eta^\alpha(r)\Pi_\eta^{\alpha\beta}(r-r')\varrho_\eta^\beta(r')}$$

$$= e^{-M_\eta[-\mathrm{i}\pi\frac{\delta}{\delta\chi_{\eta\alpha}'}]} e^{\mathrm{i}\int \mathrm{d}r\, \frac{1}{2}\chi_\eta^\alpha D_{0,\eta}^{-1}\chi_{\eta\alpha}}$$

$$= e^{\mathrm{i}\int \mathrm{d}r\, \frac{1}{2}\chi_\eta^\alpha D_{0,\eta}^{-1}\chi_{\eta\alpha}} \left[e^{-\mathrm{i}\int \mathrm{d}r\, \frac{1}{2}\chi_\eta^\alpha D_{0,\eta}^{-1}\chi_{\eta\alpha}} e^{-M_\eta[-\mathrm{i}\pi\frac{\delta}{\delta\chi_{\eta\alpha}'}]} e^{\mathrm{i}\int \mathrm{d}r\, \frac{1}{2}\chi_\eta^\alpha D_{0,\eta}^{-1}\chi_{\eta\alpha}} \right] ,$$

where in the second line we integrated over ϱ_η and used the linear bosonization results (2.28) and (2.29) and in the third line we multiplied and divided by $e^{\mathrm{i}\int \mathrm{d}r\, \frac{1}{2}\chi_\eta^\alpha D_{0,\eta}^{-1}\chi_{\eta\alpha}}$. Expanding the first term in a Taylor series in $-\mathrm{i}\pi\frac{\delta}{\delta\chi_\alpha'}$ and inserting $1 = e^{\mathrm{i}\int \mathrm{d}r\, \frac{1}{2}\chi_\eta^\alpha D_{0,\eta}^{-1}\chi_{\eta\alpha}} e^{-\mathrm{i}\int \mathrm{d}r\, \frac{1}{2}\chi_\eta^\alpha D_{0,\eta}^{-1}\chi_{\eta\alpha}}$ between each derivative, we obtain the shift $-\mathrm{i}\pi\frac{\delta}{\delta\chi_\alpha'} \to -\eta\partial_\eta\chi_\eta^\alpha - \mathrm{i}\pi\frac{\delta}{\delta\chi_\alpha'}$, where we defined,

$$\partial_\eta = \partial_t + \eta v_\mathrm{F}\partial_x ,$$

that leads to,

$$\tilde{Z}_\eta[\chi_\eta] = e^{\mathrm{i}\int \mathrm{d}r\, \frac{1}{2}\chi_\eta^\alpha D_{0,\eta}^{-1}\chi_{\eta\alpha} - M_\eta[-\eta\partial_\eta\chi_\eta^\alpha - \mathrm{i}\pi\frac{\delta}{\delta\chi_{\eta\alpha}'}]} .$$

Inserting this result in the first line of Eq. (2.19) and using Eq. (2.31) we find,

$$Z[u] = \int \mathcal{D}\chi_\pm e^{\mathrm{i}\int \mathrm{d}r\, \left[\frac{1}{2}\chi_\eta^\alpha D_{\eta\eta'}^{-1}\chi_{\eta'\alpha} - \frac{1}{\pi}\partial_x\chi_\eta^\alpha u_{\eta\alpha}\right] - \sum_\eta M_\eta[-\eta\partial_\eta\chi_\eta^\alpha - \mathrm{i}\pi\frac{\delta}{\delta\chi_{\eta\alpha}'}]} . \tag{2.37}$$
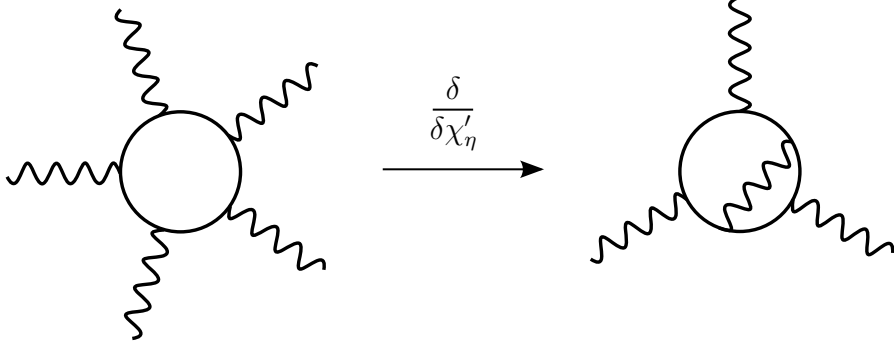
Figure 2.7: Example of contraction of two legs of the five-loop caused by the term $\sim \frac{\delta}{\delta \chi'_\eta}$ inside M_η in partition function (2.37). The contraction gives a correction to the semiclassical three-loop shown in Fig. 2.5.

This partition function contains two contributions in the exponent: the first term is the linear contribution found previously and the second term is the non-linear contribution. The derivative in the argument of M_η generates contractions between pairs of legs. For example, as shown in Fig. 2.7, the derivative acting on a five-leg vertex contracts two legs leading to a correction to the three-leg vertex. Neglecting the derivative in the argument of M_η amounts to a semiclassical approximation [39]. In other words, we are considering just the first term in powers of $q/mc \ll 1$ for each n-loop diagram. This means that we consider n-loops where there are no contractions inside the bosonic loop, such as the one in Fig. 2.7. Because our endpoint is an equation for the classical field, χ^{cl}_η, we neglect the term $\sim \frac{\delta}{\delta \chi'_\eta}$ and consider the first non-linear correction, the three-leg vertex, whose additional term to the action is,

$$S_{\text{nl}}[\chi^\alpha_\eta] = \frac{\eta}{3} \int dr_1 dr_2 dr_3 \Gamma^{\alpha_1 \alpha_2 \alpha_3}_{3,\eta}(r_1, r_2, r_3) \partial_\eta \chi^{\alpha_1}_\eta(r_1) \partial_\eta \chi^{\alpha_2}_\eta(r_2) \partial_\eta \chi^{\alpha_3}_\eta(r_3) \,. \qquad (2.38)$$

More specifically, since we are interested in the semiclassical equation for χ^{cl}_η, we need the product of two classical fields and one quantum field,

$$S_{\text{nl}}[\chi^\alpha_\eta] = \frac{\eta}{3} \int dr_1 dr_2 dr_3 \Gamma^{\text{clclq}}_{3,\eta}(r_1, r_2, r_3) \partial_\eta \chi^{\text{cl}}_\eta(r_1) \partial_\eta \chi^{\text{cl}}_\eta(r_2) \partial_\eta \chi^{\text{q}}_\eta(r_3) \,, \qquad (2.39)$$

where the vertex is,

$$\Gamma_{3,\eta}^{\text{clclq}}(r_1, r_2, r_3) = G_\eta^{\text{R}}(r_1 - r_2)G_\eta^{\text{K}}(r_2 - r_3)G_\eta^{\text{R}}(r_3 - r_1)$$

$$+ G_\eta^{\text{K}}(r_1 - r_2)G_\eta^{\text{A}}(r_2 - r_3)G_\eta^{\text{R}}(r_3 - r_1)$$

$$+ G_\eta^{\text{A}}(r_1 - r_2)G_\eta^{\text{A}}(r_2 - r_3)G_\eta^{\text{K}}(r_3 - r_1)\,.$$

To calculate the vertex we Fourier transform,

$$-\frac{i\eta}{3} \int dQ_1 dQ_2\, \Gamma_{3,\eta}^{\text{clclq}}(Q_1, Q_2)(\omega_1 - \eta c q_1)\chi_\eta^{\text{cl}}(Q_1)(\omega_2 - \eta c q_2)\chi_\eta^{\text{cl}}(Q_2)$$

$$\times (\omega_1 + \omega_2 - \eta c(q_1 + q_2))\chi_\eta^{\text{q}}(-Q_1 - Q_2)\,,$$

where we use the shorthand notation $Q_i = (q_i, \omega_i)$ and,

$$\Gamma_{3,\eta}^{\text{clclq}}(Q_1, Q_2) = \int \frac{dk}{2\pi}\frac{d\varepsilon}{2\pi} \left[G_\eta^{\text{R}}(K)G_\eta^{\text{K}}(K + Q_1)G_\eta^{\text{R}}(K + Q_1 + Q_2) \right.$$

$$+ G_\eta^{\text{K}}(K)G_\eta^{\text{A}}(K + Q_1)G_\eta^{\text{R}}(K + Q_1 + Q_2)$$

$$\left. + G_\eta^{\text{A}}(K)G_\eta^{\text{A}}(K + Q_1)G_\eta^{\text{K}}(K + Q_1 + Q_2) \right]\,.$$

Integrating over ε we have,

$$\Gamma_{3,\eta}^{\text{clclq}}(Q_1, Q_2) =$$
$$= -i \int \frac{dk}{2\pi} \left[-\frac{\tanh(\varepsilon_\eta(k + q_1)/2T)}{[\omega_1 - \varepsilon_\eta(k + q_1) + \varepsilon_\eta(k)][\omega_2 - \varepsilon_\eta(k + q_1 + q_2) + \varepsilon_\eta(k + q_1)]} \right.$$
$$+ \frac{\tanh(\varepsilon_\eta(k)/2T)}{[\omega_1 - \varepsilon_\eta(k + q_1) + \varepsilon_\eta(k)][\omega_1 + \omega_2 - \varepsilon_\eta(k + q_1 + q_2) + \varepsilon_\eta(k)]}$$
$$\left. + \frac{\tanh(\varepsilon_\eta(k + q_1 + q_2)/2T)}{[\omega_2 - \varepsilon_\eta(k + q_1 + q_2) + \varepsilon_\eta(k + q_1)][\omega_1 + \omega_2 - \varepsilon_\eta(k + q_1 + q_2) + \varepsilon_\eta(k)]} \right]\,,$$

where $\varepsilon_\eta(k) = \eta c k + k^2/2m$. We split the first term using the identity $1/ab = (1/a + $

$1/b)/(a + b)$ and get

$$\Gamma_{3,\eta}^{\text{clclq}}(Q_1, Q_2) =$$
$$= i \int \frac{dk}{2\pi} \left[\frac{\tanh(\varepsilon_\eta(k + q_1)/2T) - \tanh(\varepsilon_\eta(k)/2T)}{[\omega_1 - \varepsilon_\eta(k + q_1) + \varepsilon_\eta(k)][\omega_1 + \omega_2 - \varepsilon_\eta(k + q_1 + q_2) + \varepsilon_\eta(k)]} \right.$$
$$\left. - \frac{\tanh(\varepsilon_\eta(k + q_1 + q_2)/2T) - \tanh(\varepsilon_\eta(k + q_1)/2T)}{[\omega_2 - \varepsilon_\eta(k + q_1 + q_2) + \varepsilon_\eta(k + q_1)][\omega_1 + \omega_2 - \varepsilon_\eta(k + q_1 + q_2) + \varepsilon_\eta(k)]} \right].$$

We expand the integral up to the second power in the small spectrum curvature, m^{-1}, which, as we saw previously, is equivalent to a small momentum expansion, $q \ll k_\text{F}$. This expansion is convergent term by term and the first two are calculated more rigorously in Appendix B using the Matsubara formalism. As the vertices are symmetric for the exchange of external legs, we consider only their symmetrised part. The zero order symmetrised term in $1/m$ is zero, consistent with the Dzyaloshinski-Larkin theorem. Up to the third order we have,

$$\Gamma_{3,\eta}^{\text{clclq}}(Q_1, Q_2) = -\frac{i\eta}{2\pi m} \frac{q_1 q_2 (q_1 + q_2)}{(\omega_1 - \eta c q_1)(\omega_2 - \eta c q_2)(\omega_1 + \omega_2 - \eta c(q_1 + q_2))} + \mathcal{O}\left(m^{-3}\right).$$

This result is already symmetric and does not need symmetrisation. We also multiplied by a factor 3, as there are three ways of choosing the quantum field in Eq. (2.38). We note the absence of the second order term in m^{-1}. Then, Eq. (2.39) becomes,

$$iS_{\text{nl}}[\chi_\eta^\alpha] \approx \frac{1}{2\pi m} \int dQ_1 dQ_2 \, q_1 \chi_\eta^{\text{cl}}(Q_1) q_2 \chi_\eta^{\text{cl}}(Q_2)(q_1 + q_2)\chi_\eta^{\text{q}}(-Q_1 - Q_2).$$

Taking the Fourier transform we have,

$$S_{\text{nl}}[\chi_\eta^\alpha] = -\frac{1}{2\pi m} \int dr \left(\chi_\eta'^{\text{cl}}(r)\right)^2 \chi_\eta'^{\text{q}}(r), \tag{2.40}$$

and adding this term to the quadratic part of the action in partition function (2.30), we

have,

$$Z[u] = \int \mathcal{D}\chi_\pm \exp i \int dr \left[\frac{1}{2} \chi_\eta^\alpha D_{\eta\eta'}^{-1} \chi_{\eta'\alpha} - \frac{1}{2\pi m} \left(\chi_\eta^{\prime cl} \right)^2 \chi_\eta^{\prime q} - \frac{1}{\pi} \chi_\eta^{\prime \alpha} u_{\eta\alpha} \right] .$$

Moreover, in $\theta - \phi$ representation the non-linear term (2.40) becomes,

$$S_{nl}[\theta^\alpha, \phi^\alpha] = -\frac{1}{\pi m} \int dr \left\{ \left[\left(\theta^{\prime cl}(r) \right)^2 + \left(\phi^{\prime cl}(r) \right)^2 \right] \theta^{\prime q}(r) + 2\theta^{\prime cl}(r)\phi^{\prime cl}(r)\phi^{\prime q}(r) \right\} . \quad (2.41)$$

For the chiral fields, $\chi_\pm$, and the phase fields, θ and ϕ, the mass curvature, m^{-1}, is the parameter that control the interaction. Then, as discussed in the last subsection, we consider m^{-1} as a parameter that is zero in the infinite past and is adiabatically switched on with time.

The three-leg correction, being proportional to the mass curvature, is smaller and smaller the closer we are to the Fermi points or the smaller the cut-off, q_0, is, as can be understood by Fig. 2.6. This fact, however, does not exclude the presence of higher non-linear terms, such as the four-leg diagram in Fig. 2.5. To exclude them, we have to show that higher non-linear terms are smaller than the three-leg term in the mass curvature. We do this in Appendix B and show that, calling $\widetilde{\Gamma}_{n,\eta}$ the symmetrised n-leg vertex, we have $\widetilde{\Gamma}_3 = \mathcal{O}(m^{-1})$, $\widetilde{\Gamma}_4 = \mathcal{O}(m^{-2})$ and $\widetilde{\Gamma}_5 = \mathcal{O}(m^{-3})$. Moreover, the first non-zero terms in powers of m^{-1}, respectively proportional to m^{-1}, m^{-2} and m^{-3}, are temperature independent. These results prompt the following conjecture:

1. $\widetilde{\Gamma}_n = \mathcal{O}(m^{-(n-2)})$ for $m^{-1} \to 0$;

2. $\widetilde{\Gamma}_n$ does not depend on temperature at the lowest order in m^{-1}, that is, $m^{-(n-2)}$.

Moreover, this conjecture is supported by a dimensional analysis of the n-loop: if momenta and energies are rescaled by mv_F and mv_F^2 and made dimensionless, the n-loop behaves as $\widetilde{\Gamma}_n \sim (mv_F^2)^{-(n-2)}$. Within this conjecture, successive terms of series (2.22), given by fermionic loops with an increasing number of phononic external legs as in Fig. 2.5, are smaller and smaller in the spectrum curvature or closer to the Fermi points, justifying the

dropping of loops with more than three legs for small momenta.

2.2 Boson hydrodynamics

In the previous section we derived a low-energy hydrodynamic description of weakly interacting fermionic particles in one dimension using the technique of functional bosonization. In this section, we derive the low-energy hydrodynamic description of bosonic particles with repulsive contact interaction in the limits of weak and strong interaction.

The Lagrangian of the system is,

$$L\left[\bar{\varphi}, \varphi\right] = \int \mathrm{d}x \left[\bar{\varphi}\left(\mathrm{i}\partial_t + \frac{1}{2m}\partial_x^2 + \mu\right)\varphi - \frac{g}{2}(\bar{\varphi}\varphi)^2\right], \tag{2.42}$$

where $\varphi(x,t)$ is the bosonic particle field, m is the mass of the particle, μ the chemical potential and g the interaction strength of the density-density interaction. The system described by Lagrangian (2.42) is homogeneous as it is not subject to any external potential. Then, we consider the mean homogeneous density of the system, n, and distinguish two cases [40, 29]:

1. Weak interaction or high density, $mg \ll n$;

2. Strong interaction or low density, $mg \gg n$ (Tonks-Girardeau gas);[6]

We start from the simpler case of weak interaction.

2.2.1 Weak interactions

For weak interactions or high density, it is useful to introduce the healing length, $\xi = \frac{1}{2\sqrt{mgn}}$, the characteristic length of the interacting system. The number of particles within a healing length is $n\xi = \frac{1}{2}\sqrt{\frac{n}{mg}} \propto \sqrt{n}$ and increases with density. At high densities, there are many particles in a healing length, satisfying the criterion for the applicability of the mean

---

[6]Reintroducing $\hbar$, the left and right terms in the inequalities read $\hbar n$ and $mg/\hbar$. Setting $\hbar = 1$, n and mg have the dimensions of a momentum.

field theory [29]. Then, the dominant contribution to the functional integral is the mean field solution $\varphi = \bar{\varphi} = \sqrt{n}$ and minimisation of the energy $H[\bar{\varphi}, \varphi] = \int \mathrm{d}x\, \bar{\varphi} \mathrm{i} \partial_t \varphi - L[\bar{\varphi}, \varphi]$ gives the condition,

$$\mu = gn\,. \tag{2.43}$$

Now we consider small fluctuations of the bosonic field, φ, around its mean value, $\sqrt{n}$. To do this, we write the bosonic field using the phase-density representation,

$$\varphi(x,t) = \sqrt{n + \rho(x,t)} e^{i\phi(x,t)}\,, \tag{2.44}$$

where ρ and ϕ are small density and phase fluctuations. Substituting phase-density representation (2.44) in Lagrangian (2.42) we find,

$$L[\rho, \phi] = \int \mathrm{d}x\, \left[-\rho \partial_t \phi - \frac{n}{2m} \left(\partial_x \phi \right)^2 - \frac{g}{2} \rho^2 - \frac{1}{2m} \rho \left(\partial_x \phi \right)^2 - \frac{1}{8m} \frac{\left(\partial_x \rho \right)^2}{n + \rho} \right]\,, \tag{2.45}$$

where we omitted constant and boundary terms. The last term is called quantum pressure and accounts for quantum effects. As we consider small density fluctuations, ρ, that is, fluctuations with size greater than the healing length, the quantum pressure can be neglected [29]. Comparing this hydrodynamic Lagrangian with Hamiltonian (2.1), the compressibility of the system is $\kappa = 1/gn^2$ and, as one would expect, it is harder to compress the system when the repulsion is stronger or the density is higher. Expressing the density in term of the phase θ, as $\rho = \frac{1}{\pi} \partial_x \theta$, the Lagrangian becomes,

$$L[\theta, \phi] = \int \mathrm{d}x\, \left[-\frac{1}{\pi} \partial_x \theta \partial_t \phi - \frac{n}{2m} \left(\partial_x \phi \right)^2 - \frac{g}{2\pi^2} (\partial_x \theta)^2 - \frac{1}{2m\pi} \partial_x \theta \left(\partial_x \phi \right)^2 \right]\,,$$

where the first three terms are the linear part and the last term the non-linear part. Integrating by parts we have,

$$L[\theta, \phi] = \int \mathrm{d}x\, \frac{1}{2} \begin{pmatrix} \theta \\ \phi \end{pmatrix}^{\mathrm{T}} \begin{pmatrix} \frac{c}{\pi K} \partial_x^2 & \frac{1}{\pi} \partial_t \partial_x \\ \frac{1}{\pi} \partial_t \partial_x & \frac{cK}{\pi} \partial_x^2 \end{pmatrix} \begin{pmatrix} \theta \\ \phi \end{pmatrix} - \int \mathrm{d}x\, \left[\frac{1}{2m\pi} \partial_x \theta \left(\partial_x \phi \right)^2 \right]\,, \tag{2.46}$$

59

where,

$$c = \sqrt{\frac{ng}{m}},$$
$$\frac{K}{\pi} = \sqrt{\frac{n}{mg}}, \qquad (2.47)$$

are the speed of sound and the Luttinger parameter. Finally, we consider the action $S[\theta, \phi] = \int_{\rightleftarrows} dt L[\theta, \phi]$ and perform a Keldysh rotation to find the hydrodynamic action: the linear part is the same as the fermionic one, Eq. (2.34); however, the non-linear part does not contain the term cubic in $\partial_x \theta$, present in the fermionic case, Eq. (2.41).

2.2.2   Strong interactions

In the case of strong interaction or low density, the system becomes a Tonks-Girardeau gas of hard-core bosons [41, 42]. The partition function can be written as

$$Z = \int \mathcal{D}[\bar{\varphi}, \varphi] e^{i \int dt dx \left[\bar{\varphi} \left(i \partial_t + \frac{1}{2m} \partial_x^2 + \mu \right) \varphi - \frac{g}{2} \bar{\varphi}^2 \varphi^2 \right]}$$

$$= \int \mathcal{D}[\bar{\varphi}, \varphi] e^{i \int dt dx \left[\bar{\varphi} \left(i \partial_t + \frac{1}{2m} \partial_x^2 + \mu \right) \varphi \right]} \int \mathcal{D}[\bar{\xi}, \xi] e^{i \int dt dx \left[\frac{2}{g} \bar{\xi} \xi + \xi \bar{\varphi}^2 + \bar{\xi} \varphi^2 \right]},$$

where in the second line we introduced the field ξ through a Hubbard-Stratonovich transformation. The last term in the limit $mg \gg n$ becomes,

$$\int \mathcal{D}[\bar{\xi}, \xi] e^{i \int dt dx \left[\frac{2}{g} \bar{\xi} \xi + \xi \bar{\varphi} \bar{\varphi} + \bar{\xi} \varphi \varphi \right]} \approx \int \mathcal{D}[\bar{\xi}, \xi] e^{i \int dt dx \left[\xi \bar{\varphi} \bar{\varphi} + \bar{\xi} \varphi \varphi \right]} =$$

$$= \delta(\mathrm{Re}(\varphi^2)) \delta(\mathrm{Im}(\varphi^2))$$

$$= \delta(\bar{\varphi}^2) \delta(\varphi^2),$$

which imposes the constraint $\varphi(x)\varphi(x) = \bar{\varphi}(x)\bar{\varphi}(x) = 0$, that is, two bosons cannot be at the same position.[7] The partition function simplifies to

$$Z = \int \mathcal{D}[\bar{\varphi}, \varphi]\delta(\bar{\varphi}^2)\delta(\varphi^2)e^{i\int dtdx\left[\bar{\varphi}\left(i\partial_t + \frac{1}{2m}\partial_x^2 + \mu\right)\varphi\right]}. \qquad (2.48)$$

The constraint means that the boson fields anti-commute at the same position, $[\varphi(x), \varphi(x)]_- = 2\varphi(x)\varphi(x) = 0$, and commute at different positions, $[\varphi(x), \varphi(x')]_+ = 0$, $x \neq x'$. The anti-commutation property suggests to change the bosonic complex fields $\varphi(x)$ and $\bar{\varphi}(x)$ to the fermionic Grassmann fields $\psi(x)$ and $\bar{\psi}(x)$. Through the anti-commutativity of the fermions, the constraint $\varphi(x)\varphi(x) = \psi(x)\psi(x) = 0$ is automatically satisfied. However, the change of variables must respect the commutativity $[\varphi(x), \varphi(x')] = 0$ for $x \neq x'$. In other words, moving a boson through other bosons must not produce any change of sign. However, moving a fermion through an odd number of fermions produces a minus sign. This minus sign can be compensated by a phase factor through a Jordan-Wigner transformation [14],

$$\varphi(x) = \psi(x)e^{i\pi\int_{-\infty}^x dy\,\bar{\psi}(y)\psi(y)} \qquad (2.49)$$

The integral at the exponent, $\int_{-\infty}^x dy\,\bar{\psi}(y)\psi(y) = \int_{-\infty}^x dy\sum_{j\in\text{particles}}\delta(y - y_j)$, counts the number of particles at the left of position x. Therefore, the minus sign coming from moving a fermion through an odd number of fermions is compensated by the one coming from the phase factor. Substituting Eq. (2.49) into partition function (2.48) and using the Grassmann variable identities, $\psi^2 = \bar{\psi}^2 = 0$, we obtain

$$Z = \int \mathcal{D}[\bar{\psi}, \psi]e^{i\int dtdx\left[\bar{\psi}\left(i\partial_t + \frac{1}{2m}\partial_x^2 + \mu\right)\psi\right]}$$

---

[7]Note that, alternatively, the interaction term can be split as $\int \mathcal{D}\varrho e^{i\int dtdx\left[\frac{1}{2g}\varrho^2 + \varrho\bar{\varphi}\varphi\right]}$, which, in the limit $mg \gg n$, would lead to the constraint $\bar{\varphi}(x)\varphi(x) = 0$. However, this imposes that the density is zero or, in other words, that there are no particles in the system. Having no particles in the system implies that no two bosons are at the same position, but the constraint that two bosons cannot be at the same position does not imply that there are no particles in the system. Therefore, for a more general constraint we need the weaker condition, that is, two bosons cannot be at the same position.

This shows that a system of strongly-interacting or hard-core bosons can be mapped to a system of free fermions. As a consequence, the chemical potential corresponds to the ground state energy of a system of fermions with density n, that is, $\mu = (\pi n)^2/2m = \varepsilon_{\mathrm{F}}$. It follows that the Tonks-Girardeau gas of hard-core bosons is mapped into the Tomonaga-Luttinger liquid with,

$$c = v_{\mathrm{F}} = \frac{\pi n}{m}\,,$$
$$K = 1\,. \tag{2.50}$$

2.3   Refermionisation

In this chapter we have derived the low energy hydrodynamic theory, Eq. (2.3), starting from interacting fermionic and bosonic particles. In the case of weakly interacting fermions, the speed of sound, c, and the Luttinger parameter, K, are given by Eqs. (2.35) and the coefficient characterising the cubic density non-linearity is $\alpha = \pi^2/m$. In the case of weakly interacting bosons, c and K are given by Eqs. (2.47) and $\alpha = 0$. Instead, we saw that strongly interacting bosons behave like free fermions, leading to c and K given by Eqs. (2.50) and $\alpha = \pi^2/m$. Corresponding to the quadratic part of hydrodynamic Hamiltonian (2.3) are action (2.34) for fermions and the quadratic part of action (2.46) for bosons. These actions are not diagonal and it would be interesting to know what the excitations of the systems are by diagonalising them. First, we rescale the phase fields θ and ϕ to the effective phase fields $\tilde{\theta}$ and $\tilde{\phi}$ as $\theta = \sqrt{K}\,\tilde{\theta}$ and $\phi = \tilde{\phi}/\sqrt{K}$ and the quadratic part of the action becomes,

$$S_0[\tilde{\theta}^\alpha, \tilde{\phi}^\alpha] = \int \mathrm{d}r \left[\begin{pmatrix} \tilde{\theta}^\alpha \\ \tilde{\phi}^\alpha \end{pmatrix}^{\mathrm{T}} \begin{pmatrix} \frac{c}{\pi}\partial_x^2 & \frac{1}{\pi}\partial_t\partial_x \\ \frac{1}{\pi}\partial_t\partial_x & \frac{c}{\pi}\partial_x^2 \end{pmatrix} \begin{pmatrix} \tilde{\theta}_\alpha \\ \tilde{\phi}_\alpha \end{pmatrix} - \begin{pmatrix} \frac{2\sqrt{K}}{\pi}\partial_x\tilde{\theta}^\alpha \\ \frac{2}{\pi\sqrt{K}}\partial_x\tilde{\phi}^\alpha \end{pmatrix} \begin{pmatrix} u_{\theta\alpha} \\ u_{\phi\alpha} \end{pmatrix} \right].$$

This action is equal in form to the hydrodynamic action of non-interacting fermions with a renormalised Fermi velocity c and a rescaled coupling to the source fields. Since the action of non-interacting fermions is diagonal in the chiral fields representation, the action

is diagonalised by a transformation to the effective chiral fields $\tilde{\chi}_\pm = \tilde{\theta} \pm \tilde{\phi}$,

$$S_0[\tilde{\chi}_\eta^\alpha] = \int \mathrm{d}r \left[\frac{1}{2} \tilde{\chi}_\eta^\alpha \tilde{D}_{0,\eta}^{-1} \tilde{\chi}_{\eta\alpha} - \frac{2\sqrt{K}}{\pi} \partial_x (\tilde{\chi}_+^\alpha + \tilde{\chi}_-^\alpha) u_{\theta\alpha} - \frac{2}{\pi\sqrt{K}} \partial_x (\tilde{\chi}_+^\alpha - \tilde{\chi}_-^\alpha) u_{\phi\alpha} \right],$$

where,

$$\tilde{D}_{0,\eta}^{-1}(r) = \frac{\eta}{\pi} \partial_x (\partial_t + \eta c \partial_x), \tag{2.51}$$

is the inverse propagator (2.29) with a renormalised sound velocity, c. Now we turn to the non-linear part of the action.

The non-linear terms are different for fermions and bosons. We start with fermions. In terms of the rescaled fields $\tilde{\theta}$ and $\tilde{\phi}$, the non-linear part of the fermionic hydrodynamic action, Eq. (2.41), becomes,

$$S_{\mathrm{nl}}[\tilde{\theta}^\alpha, \tilde{\phi}^\alpha] = -\frac{1}{\pi m} \int \mathrm{d}r \left\{ \left[K(\tilde{\theta}'^{\mathrm{cl}})^2 + \frac{1}{K}(\tilde{\phi}'^{\mathrm{cl}})^2 \right] \sqrt{K} \tilde{\theta}'^{\mathrm{q}} + \frac{2}{\sqrt{K}} \tilde{\theta}'^{\mathrm{cl}} \tilde{\phi}'^{\mathrm{cl}} \tilde{\phi}'^{\mathrm{q}} \right\},$$

and in terms of the effective chiral fields, $\tilde{\chi}_\pm$, we have,

$$\begin{aligned}
S_{\mathrm{nl}}[\tilde{\chi}_\eta^\alpha] = &-\frac{1}{2\pi m^*} \int \mathrm{d}r \, (\tilde{\chi}_\eta'^{\mathrm{cl}})^2 \tilde{\chi}_\eta'^{\mathrm{q}} \\
&+ \frac{1}{8\pi m} \frac{1}{\sqrt{K}} \left(1 - K^2 \right) \int \mathrm{d}r \left[(\tilde{\chi}_{\bar{\eta}}'^{\mathrm{cl}})^2 + 2\tilde{\chi}_{\bar{\eta}}'^{\mathrm{cl}} \tilde{\chi}_\eta'^{\mathrm{cl}} \right] \tilde{\chi}_\eta'^{\mathrm{q}},
\end{aligned} \tag{2.52}$$

where $\bar{\eta}$ is the opposite of η and we defined the effective mass,

$$m^* = m \frac{4\sqrt{K}}{3 + K^2} \approx m \left(1 - \frac{3}{8} \delta K^2 \right) \tag{2.53}$$

where we expanded the Luttinger parameter in the weak interaction limit, $K = 1 + \delta K$ with $\delta K \ll 1$.

In the case of weakly interacting bosons, the non-linear part in Eq. (2.46) does not have the density-cube term, $\sim \theta'^3$, present in the fermionic one, Eq. (2.41). Rescaling the

fields, Eq. (2.46) becomes,

$$S_{\mathrm{nl}}[\tilde{\theta}^\alpha, \tilde{\phi}^\alpha] = -\frac{1}{\pi\sqrt{K}m} \int \mathrm{d}r \left\{ (\tilde{\phi}'^{\mathrm{cl}})^2 \tilde{\theta}'^{\mathrm{q}} + 2\tilde{\theta}'^{\mathrm{cl}}\tilde{\phi}'^{\mathrm{cl}}\tilde{\phi}'^{\mathrm{q}} \right\},$$

and in terms of $\tilde{\chi}_\pm$ we have,

$$\begin{aligned}
S_{\mathrm{nl}}[\tilde{\chi}_\eta^\alpha] &= -\frac{1}{2\pi m^*} \int \mathrm{d}r\, (\tilde{\chi}_\eta'^{\mathrm{cl}})^2 \tilde{\chi}_\eta'^{\mathrm{q}} \\
&\quad + \frac{1}{8\pi m}\frac{1}{\sqrt{K}} \int \mathrm{d}r \left[(\tilde{\chi}_{\bar{\eta}}'^{\mathrm{cl}})^2 + 2\tilde{\chi}_{\bar{\eta}}'^{\mathrm{cl}}\tilde{\chi}_\eta'^{\mathrm{cl}} \right] \tilde{\chi}_\eta'^{\mathrm{q}}
\end{aligned} \tag{2.54}$$

where we defined the effective mass,

$$m^* = \frac{4}{3}m\sqrt{K}, \tag{2.55}$$

and we remind that for weakly interacting bosons $K \gg 1$.

In the non-linear actions (2.52) and (2.54) the first line describes interactions between effective chiral fields moving in the same directions, either $\eta = +1$ or $\eta = -1$; instead, the second line describes mixed interactions between right, $\eta = +1$, and left, $\eta = -1$, effective chiral fields. Since the interaction time between chiral fields moving in opposite directions is negligible compared to that of those moving in the same direction, we neglect the second lines of Eqs. (2.52) and (2.54). Then, the hydrodynamic partition functions for fermionic and bosonic particles have the same form,

$$Z[u] = \int \mathcal{D}\tilde{\chi}_\pm e^{\mathrm{i}\int \mathrm{d}r \left[\frac{1}{2}\tilde{\chi}_\eta^\alpha \tilde{D}_{0,\eta}^{-1}\tilde{\chi}_{\eta\alpha} - \frac{1}{2\pi m^*}\left(\tilde{\chi}_\eta'^{\mathrm{cl}}\right)^2 \tilde{\chi}_\eta'^{\mathrm{q}} - \frac{2\sqrt{K}}{\pi}\partial_x(\tilde{\chi}_+^\alpha + \tilde{\chi}_-^\alpha)u_{\theta\alpha} - \frac{2}{\pi\sqrt{K}}\partial_x(\tilde{\chi}_+^\alpha - \tilde{\chi}_-^\alpha)u_{\phi\alpha} \right]}. \tag{2.56}$$

Integrating over the quantum component of right and left chiral field we obtain, as seen in Chap. 1, the equations of motion for the classical component,

$$(\partial_t + \eta c \partial_x)\tilde{\chi}_\eta^{\mathrm{cl}} = -\frac{\eta}{2m^*}(\tilde{\chi}_\eta^{\mathrm{cl}})^2, \tag{2.57}$$

where we omitted the source fields. This equation of motion will be important in the next

chapter.

Partition function (2.56) looks like the partition function of bosonized free fermions with effective mass m^* and a different coupling to density and phase source fields u_θ and u_ϕ. Comparing the transformation between fermionic fields and chiral fields, Eq. (2.32), we transform to the effective fermionic fields $\bar{\tilde{\psi}}$ and $\tilde{\psi}$ as,[4]

$$\frac{1}{2\pi}\partial_x\tilde{\chi}_\eta \longleftrightarrow \bar{\tilde{\psi}}_\eta\tilde{\psi}_\eta\,.$$

Then, the effective chiral fields partition function, Eq. (2.56), corresponds to the effective fermions partition function,

$$Z[u] = \int \mathcal{D}\big[\bar{\tilde{\psi}}_\pm,\tilde{\psi}_\pm\big]e^{\mathrm{i}\int_{\rightleftarrows}\mathrm{d}r\left[\bar{\tilde{\psi}}_\eta(r)\tilde{G}_\eta^{-1}(r)\tilde{\psi}_\eta(r)-\sqrt{K}(\bar{\tilde{\psi}}_+\tilde{\psi}_++\bar{\tilde{\psi}}_-\tilde{\psi}_-)u_{\theta\alpha}-\frac{1}{\sqrt{K}}(\bar{\tilde{\psi}}_+\tilde{\psi}_+-\bar{\tilde{\psi}}_-\tilde{\psi}_-)u_{\phi\alpha}\right]}\,, \quad (2.58)$$

where the Green's functions is,

$$\tilde{G}_\eta^{-1}(r) = \mathrm{i}\partial_t + \eta\mathrm{i}c\partial_x + \frac{\partial_x^2}{2m^*}\,, \quad (2.59)$$

which leads to the spectrum,

$$\varepsilon_\eta(k) = \eta ck + \frac{k^2}{2m^*}\,. \quad (2.60)$$

The coupling to the source fields tells us that density and phase in terms of the effective fermions are $\sqrt{K}(\bar{\tilde{\psi}}_+\tilde{\psi}_++\bar{\tilde{\psi}}_-\tilde{\psi}_-)$ and $(\bar{\tilde{\psi}}_+\tilde{\psi}_+-\bar{\tilde{\psi}}_-\tilde{\psi}_-)/\sqrt{K}$. These relations together with Eqs. (2.58) and (2.59) are known as *refermionisation.* We do not prove it rigorously here and we refer to Refs. [43, 44, 45] for a rigorous derivation. As in the case of bosonization, for which the non-linearity of the spectrum must be small, $k \ll mv_{\mathrm{F}}$, for refermionisation to be possible the condition $k \ll m^*c$ must hold. An additional condition in the case of weakly interacting bosons requires $p \ll p_{\mathrm{G}}$, where $p_{\mathrm{G}} = (m/m^*)mc = 3mc/\sqrt{K}$ is the Ginzburg momentum [46, 47]. As $K \gg 1$ for weakly interacting bosons, this condition is restrictive. We leave the discussion of the Ginzburg momentum to Sec. 3.8. Finally, we note that fermionic quasiparticles are lighter than the initial particles, $m^* < m$, for
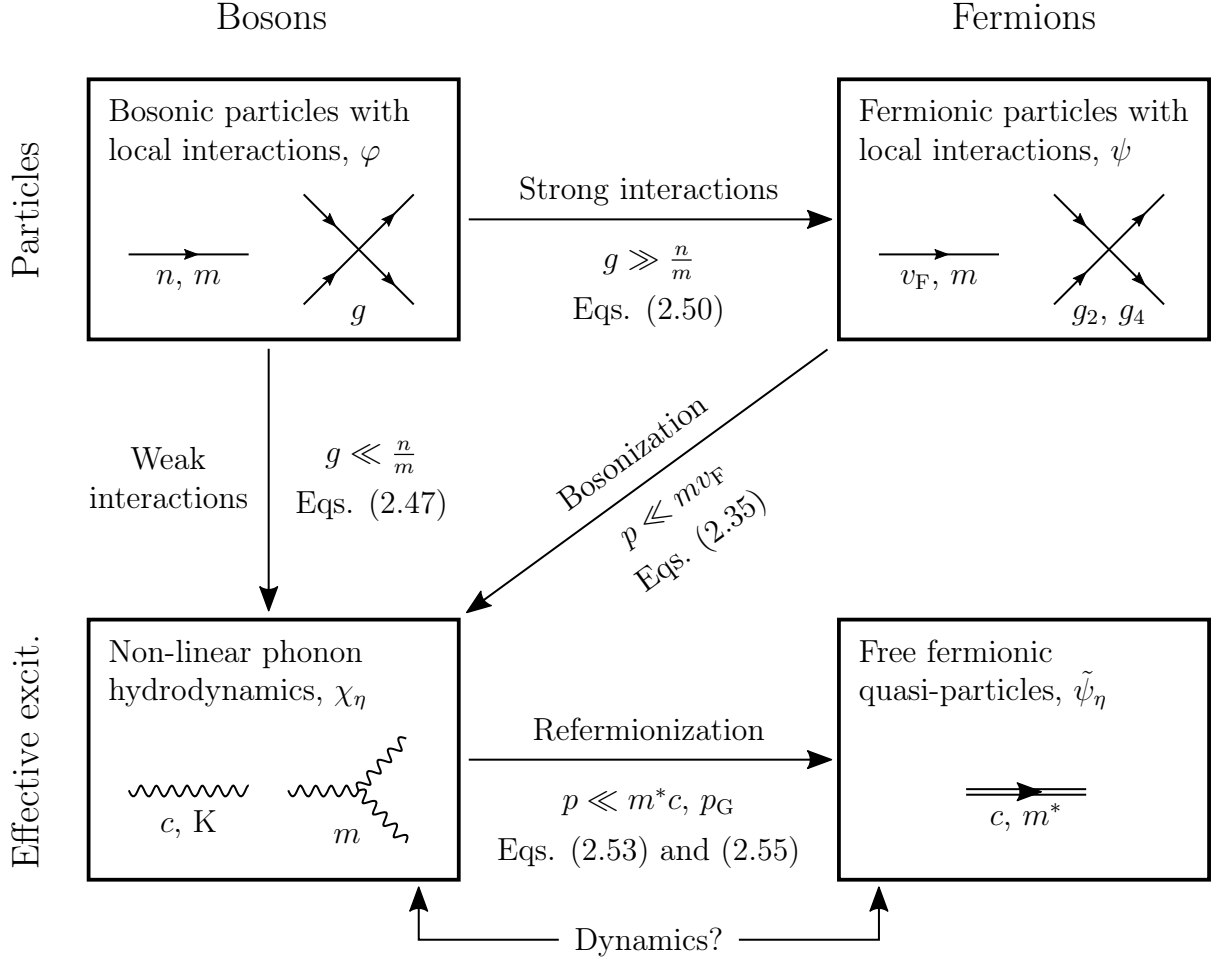
Figure 2.8: Schematic summary of the main results of the chapter. Left and right columns refer to bosonic and fermionic statistics and top and bottom rows to particles and effective excitations. The equation references give the relation between the parameters of the related theories.

interacting fermions and heavier, $m^* > m$, for weakly interacting bosons.

2.4 A paradox in one-dimensional dynamics

In this chapter we derived the low-energy hydrodynamic and the fermionic quasiparticle theories for interacting fermionic and bosonic particles. The relations between these theories are depicted in Fig. 2.8 with the help of Feynman diagrams. We started from fermions, the top-right box in Fig. 2.8. The fermionic theory is characterised by the propagator and the local density-density interaction term, represented by the straight line and the cross diagrams. The propagator depends on the Fermi velocity, $v_{\rm F}$, and mass,

m, and the interaction terms correspond to scattering with strengths g_2 and g_4 between two fermions. Using functional bosonization, we showed that the low-energy particle-hole excitations around the two Fermi points give rise to phononic excitations. The theory of phononic excitations is characterised by the two diagrams in the bottom-left box in Fig. 2.8. The wiggly line is the phonon propagator that depends on the speed of sound, c, and the Luttinger parameter, K. The three-leg diagram represents the non-linear contribution that comes from the mass curvature, m, of the fermionic spectrum and corresponds to the three-loop of Fig. 2.5. This non-linear term, as suggested by the diagram, corresponds to the processes of splitting a phonon into two or recombining two into one. Additional non-linear terms with more legs are present, but can be neglected for small momenta, $p \ll m v_{\mathrm{F}}$. Then, we considered bosonic particles with contact interactions, the top-left box in Fig. 2.8. The bosonic theory is characterised by the propagator and the contact density-density interaction term, represented by the straight line and the cross diagrams. The propagator depends on the density, n, and mass, m, and the interaction term corresponds to the scattering with strength g between two bosons. We considered the two limits of weak and strong interactions. In the case of weak interactions, $g \ll \frac{n}{m}$, a the hydrodynamic theory was derived in terms of density and phase fluctuations over the average values. In the case of strong interactions, $g \gg \frac{n}{m}$, bosons become impenetrable, a feature that allows the mapping to free fermions and, in turn, to the hydrodynamic theory with $K = 1$. Finally, we mapped the non-linear hydrodynamic theory to free fermionic quasiparticles with an effective Fermi velocity c and an effective mass m^*, the bottom-right box in Fig. 2.8. The mapping requires the additional low-momentum condition $p \ll m^* c$ and in the case of weakly interacting bosons the additional condition $p \ll p_{\mathrm{G}} \sim 1/\sqrt{K}$.

Non-linear phonons and free fermionic quasiparticles are equally good at describing static properties [7]. However, this is not the case for dynamical ones. In fact, to realise this, it is sufficient to compare the dynamical structure factor, $S(q, \omega)$, calculated using the two representations. We have already calculated $S(q, \omega)$ using free fermions and the result is represented in Fig. 2.3. In the case of fermionic quasiparticles, Fermi velocity,

v_{F}, and mass, m, are replaced by c and m^* but the width depends on q in the same way: $\delta\omega(q) \sim q^2$ at $T = 0$ and $\delta\omega_T(q) \sim q$ at $T > 0$. Using phonons, we start deriving the dynamical structure factor using the quadratic approximation. We do not need to do the calculation explicitly, we just need to know that the density structure factor is non-zero where the spectrum of particle-holes excitations is non-zero. Because the quadratic phonons approximation corresponds to fermions with linearised spectrum, there is no spectrum curvature and particle-hole excitations can only satisfy the relation $\omega = cq$. It follows that the density structure factor is a straight line with slope c and no width in the $q - \omega$ plane of Fig. 2.3. This result is in clear contrast with the one derived using fermionic quasiparticles. But we know that, when there are no interactions between fermions, particles and quasiparticles coincide, giving the correct result. Then, we may add the three-leg term to the quadratic phonons. With this term, the calculation of the width of the dynamical structure factor is not straightforward as it involves a self-consistent approach to avoid a resonant behaviour. We do not give the explicit calculation here and refer to Refs. [48, 49]. The resulting width is $\delta\omega(q) \sim q^2$ at $T = 0$ and $\delta\omega_T(q) \sim q^{3/2}$ at $T > 0$. Now, fermionic quasiparticles and phonons give the same result at $T = 0$ but differ at $T > 0$: even with the three-leg correction, the two representations lead to different thermal dynamics in the small-momentum limit, where the three-leg approximation should hold better. This leads to an apparent paradox: which one is the correct representation to describe the thermal dynamics of one-dimensional systems, non-linear phonons or free fermionic quasiparticles? We will answer this question in the next chapter.

Chapter 3

Thermal dynamics of one-dimensional systems

In this chapter we explore the thermal dynamics of non-linear phonons and fermionic quasiparticles and solve the apparent paradox raised in last chapter. We approach the problem by introducing a system of phononic and fermionic excitations that interact with each other. Phonons and fermions will represent long wavelength fluctuations and local excitations respectively, so that there is a scale separation assuring that they represent different entities of the system. We introduce fermionic quasiparticles using the concept of a depleton, developed in Ref. [50] to describe the dynamic of a single impurity in a one-dimensional system. A depleton is a quasiparticle constituted by an impurity together with the depletion cloud that it induces to the liquid. The peculiarity of the depleton approach is the ability to account for the changes induced by an impurity to the liquid. As we will see in detail in the chapter, a local excitation of the liquid can be modelled by a massless impurity, such that the depleton is just the depletion cloud characterising the excitation of the system. The advantage of this approach is that we can define the position of the excitation through the position of the massless impurity. This will allow us to second-quantise the system of a single depleton into a system of many depletons interacting with the phonons following the standard rules of second-quantisation. The depletons will

represent the fermionic quasiparticles derived in the previous chapter. Following Ref. [50], we will dedicate the first two sections of this chapter to the introduction of the single depleton theory. Then, we will proceed to the original part of this thesis (see Ref. [1] in the Publication section at the beginning of this thesis): we will extend the single depleton to a many-depleton picture and study the dynamics of phonons and depletons using the dynamical structure factor.

3.1 The depleton

In this section we consider a single impurity immersed in a liquid with Hamiltonian (2.1). The Hamiltonian of the liquid consists of a static part, given by the first term, and a dynamical part, given by the second term. We will start by considering a static liquid and later extend the results to the dynamics. The Lagrangian of the static liquid in thermodynamic equilibrium is the Legendre transform of the first term of Hamiltonian (2.1),

$$L_0(\mu) = \int \mathrm{d}x \, [\mu(n)n - e_0(n)] \,. \tag{3.1}$$

The Lagrangian does not depend explicitly on the density, n, because in thermodynamic equilibrium n is related to μ through $\partial_n e_0[n] = \mu$, as we saw at the beginning of Chap. 2. Now, we introduce an impurity of mass M at coordinate $X(t)$, moving with velocity $\partial_t X = V$ with respect to the liquid. To do so, we perform a Galilean transformation to a reference frame moving with velocity V with respect to the liquid, as shown in Fig. 3.1. Denoting with prime the quantities in the moving reference frame, the energy of the liquid transforms as $e_0'(n, V) = e_0(n) + \frac{1}{2}nV^2$, leading to the new Lagrangian,

$$L_0'(\mu', V) = \int \mathrm{d}x \, [\mu'(n, V)n - e_0'(n, V)] \,,$$
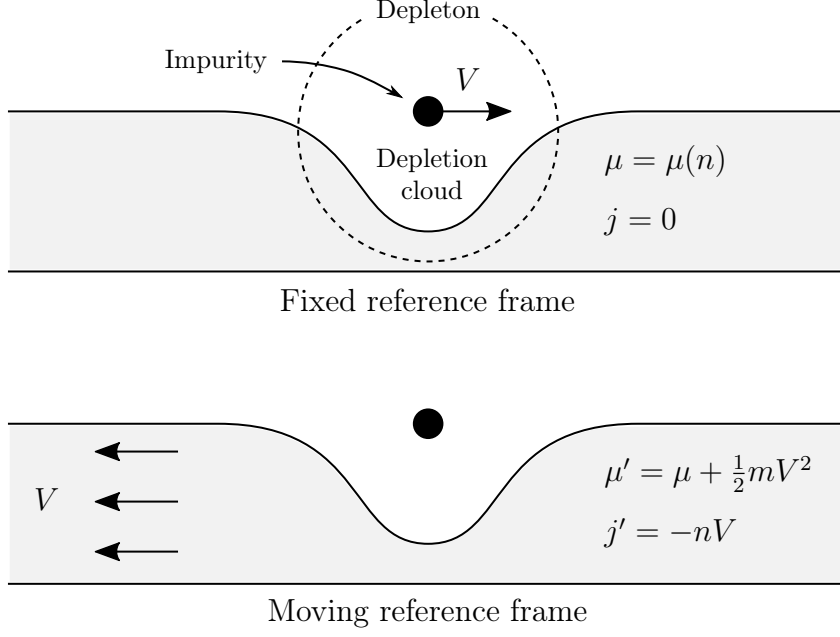
Figure 3.1: Galilean transformation from the fixed reference frame, where the liquid is static (top), to the reference frame moving with velocity V, where the particle is still (bottom). The height represents the density profile. The impurity generates a depletion of the liquid in its vicinity and the impurity together with the depletion cloud is the depleton.

where the chemical potential, μ', in the moving frame is related to μ as,

$$\mu'(n, V) = \mu(n) + \frac{1}{2}MV^2 \,. \tag{3.2}$$

In the moving frame, we immerse the impurity in the liquid. The impurity causes a depletion of the liquid in its vicinity that we call *depletion cloud*, as shown in Fig. 3.1. We account for this depletion using the number N_d of particles expelled from the liquid by the impurity. Moreover, the impurity experiences the flow of the fluid given by the supercurrent,

$$j' = -nV \,. \tag{3.3}$$

The total Lagrangian of the system is now the Lagrangian of the liquid, L'_0, plus the Lagrangian of the depletion cloud,

$$L'_D(n, V) = \mu'(n, V)N_D - E'_D \,, \tag{3.4}$$

71

where E'_{D} is the energy of the impurity in the moving frame and the Lagrangian depends on n and V through μ'.

We take advantage of the system being in thermodynamic equilibrium. To this end, we note that the right hand side of Lagrangian (3.1) coincides with minus the grand canonical thermodynamical potential of the liquid, $\Omega_0(\mu)$,

$$L_0(\mu) = -\Omega_0(\mu) .$$

Due to the Galilean invariance of the static liquid, in the moving frame we have the same equality, $L'_0(\mu', V) = -\Omega'_0(\mu', j')$, where we used relation (3.3) between V and j'. Then, the addition of the impurity Lagrangian, L'_d, to the liquid Lagrangian, L'_0, is seen as the change of the grand canonical potential of the liquid due to the presence of the impurity, $\Omega'_0(\mu', j') \to \Omega'_0(\mu', j') + \Omega'_{\mathrm{D}}(\mu', j')$, and we obtain the relation,

$$L'_{\mathrm{D}}(\mu', j') = -\Omega'_{\mathrm{D}}(\mu', j') . \tag{3.5}$$

As a consequence of the Galilean transformation, this equality relates the dynamics of the depletion of the liquid, the left hand side, with its thermodynamics, the right hand side. This relation is useful because we can study the change induced to the depletion cloud, $\mathrm{d}\Omega'_{\mathrm{D}}(\mu', j')$, by a change of the state of the liquid, $\mathrm{d}j'$ and $\mathrm{d}\mu'$,

$$
\begin{aligned}
&\mathrm{d}\Omega'_{\mathrm{D}}(\mu', j') = N\,\mathrm{d}\mu' + \Phi\,\mathrm{d}j', \\
&N = \partial_{\mu'}\Omega'_{\mathrm{D}}, \quad \Phi = \partial_{j'}\Omega'_{\mathrm{D}} .
\end{aligned}
\tag{3.6}
$$

Here, N is the response to a variation of the chemical potential μ' and is related by Eqs. (3.4) and (3.5) to the number of depleted particles as $N = -N_{\mathrm{d}}$. The response Φ to a change of the superfluid current, j', is the superfluid phase and has no analogy in classical thermodynamics. We are in the situation where we have linked the dynamics of the depletion cloud to its thermodynamics in terms of the independent equilibrium parameters,

μ' and j', characterising the liquid. Instead, the parameters characterising the depletion cloud, N and Φ, depend on μ' and j'. Since our final goal is to consider the effect of the liquid dynamics on the depletion cloud, instead of μ' and j', it is convenient to consider N and Φ as independent variables. This is achieved through a Legendre transformation to a new thermodynamic potential,

$$H_{\mathrm{D}}(\Phi, N) = \Omega_{\mathrm{D}}' - j'\Phi - \mu'N \,,$$

$$\mathrm{d}H_{\mathrm{D}}(\Phi, N) = -j'\mathrm{d}\Phi - \mu'\mathrm{d}N \,. \tag{3.7}$$

After this transformation, the independent variables N and Φ describe the state of the local depletion cloud around the impurity which may or may *not* be in equilibrium with imposed j' and μ'. In this way, by considering fluctuations of j' and μ', in the next section, we will be able to introduce the dynamics of the liquid. Putting Eqs. (3.4), (3.5) and (3.7) together, we find the Lagrangian,

$$L_{\mathrm{D}}' = \frac{1}{2}MV^2 - j'\Phi - \mu'N - H_{\mathrm{D}}(\Phi, N) \,, \tag{3.8}$$

and performing a Galilean transformation back to the liquid reference frame by means of Eqs. (3.2) and (3.3), we obtain,

$$L_{\mathrm{D}} = \frac{1}{2}(M - mN)V^2 + nV\Phi - \mu(n)N - H_{\mathrm{D}}(\Phi, N) \,. \tag{3.9}$$

This Lagrangian describes the impurity together with the induced depletion cloud, that is, a dressed impurity called *depleton* [50]. The depleton is shown by the dashed circle in Fig. 3.1.

In this chapter we will be interested, not in a single depleton, but in many of them. The standard procedure to go from a single to many depletons is second quantisation, for which it is convenient to recast Lagrangian (3.9) in a suitable form. First, we need the

momentum of the depleton,

$$P = \frac{\partial L}{\partial V} = (M - mN)V + n\Phi. \tag{3.10}$$

Here, $M - mN$, is the mass of the depleton, that is, the mass of the impurity minus the mass of the depleted particles and $n\Phi$ is the supercurrent momentum induced to the liquid by the impurity. Inverting Eq. (3.10) we find the velocity of the depleton in terms of its momentum,

$$\partial_t X = V = V(P, \Phi, N) = \frac{P - n\Phi}{M - mN}, \tag{3.11}$$

and substituting it into Eq. (3.9), the depleton Lagrangian takes the standard form,

$$L_{\mathrm{D}} = PV - H, \tag{3.12}$$

with Hamiltonian,

$$H(P, \Phi, N) = \frac{1}{2}\frac{(P - n\Phi)^2}{M - mN} + \mu N + H_{\mathrm{D}}(\Phi, N). \tag{3.13}$$

The Hamiltonian of the depleton depends on the impurity momentum and mass and on the depletion cloud phase and number of expelled particles.

When the impurity is initially immersed in the liquid, the depletion cloud is out of equilibrium. After some time, the cloud equilibrates to the values $\Phi = \Phi_0(P, n)$ and $N = N_0(P, n)$, for which the Hamiltonian becomes,

$$E(P, n) = H(P, \Phi_0(P, n), N_0(P, n)). \tag{3.14}$$

Here, $E(P, n)$ is the dispersion relation of the dressed impurity at equilibrium. The equilibrium values $\Phi_0(P, n)$ and $N_0(P, n)$ are an extremum of the Hamiltonian, that is,

they satisfy the following equations,

$$0 = -\partial_\phi H = nV - \partial_\phi H_d \,,$$

$$0 = -\partial_N H = -\mu - \frac{1}{2}mV^2 - \partial_N H_d \,,$$

(3.15)

where we used Eq. (3.11) for the velocity of the depleton. By differentiating both sides of Eq. (3.14) by P and N and using Eqs. (3.13) and (3.15), we find the equivalent equations for the equilibrium values $\Phi_0(P,n)$ and $N_0(P,n)$,

$$\partial_P E(P,n) = V_0(P,n) = \frac{P - n\Phi_0}{M - mN_0} \,,$$

$$\partial_n E(P,n) = \frac{mc^2}{n} N_0 - V_0(P,n)\Phi_0 \,,$$

(3.16)

that has to be solved for fixed P.

We conclude this section by connecting the depleton to the fermionic quasiparticles derived at the end of the last section. Those fermionic quasiparticles are excitations of the system associated to a depletion cloud without an external impurity. However, the concept of impurity turns out to be useful as it defines the position and velocity of the depleton. Having no impurity amounts to setting its mass to zero, $M = 0$. Given this connection, the equilibrium spectrum of the depleton is identified by Eq. (2.60) with,

$$E_\eta(P,n) = \eta c(n)P + \frac{P^2}{2m^*(n)} \,.$$

(3.17)

In the case of bosons, this spectrum would correspond, in the low energy limit, to localised excitations in the superfluid, such as grey solitons in Bose-Einstein condensates [51, 52]. The depleton picture equally applies to a foreign particle, for example an atom in a different hyperfine state considered in Refs. [53, 50].

3.2 Depleton-Phonon coupling

In the previous section, the liquid we considered was static, that is, we just considered the first term of Hamiltonian (2.1), constant in time and space. In this section, we introduce the dynamics of the liquid, that, in the case where no depleton was present, amounted to the second term of Hamiltonian (2.1). However, in presence of the depleton, the liquid and the depleton interact, giving rise to an additional term in the Lagrangian of our system. To find this interaction term, we consider a liquid that can fluctuate, which means that the density and velocity of the liquid considered in last section are modified as,

$$
\begin{aligned}
n &\rightarrow n + \rho\,, \\
V &\rightarrow V + v\,,
\end{aligned}
\tag{3.18}
$$

where, following the definitions in Eq. (2.2), $\rho = \frac{1}{\pi}\partial_x\theta$ and $v = \frac{1}{m}\partial_x\phi$ are the density and velocity phononic fluctuations. The fluctuations due to phonons have a size that is much larger compared to the depleton. As a consequence, the depleton experiences phonons as a temporary change of the liquid density and velocity, as shown in Fig. 3.2. However, in our formalism, as we see from Eq. (3.9), the depleton experiences the density and velocity of the liquid indirectly, through the chemical potential, μ', and supercurrent, j'. Then, we have to find the change to μ' and j' due to the density, ρ, and velocity, v, of phonons. For the change to the chemical potential due to phonons, we need the Lagrangian corresponding to the second term of Hamiltonian (2.1),

$$
\begin{aligned}
L_{\mathrm{Ph}}[\rho, v] &= \int \mathrm{d}x\,\left[-\rho\partial_t\phi - \frac{1}{2}m(n+\rho)v^2 - e_0(n+\rho) + \mu(n+\rho)\right] - \int \mathrm{d}x\,[\mu n - e_0(n)] \\
&= \int \mathrm{d}x\,\left[-(n+\rho)\partial_t\phi + n\partial_t\phi - \frac{1}{2}m(n+\rho)v^2 - e_0(n+\rho) + e_0(n) + \mu\rho\right]\,.
\end{aligned}
$$

From the factor multiplying $(n+\rho)$, we deduce that the chemical potential changes as,

$$
\mu \rightarrow \mu - \partial_t\phi - \frac{1}{2m}(\partial_x\phi)^2\,,
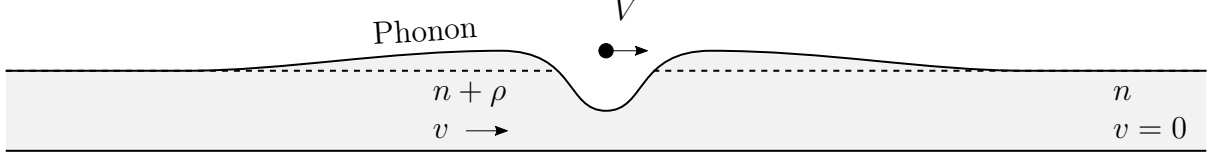$$

Figure 3.2: Depleton experiencing a phonon through a change of density and velocity of the liquid.

where we used the relation between velocity and phase, $v = \frac{1}{m}\partial_x\phi$. In the reference frame moving with velocity V, we have,

$$\mu' = \mu + \frac{m}{2}V^2 \rightarrow \mu - \partial_t\phi - \frac{1}{2m}(\partial_x\phi)^2 + \frac{m}{2}(V - \frac{1}{m}\partial_x\phi)^2 = \mu + \frac{m}{2}V^2 + \frac{d\phi}{dt}, \quad (3.19)$$

where we defined the total time derivative,

$$\frac{d}{dt} = \partial_t + V\partial_x.$$

The change induced by phonons to the supercurrent is found using substitution (3.18),

$$j' = -nV \rightarrow -\left(n + \frac{1}{\pi}\partial_x\theta\right)\left(V - \frac{1}{m}\partial_x\phi\right) = -nV - \frac{1}{\pi}\frac{d\theta}{dt}, \quad (3.20)$$

where we expressed density and velocity through the phase fields, θ and ϕ, and in the last equality we used the continuity equation in the form $\partial_t\theta/\pi = -(n + \rho)v$, following from the gauge invariance of the system [50]. Dynamic Eqs. (3.19) and (3.20) replace static Eqs. (3.2) and (3.3) for the chemical potential and supercurrent. Substituting Eqs. (3.19) and (3.20) into Lagrangian (3.8) we obtain Lagrangian (3.9) and the additional interaction term between depleton and liquid,

$$L_{\text{Ph-D}} = \frac{1}{\pi}\Phi\frac{d}{dt}\theta(X,t) + N\frac{d}{dt}\phi(X,t). \quad (3.21)$$

This Lagrangian provides the dynamics of the depletion cloud through the collective coordinates Φ and N. It also shows that the canonical momenta correspond respectively to the liquid density and velocity phases, $\theta(X,t)$ and $\phi(X,t)$, at the position of the impurity,

$X(t)$. It is convenient to express the interaction term, Eq. (3.21), in the effective chiral field representation, that follows from Eq. (2.33) and the relations at page 62,

$$
\begin{aligned}
\theta &= \sqrt{K}\,\frac{\tilde{\chi}_+ + \tilde{\chi}_-}{2}\,, \\
\phi &= \frac{1}{\sqrt{K}}\,\frac{\tilde{\chi}_+ - \tilde{\chi}_-}{2}\,.
\end{aligned}
\tag{3.22}
$$

Then, Eq. (3.21) becomes,

$$
L_{\text{Ph}-\text{D}}[\tilde{\chi}_\eta, \Lambda_\eta, X] = \Lambda_\eta \frac{\mathrm{d}}{\mathrm{d}t}\tilde{\chi}_\eta(X, t)\,,
\tag{3.23}
$$

where we defined the chiral collective variables of the depletion cloud,

$$
\Lambda_\eta = \frac{1}{2}\left(\frac{\sqrt{K}}{\pi}\Phi \pm \frac{1}{\sqrt{K}}N\right)\,.
\tag{3.24}
$$

With the interaction term between depleton and liquid, Eq. (3.23), we have completed the derivation of the Lagrangian of the system. In the following section we will extend the system of a single depleton to a system of many depletons.

3.3 Many depletons

Putting together the Lagrangians of phonons, depletons and the interaction term, the partition function in the closed time contour representation is,

$$
Z = \int \mathcal{D}\tilde{\chi}_\pm \mathcal{D}\Lambda_\pm \mathcal{D}X \mathcal{D}P\, e^{\mathrm{i}\int_{\rightleftarrows}\mathrm{d}t\left\{\sum_\eta L_{\text{Ph},\eta}[\tilde{\chi}_\eta]+L_{\text{D}}[X,P,\Lambda_\pm]+L_{\text{Ph}-\text{D}}[\tilde{\chi}_\eta,\Lambda_\eta,X]\right\}}\,.
\tag{3.25}
$$

The phononic Lagrangian before the Keldysh rotation is derived by Eq. (2.56),

$$
L_{\text{Ph},\eta}[\tilde{\chi}_\eta] = \int \mathrm{d}x \left[\frac{1}{4\pi}\tilde{\chi}_\eta\left(\eta\partial_t\partial_x + c\partial_x^2\right)\tilde{\chi}_\eta - \frac{1}{12\pi m^*}(\partial_x\tilde{\chi}_\eta)^3\right]\,,
\tag{3.26}
$$

where we dropped the source terms. The depleton Lagrangian in terms of $\Lambda_\pm$ is derived from Eqs. (3.12) and (3.13),

$$L_{\mathrm{D}}[X, P, \Lambda_\pm] = P\partial_t X - H[P, \Lambda_\pm],$$

where $H[P, \Lambda_\pm]$ is Hamiltonian (3.13) in terms of $\Lambda_\pm$.

As we saw in the previous section through Eq. (3.23), the presence of phonons affect the depletion cloud. Assuming that the change due to phonons is small, we expand $H(P, \Lambda_\pm)$ around the equilibrium values of the depletion cloud, $\Lambda_{0,\pm}$, obtained by Eqs. (3.16) and (3.24), as,

$$H(P, \Lambda_{0,\pm} + \delta\Lambda_\pm) \approx E(P) + 2\pi\,\delta\Lambda_\eta\,\Gamma^{-1}_{\eta\eta'}(P)\,\delta\Lambda_{\eta'}\,, \tag{3.27}$$

where the matrix $\Gamma^{-1}_{\eta\eta'}(P)$ is the Hessian,

$$\Gamma^{-1}_{\eta\eta'}(P) = \begin{pmatrix} \Gamma^{-1}_{++}(P) & \Gamma^{-1}_{+-}(P) \\ \Gamma^{-1}_{-+}(P) & \Gamma^{-1}_{--}(P) \end{pmatrix} = \frac{1}{4\pi}\begin{pmatrix} \partial^2_{\Lambda_+}H & \partial_{\Lambda_+}\partial_{\Lambda_-}H \\ \partial_{\Lambda_-}\partial_{\Lambda_+}H & \partial^2_{\Lambda_-}H \end{pmatrix}_{\Lambda_\pm = \Lambda_{0,\pm}}\,, \tag{3.28}$$

evaluated at constant P (see also Ref. [50]) and characterises the scattering rate of phonons by a moving impurity. Expanding the interaction term, Eq. (3.23), around the equilibrium values of the depletion cloud, $\Lambda_{0,\pm}$, and integrating over $\delta\Lambda_\pm$ in partition function (3.25), we obtain the effective Lagrangian of a depleton coupled to the bath of phonons,

$$L_{\mathrm{D}} + L_{\mathrm{Ph-D}} \to P\partial_t X - E(P) + \Lambda_{0,\eta}\frac{\mathrm{d}}{\mathrm{d}t}\tilde{\chi}_\eta(X, t) + \frac{1}{8\pi}\left(\frac{\mathrm{d}}{\mathrm{d}t}\tilde{\chi}_\eta(X, t)\right)\Gamma_{\eta\eta'}(P)\left(\frac{\mathrm{d}}{\mathrm{d}t}\tilde{\chi}_{\eta'}(X, t)\right). \tag{3.29}$$

Using the results obtained in Appendix C, $\Lambda_{0,\eta}(P)$ can be shown to be independent of P at small momenta, so that the third term on the right hand side of Eq. (3.29) is a total derivative and can be omitted. The full time derivative of phononic fields can be evaluated with the help of the equation of motion of the impurity, $\partial_t X = V(P)$, leading
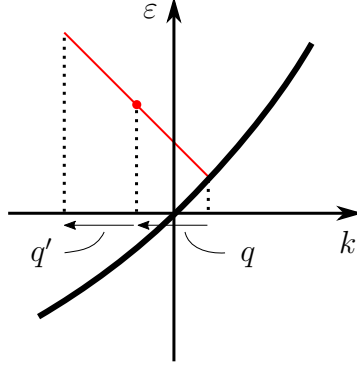
Figure 3.3: Conservation of momentum and energy for the scattering of a right moving depleton and a left moving phonon. The curved line represents the depleton spectrum and the straight line represents the phonon spectrum. The conservation of momentum and energy amounts to connecting two points of the depleton spectrum with two straight lines of the phonon spectrum and the only way of doing it is by having $q' = -q$.

to $\mathrm{d}\tilde{\chi}_\pm(X,t)/\mathrm{d}t \approx (\partial_t + V(P)\partial_x)\,\tilde{\chi}_\pm$. Then, Eq. (3.29) becomes,

$$L_{\mathrm{D}} + L_{\mathrm{Ph-D}} \to P\partial_t X - E(P) + \frac{1}{8\pi}\left(\partial_t + V(P)\partial_x\right)\tilde{\chi}_\eta\,\Gamma_{\eta\eta'}(P)\left(\partial_t + V(P)\partial_x\right)\tilde{\chi}_{\eta'}, \quad (3.30)$$

Considering a right moving impurity, $V(P) = c + P/m$, and evaluating the last term of Eq. (3.30) with the help of the linear equations of motion of phonons, $\partial_t\tilde{\chi}_\pm = \mp c\partial_x\tilde{\chi}_\pm$, we find

$$\frac{\mathrm{d}}{\mathrm{d}t}\tilde{\chi}_+\Gamma_{++}(P)\frac{\mathrm{d}}{\mathrm{d}t}\tilde{\chi}_+ = \left(\frac{P}{m^*}\right)^2\partial_x\tilde{\chi}_+\Gamma_{++}(P)\partial_x\tilde{\chi}_+,$$

$$\frac{\mathrm{d}}{\mathrm{d}t}\tilde{\chi}_-\Gamma_{-+}(P)\frac{\mathrm{d}}{\mathrm{d}t}\tilde{\chi}_+ = \frac{\mathrm{d}}{\mathrm{d}t}\tilde{\chi}_+\Gamma_{+-}(P)\frac{\mathrm{d}}{\mathrm{d}t}\tilde{\chi}_- = \left(\frac{P}{m^*}\right)\left(2c + \frac{P}{m^*}\right)\partial_x\tilde{\chi}_+\Gamma_{+-}(P)\partial_x\tilde{\chi}_-$$

$$\approx \frac{2c}{m^*}P\partial_x\tilde{\chi}_+\Gamma_{+-}(P)\partial_x\tilde{\chi}_-,$$

$$\frac{\mathrm{d}}{\mathrm{d}t}\tilde{\chi}_-\Gamma_{--}(P)\frac{\mathrm{d}}{\mathrm{d}t}\tilde{\chi}_- = \left(2c + \frac{P}{m^*}\right)^2\partial_x\tilde{\chi}_-\Gamma_{--}(P)\partial_x\tilde{\chi}_- \approx 4c^2\partial_x\tilde{\chi}_-\Gamma_{--}(P)\partial_x\tilde{\chi}_-,$$

$$(3.31)$$

where we have simplified the expression leaving only the leading terms in $P \ll m^*c$, the low momentum condition for the validity of refermionisation seen in Sec. 2.3. The first term, coupling right moving phonons, is quadratic and can be neglected in the small momentum limit. The second term, coupling phonons with different chiralities, has been approximated in the small momentum limit. The third term, corresponding to the scattering of a depleton moving to the right with a phonon moving to the left, does not contribute to

dynamical quantities because the corresponding scattering process is suppressed by the conservation of energy and momentum. The conservation of momentum and energy can be approached graphically with the help of Fig. 3.3. The curved line represents the right moving depleton spectrum and the straight red lines represent the left moving phononic spectrum. The scattering process is allowed by momentum and energy conservation if we can connect two points of the depleton spectrum by two straight lines of the phononic spectrum. It is easy to realise that the only way of doing it is to come back to the original point with the second straight line, that is $q' = -q$ in Fig. 3.3, which means that depleton and phonons do not change their states and as a consequence do not contribute to the dynamics. Since only vertices proportional to $\Gamma_{+-}(P)$ and $\Gamma_{-+}(P)$ are left, we denote $\Gamma_{+-}(P) = \Gamma_{-+}(P) \equiv \Gamma(P)$. This vertex, introduced in Refs. [53, 51, 50], is the amplitude of the process where a phonon scatters against a depleton and changes its chirality, that is a *backscattering* process. Since we are dealing with small momenta, P, we may expand $\Gamma(P)$ around $P = 0$. Using the definition $\Gamma^{-1}(P) = [\partial_{\Lambda_+}\partial_{\Lambda_-} H]_{\Lambda_{\pm}=\Lambda_{0,\pm}}$, Hamiltonian (3.13), Eq. (3.24) and the equations for the equilibrium values, $\Phi_0(P, n)$ and $N_0(P, n)$, in Appendix C we show that, for small momenta,

$$\Gamma(P) \approx \Gamma'_0 P\,, \quad P \ll m^* c\,, \tag{3.32}$$

where,

$$\Gamma'_0 = [\partial_P \Gamma(P)]_{P=0} = -\frac{1}{4nc}\left(\left(1 + \frac{n}{c}\frac{\partial c}{\partial n}\right) + n\frac{\partial}{\partial n}\right)\left[\frac{1}{mc}\left(\frac{n}{m^*}\frac{\partial m^*}{\partial n} - \left(1 - \frac{n}{c}\frac{\partial c}{\partial n}\right)\right)\right]. \tag{3.33}$$

Substituting Eq. (3.32) into Eq. (3.30) we find,

$$L_{\mathrm{D}} + L_{\mathrm{Ph\text{-}D}} \to P\partial_t X - E(P) + \frac{1}{2\pi}\frac{c\Gamma'_0}{m^*}P^2\,\tilde{\chi}'_+(X,t)\tilde{\chi}'_-(X,t)\,, \tag{3.34}$$

valid for a right moving depleton. In the case of a left moving depleton, the second line of Eq. (3.31) gets and additional minus sign, which causes the last term of Eq. (3.34) to

change sign.

We have derived the partition function for a system with a single depleton, describing a quasiparticle excitation, interacting with phonons in the small momentum limit, $P \ll m^* c$. The total Lagrangian of the system is given by the sum of Eqs. (3.26) and (3.34). Now, we extend the Lagrangian of a single depleton to the Lagrangian of many depletons with the standard rules for second-quantising a single particle Lagrangian, as explained, for example, in Ref. [14]. It follows that L_D and $L_\mathrm{Ph-D}$ get replaced by the fermionic Lagrangians,

$$L_{\mathrm{F},\eta} = \int \mathrm{d}x \, \bar{\psi}_\eta \left[\mathrm{i}\partial_t - E_\eta(-\mathrm{i}\partial_x) \right] \psi_\eta \,, \tag{3.35}$$

and,

$$L_{\mathrm{Ph\text{-}F},\eta} = \pm \int \mathrm{d}x \, \frac{1}{2\pi} \frac{c\Gamma_0'}{m^*} \partial_x \tilde{\chi}_+ \partial_x \tilde{\chi}_- \left(\bar{\psi}_\eta (\overset{\leftrightarrow}{P})^2 \psi_\eta \right) \,, \tag{3.36}$$

where $\bar{\psi}_\eta$ and ψ_η are the fermionic quasiparticle fields introduced in Sec. 2.3 and we dropped the tildes. We defined $\overset{\leftrightarrow}{P}$ as the symmetric version of the momentum operator, $\bar{\psi} \overset{\leftrightarrow}{P} \psi = \frac{\mathrm{i}}{2} \left[(\partial_x \bar{\psi}) \psi - \bar{\psi} (\partial_x \psi) \right]$, in order for it to be Hermitian. Then, the respective term in Eq. (3.36) is explicitly given by $\bar{\psi}(\overset{\leftrightarrow}{P})^2 \psi = -\frac{1}{4} \left[(\partial_x^2 \bar{\psi}) \psi - 2 (\partial_x \bar{\psi}) (\partial_x \psi) + \bar{\psi} (\partial_x^2 \psi) \right]$. In order to go from a single depleton to many depletons we assumed that depletons are dilute, so that we can neglect collisions between themselves. This assumption will be justified when we will see that depletons describe excitations with higher energy than phonons, which means that at low energies there are only few of them. In Lagrangians (3.35) and (3.36), we refer to the quasiparticles as fermions to distinguish them from the single depleton ones. However, in the following we will use the terms fermions and Depletons interchangeably. We are now ready to derive the Feynman rules of the system that we will use to calculate dynamical quantities in the following sections.

82

3.4 Feynman rules

For the calculations that follow, it is useful to write the Feynman rules in momentum-energy space and in the Keldysh formalism. The action of the whole system is,

$$S = \int_{\rightleftarrows} \mathrm{d}t \sum_{\eta} \left(L_{\mathrm{Ph},\eta} + L_{\mathrm{F},\eta} + L_{\mathrm{Ph\text{-}F},\eta} \right) , \tag{3.37}$$

with $L_{\mathrm{Ph},\eta}$, $L_{\mathrm{F},\eta}$ and $L_{\mathrm{Ph\text{-}F},\eta}$ defined respectively by Eqs. (3.26), (3.35) and (3.36). Denoting with the superscripts $\pm$ the fields in upper and lower time branches, as explained in Chap. 1, we perform a Keldysh rotation for real bosonic fields,

$$\tilde{\chi}^{\pm} = \tilde{\chi}^{\mathrm{cl}} \pm \tilde{\chi}^{\mathrm{q}} ,$$

and for fermionic fields,

$$\psi^{\pm} = \frac{\psi_1 \pm \psi_2}{\sqrt{2}} ,$$
$$\bar{\psi}^{\pm} = \frac{\bar{\psi}_1 \mp \bar{\psi}_2}{\sqrt{2}} .$$

The Keldysh rotation of phononic Lagrangian (3.26) leads to the Lagrangian in Eq. (2.56) without source fields,

$$L_{\mathrm{Ph},\eta} = \int \mathrm{d}x \left[\frac{1}{2} \tilde{\chi}_\eta^\alpha \tilde{D}_{0,\eta}^{-1} \tilde{\chi}_{\eta\alpha} - \frac{1}{2\pi m^*} (\tilde{\chi}_\eta'^{\mathrm{cl}})^2 \tilde{\chi}_\eta'^{\mathrm{q}} \right] , \tag{3.38}$$

where the phononic propagator, defined in Eq. (2.51), in momentum space reads,

$$\tilde{D}_{0,\pm}^{-1}(q,\omega) = \pm \frac{1}{\pi} q(\omega \mp cq) .$$

Inverting it, we define the Feynman diagram for the right and left phononic propagators as black and red wiggly lines,

$$\overset{q\,,\,\beta\alpha}{\wwwwww} \quad = \tilde{D}_+^{\alpha\beta}(q,\omega) = \begin{pmatrix} \tilde{D}_+^{\mathrm{K}}(q,\omega) & \tilde{D}_+^{\mathrm{R}}(q,\omega) \\ \tilde{D}_+^{\mathrm{A}}(q,\omega) & 0 \end{pmatrix} , \tag{3.39}$$

and,

$$
\underset{q\,,\,\beta\alpha}{\wwwww} \;=\; \tilde{D}_{-}^{\alpha\beta}(q,\omega) = \begin{pmatrix} \tilde{D}_{-}^{\mathrm{K}}(q,\omega) & \tilde{D}_{-}^{\mathrm{R}}(q,\omega) \\[2mm] \tilde{D}_{-}^{\mathrm{A}}(q,\omega) & 0 \end{pmatrix}. \tag{3.40}
$$

Retarded and advanced propagators are defined as,

$$
\tilde{D}_{\pm}^{\mathrm{R}}(q,\omega) = \left[\tilde{D}_{\pm}^{\mathrm{A}}(q,\omega)\right]^{\dagger} = \pm\frac{\pi}{q(\omega \mp cq + \mathrm{i}0)}\,,
$$

and the Keldysh one as,

$$
\tilde{D}_{\pm}^{\mathrm{K}}(q,\omega) = F_{\mathrm{Ph}\pm}(q)\Delta_{\mathrm{Ph}\pm}(q,\omega)\,, \tag{3.41}
$$

where,

$$
\Delta_{\mathrm{Ph}\pm}(q,\omega) = \tilde{D}_{\pm}^{\mathrm{R}}(q,\omega) - \tilde{D}_{\pm}^{\mathrm{A}}(q,\omega) = \mp\frac{2\pi^2}{q}\mathrm{i}\delta\left(\omega \mp cq\right)\,, \tag{3.42}
$$

and $F_{\mathrm{Ph}\pm}(q)$ is the distribution function, that in equilibrium is given by,

$$
F_{\mathrm{Ph}\pm}(q) = \coth\left(\pm\frac{cq}{2T}\right)\,. \tag{3.43}
$$

The Keldysh rotation of fermionic Lagrangian (3.35) leads to the Lagrangian in Eq. (2.58) without source fields,

$$
L_{\mathrm{F},\eta} = \int \mathrm{d}x \left[\bar{\psi}_{\eta}(r)\tilde{G}_{\eta}^{-1}(r)\psi_{\eta}(r)\right]\,,
$$

where the fermionic propagator, defined in Eq. (2.16), in momentum space reads,

$$
\tilde{G}_{\eta}^{-1}(k,\varepsilon) = \varepsilon - \varepsilon_{\eta}(k)\,,
$$

where we used Eq. (2.60) for the spectrum,

$$
\varepsilon_{\pm}(k) = \pm ck + \frac{k^2}{2m^*}\,. \tag{3.44}
$$

Inverting $\tilde{G}_\eta^{-1}$, we define the Feynman diagram for the right and left fermionic quasiparticle propagators as black and red straight double lines,

$$\overset{k\,,\,ba}{\Longrightarrow} \quad = \tilde{G}_+^{ab}(k,\varepsilon) = \begin{pmatrix} \tilde{G}_+^{\mathrm{R}}(k,\varepsilon) & \tilde{G}_+^{\mathrm{K}}(k,\varepsilon) \\ 0 & \tilde{G}_+^{\mathrm{A}}(k,\varepsilon) \end{pmatrix}, \tag{3.45}$$

and,

$$\overset{k\,,\,ba}{\Longrightarrow} \quad = \tilde{G}_-^{ab}(k,\varepsilon) = \begin{pmatrix} \tilde{G}_-^{\mathrm{R}}(k,\varepsilon) & \tilde{G}_-^{\mathrm{K}}(k,\varepsilon) \\ 0 & \tilde{G}_-^{\mathrm{A}}(k,\varepsilon) \end{pmatrix}, \tag{3.46}$$

where retarded and advanced propagators are defined as,

$$\tilde{G}_\pm^{\mathrm{R}}(k,\varepsilon) = \left[\tilde{G}_\pm^{\mathrm{A}}(k,\varepsilon)\right]^\dagger = \frac{1}{\varepsilon - \varepsilon_\pm(k) + \mathrm{i}0},$$

and the Keldysh one as,

$$\tilde{G}_\pm^{\mathrm{K}}(k,\varepsilon) = F_{\mathrm{F}\pm}(k)\Delta_{\mathrm{F}\pm}(k,\varepsilon). \tag{3.47}$$

Here,

$$\Delta_{\mathrm{F}\pm}(k,\varepsilon) = \tilde{G}_\pm^{\mathrm{R}}(k,\varepsilon) - \tilde{G}_\pm^{\mathrm{A}}(k,\varepsilon) = -2\pi\mathrm{i}\delta\left(\varepsilon - \varepsilon_\pm(k)\right), \tag{3.48}$$
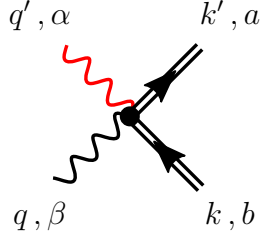
and $F_{\mathrm{F}\pm}(k)$ is the distribution function, that in equilibrium is given by,

$$F_{\mathrm{F}\pm}(k) = \tanh\left(\frac{\varepsilon_\pm(k)}{2T}\right). \tag{3.49}$$

The interaction term between fermions and phonons, Eq. (3.36), after a Keldysh rotation reads,

$$L_{\mathrm{Ph\text{-}F},\eta} = \eta \int \mathrm{d}x\, \frac{1}{2\pi}\frac{c}{m^*}\Gamma_0'\hat{\gamma}_{\alpha\beta}^{ab}\partial_x\chi_+^\alpha\partial_x\chi_-^\beta\left(\bar{\psi}_a(\overleftrightarrow{P})^2\psi_b\right).$$

Focusing only on right moving fermions, the interaction Lagrangian leads to the following vertex,

$$= \Gamma^{ac}_{\alpha\beta}(k', k; q', q)$$

$$= \frac{\mathrm{i}}{8\pi} \frac{c\Gamma'_0}{m^*} \gamma^{ab}_{\alpha\beta} qq'(k+k')^2 (2\pi)^2 \delta^2(k+q-k'-q') \,.$$

where we have introduced the Keldysh tensors, $\gamma^{ab}_{\alpha\beta}$,

$$\gamma^{ab}_{\mathrm{clcl}} = \gamma^{ab}_{\mathrm{qq}} = \begin{pmatrix} 1 & 0 \\ 0 & 1 \end{pmatrix}, \qquad \gamma^{ab}_{\mathrm{clq}} = \gamma^{ab}_{\mathrm{qcl}} = \begin{pmatrix} 0 & 1 \\ 1 & 0 \end{pmatrix}. \qquad (3.50)$$

With the Feynman rules laid down, we are ready to calculate dynamical quantities.

3.5 Depletons dynamics

In this section we study the depleton contribution to the dynamics of the system. As we did in Sec. 2.1, we study the dynamics by means of the dynamical structure factor defined in Eq. (2.5). The definition given in Eq. (2.5) can be extended to a system in the thermodynamic limit,

$$S(q, \omega) = \int_{-\infty}^{\infty} dx \int_{-\infty}^{\infty} dt \, \langle n(x, t)n(0, 0) \rangle \, e^{-iqx + i\omega t} \,, \qquad (3.51)$$

where we removed the hat from the density, $n(x, t)$, as now, instead of the operator formalism, we are dealing with the functional formalism. To calculate the fermionic contribution to the dynamical structure factor, we observe that we can decompose the density at each position and time into modes with different momenta as,

$$n(x, t) = \sqrt{K} \int \frac{\mathrm{d}k}{2\pi} \left[F_{\mathrm{F}+}(x, k, t) + F_{\mathrm{F}-}(x, k, t) \right] \,. \qquad (3.52)$$

Here $F_{F\pm}(x, k, t)$ are the fermionic density of states of right and left movers as a function of momentum k at position x and time t. The factor $\sqrt{K}$, where K is the Luttinger parameter, comes from the definition of the density in terms of fermionic quasiparticles, $\sqrt{K}(\bar{\psi}_+\psi_+ + \bar{\psi}_-\psi_-)$: this is the term multiplying the density source field, u_θ, in partition function (2.58). The reason for which we use decomposition (3.52) is because the time evolution of $F_{F\pm}(x, k, t)$ satisfy a linear differential equation, as we will see in this section. Instead, the time evolution of $n(x, t)$ is non-linear because it is the sum of many $F_{F\pm}(x, k, t)$'s with different time evolutions for every momentum k. We also note that, since we are studying the dynamics of the system, only the variations of the density over the homogenous part (static liquid) are relevant; so, the fact that in the last chapter we discarded the homogenous parts in the derivation of the phononic and fermionic actions is not a problem.

Focusing only on right moving fermions, $F_{F+}(x, k, t)$ satisfies the extension of kinetic equation (1.46) to a system dependent on position, which, in the Wigner approximation, reads [13],

$$[\mathrm{i}\partial_t + v(k)\partial_x]\, F_{F+}(x, k, t) = I^{\text{coll}}(x, k, t)\,, \tag{3.53}$$

where the velocity of excitations with momentum k is,

$$v(k) = c + \frac{k}{m^*}\,, \tag{3.54}$$

obtained by differentiating spectrum (3.44) by k, and $I^{\text{coll}}(x, k, t)$ is the collision integral,

$$\begin{aligned} I^{\text{coll}}(x, k, t) &= \mathrm{i}\Sigma^{K}(x, k, t) + 2\mathrm{Im}\Sigma^{R}(x, k, t)F_{F+}(x, k, t)\,. \\ &= \mathrm{i}\Sigma^{K}(x, k, t) - \frac{F_{F+}(x, k, t)}{\tau(x, k, t)}\,. \end{aligned} \tag{3.55}$$

defined in terms of the retarded and Keldysh fermionic self-energies, Σ^{R} and Σ^{K}. In kinetic equation (3.53) we also omitted the external source field that was present in Eq. (1.46). In the second line we used the relation between the lifetime, τ, and the retarded self-energy

[13],

$$\frac{1}{\tau(x,k,t)} = -2\mathrm{Im}\Sigma^{\mathrm{R}}(x,k,t).$$ (3.56)

In order to calculate the dynamical structure factor, Eq. (3.51), we need to determine the solution of Eq. (3.53), which requires the knowledge of the self-energy,

$$\Sigma^{ab} = \begin{pmatrix} \Sigma^{\mathrm{R}} & \Sigma^{\mathrm{K}} \\ 0 & \Sigma^{\mathrm{A}} \end{pmatrix}.$$

We proceed by calculating the self-energy.

3.5.1   Self-energy and lifetime

We calculate the fermion self-energy at the lowest order in perturbation theory in the interaction term. At the lowest order, the fermion self-energy is depicted in Fig. 3.4 and reads,

$$\begin{aligned}
-\mathrm{i}\Sigma^{ab}(k) &= \int \frac{\mathrm{d}^2 q}{(2\pi)^2} \frac{\mathrm{d}^2 q'}{(2\pi)^2} \Gamma^{ac}_{\beta\gamma}\left(k+q-q',k;q',q\right) \mathrm{i}G^{cd}_{+}(k+q-q')\mathrm{i}D^{\gamma\delta}_{-}(q') \\
&\quad \times \Gamma^{db}_{\delta\alpha}\left(k,k+q-q';q,q'\right) \mathrm{i}D^{\alpha\beta}_{+}(q) \\
&= \mathrm{i}\frac{1}{(8\pi)^2} \frac{\Gamma'^2_0 c^2}{(m^*)^2} \int \frac{\mathrm{d}^2 q}{(2\pi)^2} \frac{\mathrm{d}^2 q'}{(2\pi)^2} \left(qq'\right)^2 \left(2k+q-q'\right)^4 \\
&\quad \times \left[\gamma^{ac}_{\beta\gamma} G^{cd}_{+}(k+q-q')D^{\gamma\delta}_{-}(q')\gamma^{db}_{\delta\alpha}D^{\alpha\beta}_{+}(q)\right],
\end{aligned}$$ (3.57)

where the factor $1/2$ coming from the second order perturbation theory is cancelled by the factor 2 due to the symmetry by exchange of the vertices. In order to have a compact notation, we use only the momentum variable in the argument of functions, leaving the energy variable implicit and omitting the the position and time dependence. Also, the integration measure in energy and momentum is denoted as $\mathrm{d}^2 q = \mathrm{d}q\mathrm{d}\omega$ and similarly for the other variables. The retarded component is given by,
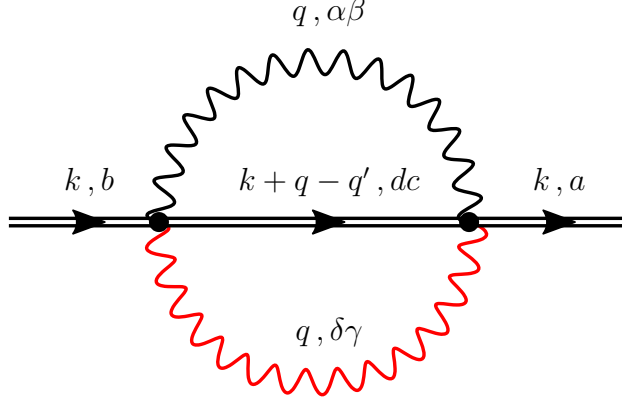
Figure 3.4: Fermion self-energy at second order in perturbation theory.

$$\Sigma^{\mathrm{R}}(k) = \Sigma^{11}(k)$$

$$= -\frac{1}{(8\pi)^2} \frac{\Gamma_0'^2 c^2}{(m^*)^2} \int \frac{\mathrm{d}^2 q}{(2\pi)^2} \frac{\mathrm{d}^2 q'}{(2\pi)^2} (qq')^2 (2k+q-q')^4$$

$$\times \left[G_+^{\mathrm{R}}(k+q-q') \left(D_-^{\mathrm{K}}(q') D_+^{\mathrm{K}}(q) - \left(D_-^{\mathrm{R}}(q') - D_-^{\mathrm{A}}(q') \right) \left(D_+^{\mathrm{R}}(q) - D_+^{\mathrm{A}}(q) \right) \right) + \right.$$

$$\left. + G_+^{\mathrm{K}}(k+q-q') \left(D_-^{\mathrm{K}}(q') D_+^{\mathrm{A}}(q) + D_-^{\mathrm{R}}(q') D_+^{\mathrm{K}}(q) \right) \right] \ .$$

Taking the imaginary part of the retarded self-energy, as needed in collision integral (3.55), and using representations (3.41) and (3.47) for the Keldysh propagators, we have,

$$2\mathrm{i}\mathrm{Im}\Sigma^{\mathrm{R}}(k) = -\frac{1}{(8\pi)^2} \frac{\Gamma_0'^2 c^2}{(m^*)^2} \int \frac{\mathrm{d}^2 q}{(2\pi)^2} \frac{\mathrm{d}^2 q'}{(2\pi)^2} \mathrm{d}^2 k' \ (qq')^2 (k+k')^4 \delta^2(k+q-q'-k')$$

$$\times \Delta_{\mathrm{F}+}(k') \Delta_{\mathrm{Ph}-}(q') \Delta_{\mathrm{Ph}+}(q) \mathcal{F}_{\mathrm{F}}^{\mathrm{R}}(k,k';q,q') ,$$

(3.58)

where the delta function, $\delta^2(...)$, imposes momentum and energy conservation and we defined,

$$\mathcal{F}_{\mathrm{F}}^{\mathrm{R}}(k,k';q,q') = F_{\mathrm{Ph}-}(q') F_{\mathrm{Ph}+}(q) - 1 + F_{\mathrm{F}+}(k') \left(F_{\mathrm{Ph}+}(q) - F_{\mathrm{Ph}-}(q') \right) \ .$$

Here we imposed the mass shell condition on the external energy since the quantities of interest in which $\mathrm{Im}\Sigma_+^{\mathrm{R}}(k)$ appears are always multiplied by $\Delta_{\mathrm{F}+}(k) \sim \delta\left(\varepsilon - \varepsilon_+(k)\right)$ [13].

Substituting in Eq. (3.58) the explicit values of $\Delta_{\mathrm{F}\pm}(k)$ and $\Delta_{\mathrm{Ph}\pm}(q)$ from Eqs. (3.48) and (3.42) and integrating over $\mathrm{d}\omega$, $\mathrm{d}\omega'$, $\mathrm{d}\varepsilon'$, we find,

$$2\mathrm{i}\mathrm{Im}\Sigma^{\mathrm{R}}(k) = \frac{\mathrm{i}}{128\pi}\frac{{\Gamma_0'}^2 c^2}{(m^*)^2}\int \mathrm{d}q\mathrm{d}q'\mathrm{d}k'\,\delta(\varepsilon_+(k) + c(q-q') - \varepsilon_+(k'))$$
$$\times\,\delta(k+q-q'-k')$$
$$\times\,qq'\,(k+k')^4\,\mathcal{F}_{\mathrm{F}}^{\mathrm{R}}(k,k';q,q')\,.$$

By integrating over $\mathrm{d}k'$, making the shift $q' = q - \tilde{q}$ and integrating over $\mathrm{d}q$, we find,

$$2\mathrm{Im}\Sigma^{\mathrm{R}}(k) = \frac{1}{128\pi}\frac{{\Gamma_0'}^2}{(2m^*)^3}\int \mathrm{d}q\,q^2\,(2k+q)^5\left[1 + \frac{2k+q}{4m^*c}\right]$$
$$\times\,\mathcal{F}_{\mathrm{F}}^{\mathrm{R}}\left(k, k+q; q\left[1 + \frac{2k+q}{4m^*c}\right], q\frac{2k+q}{4m^*c}\right)\,,$$

where in the last line we renamed the dummy variable $\tilde{q}$ to q. At the lowest order in small momenta, $k, q \ll m^*c$, we have,

$$2\mathrm{Im}\Sigma^{\mathrm{R}}(k) \approx \frac{1}{128\pi}\frac{{\Gamma_0'}^2}{(2m^*)^3}\int \mathrm{d}q\,q^2\,(2k+q)^5\,\mathcal{F}_{\mathrm{F}}^{\mathrm{R}}\left(k, k+q; q, q\frac{2k+q}{4m^*c}\right)\,. \tag{3.59}$$

The last argument of $\mathcal{F}_{\mathrm{F}}^{\mathrm{R}}$ is the momentum of the left-moving phonon in the scattering process which is small due to the conservation of energy and momentum. The reason can be understood using the graphical depiction of momentum and energy conservation in Fig. 3.5. From the picture we see that the momentum of the left-moving phonon would be zero in the case of a linear dispersion, $m^{*-1} = 0$, and the addition of a weak non-linearity, $q, k \ll m^*c$, makes it parametrically small. We evaluate the self-energy at equilibrium, as non-equilibrium terms would be smaller corrections to kinetic equation (3.53). At equilibrium we use the fluctuation-dissipation theorem in the form of Eqs. (3.43) and (3.49), for which we have,

$$\mathcal{F}_{\mathrm{F}}^{\mathrm{R}}(k, k'; q, q') = \left[\coth\left(\frac{cq'}{2T}\right) + \coth\left(\frac{cq}{2T}\right)\right]\left[\tanh\left(\frac{ck'}{2T}\right) - \coth\left(\frac{c(q+q')}{2T}\right)\right]\,. \tag{3.60}$$
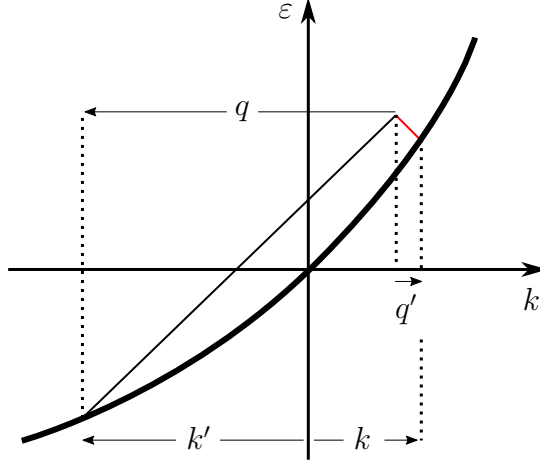
Figure 3.5: Kinematics of the scattering process described by the diagram in Fig. 3.6. The black thick line represents the spectrum of right moving fermions and the black and red thin lines the spectrum of right and left moving phonons. Given the weak non-linearity m^{*-1} of the fermionic spectrum, the momentum q' of the left-moving phonon is parametrically small with respect to q.

In the limit $k, q \ll m^* c$, the terms with the divergent factor $\coth{(cq'/2T)}$ dominate as a consequence of the conservation of energy and momentum. Substituting Eq. (3.60) into Eq. (3.59), and using the definition of lifetime, Eq. (3.56), we finally find,

$$\frac{1}{\tau(k)} = \frac{1}{2\pi} \frac{T^7 \Gamma_0'^2}{m^{*2} c^6} I\left(\frac{ck}{2T}\right) = \frac{\pi^5}{128} \frac{T^7 \Gamma_0'^2}{(m^* c^2)^2 c^2} + \left(\frac{103\pi^3}{1920} \frac{T^5 \Gamma_0'^2}{(m^* c^2)^2}\right) k^2 + o\left(k^4\right) , \quad (3.61)$$

where,

$$I(y) = \int_{-\infty}^{+\infty} \mathrm{d}x \, x \, (x + 2y)^4 \left[\coth{(x)} - \tanh{(x+y)}\right] .$$

Now we turn to, the Keldysh component of the self-energy, which is given by,

$$\Sigma^{\mathrm{K}}(k) = \Sigma^{12}(k)$$

$$= -\frac{1}{(8\pi)^2} \frac{\Gamma_0'^2 c^2}{(m^*)^2} \int \frac{\mathrm{d}^2 q}{(2\pi)^2} \frac{\mathrm{d}^2 q'}{(2\pi)^2} \, (qq')^2 \, (2k + q - q')^4$$

$$\times \left[G_+^{\mathrm{K}}(k + q - q') \left(D_-^{\mathrm{K}}(q') D_+^{\mathrm{K}}(q) - \left(D_-^{\mathrm{R}}(q') - D_-^{\mathrm{A}}(q') \right) \left(D_+^{\mathrm{R}}(q) - D_+^{\mathrm{A}}(q) \right) \right) + \right.$$

$$- D_-^{\mathrm{K}}(q') \left(G_+^{\mathrm{R}}(k + q - q') - G_+^{\mathrm{A}}(k + q - q') \right) \left(D_+^{\mathrm{R}}(q) - D_+^{\mathrm{A}}(q) \right) +$$

$$\left. + D_+^{\mathrm{K}}(q) \left(G_+^{\mathrm{R}}(k + q - q') - G_+^{\mathrm{A}}(k + q - q') \right) \left(D_-^{\mathrm{R}}(q') - D_-^{\mathrm{A}}(q') \right) \right] .$$

91

The calculation proceeds in the same way as for the retarded self-energy, with the difference that $\mathcal{F}_F^R$ gets replaced by,

$$\mathcal{F}_F^K(k, k'; q, q') = F_{F+}(k')\left(F_{Ph-}(q')F_{Ph+}(q) - 1\right) - F_{Ph-}(q') + F_{Ph+}(q),$$

and results in,

$$i\Sigma^K(k) = \int \mathrm{d}q\, M(k, q) F_{F+}(x, k + q, t), \tag{3.62}$$

where we expanded to first order in $F_{F+}(x, k + q, t)$ and defined,

$$M(k, q) = \frac{1}{128\pi} \frac{T\Gamma_0'^2}{m^{*2}} q(2k + q)^4 \left(\coth\left(\frac{cq}{2T}\right) + \tanh\left(\frac{ck}{2T}\right)\right).$$

Before moving on to the kinetic equation, we discuss the zero temperature case. The lifetime of excitations in the system of nonlinear interacting fermions was investigated in Refs. [54, 55]. Their result for a non-thermal particle scales as k^8 where k is the momentum of the quasiparticle above Fermi surface. Substituting the zero temperature limit of the distribution functions,

$$\tanh\left(\frac{E}{2T}\right) \to \mathrm{sgn}(E),$$

$$\coth\left(\frac{\omega}{2T}\right) \to \mathrm{sgn}(\omega),$$

into Eq. (3.60), we find,

$$\frac{1}{\tau(k)} = -\frac{\Gamma_0'^2 c}{256\pi m^{*2}} \int \mathrm{d}q\mathrm{d}q'\, \delta\left(q' - \frac{q(2k + q)}{4m^*c}\right) qq'(2k + q)^4$$
$$\times \left[\mathrm{sgn}(-cq')\left\{\mathrm{sgn}(cq) - \mathrm{sgn}(ck + cq)\right\} + \left\{\mathrm{sgn}(ck + cq)\mathrm{sgn}(cq) - 1\right\}\right],$$

where, as before, we considered the lowest approximation in small momentum, $q, k \ll m^*c$. We have also conveniently rearranged the distribution functions such that the expressions in curly brackets are non–zero only when $-k < q < 0$. Since $\mathrm{sgn}(-cq') = \mathrm{sgn}\left(-(2k + q)q\right) = 1$ in that region, the value of the expression in square brackets gives a factor -4 and the

decay rate becomes,

$$\tau^{-1}(k) = \frac{\Gamma_0'^2 c^2}{128\pi m^{*2}} \int_{-k}^{0} \mathrm{d}q \, \frac{q^2(2k+q)^5}{2m^*c^2} = \frac{73\Gamma_0'^2 k^8}{14336\pi m^{*3}} \, ,$$

consistent with the result of Refs. [54, 55]. In the case of thermal quasiparticles the temperature dependence T^7 in Eq. (3.61) originates from the fact that the energy of the left moving phonon cq' is controlled by the first power of temperature T, in contrast to the second power of the incoming momentum in Refs. [54, 55].

3.5.2 Kinetic equations for fermions

Inserting results (3.61) and (3.62) into collision integral (3.55), we find,

$$I^{\mathrm{coll}}(x, k, t) = \int \mathrm{d}q \, M(k, q) F_{\mathrm{F}+}(x, k+q, t) - \frac{F_{\mathrm{F}+}(x, k, t)}{\tau(k)} \, .$$

Inserting this collision integral into Eq. (3.53), we have the kinetic equation for right moving fermions,

$$[\mathrm{i}\partial_t + v(k)\partial_x] \, F_{\mathrm{F}+}(x, k, t) = \int \mathrm{d}q \, M(k, q) F_{\mathrm{F}+}(x, k+q, t) - \frac{F_{\mathrm{F}+}(x, k, t)}{\tau(k)} \, . \qquad (3.63)$$

The first term on the right hand side describes the growth of $F_{\mathrm{F}+}$ since $M(k, q)$ is positive for small momenta k and q. This term comes from the process of a right moving phonon giving an additional momentum to a right moving fermion by backscattering into a left moving phonon. This process favours the population of fermionic modes with higher energy. Instead, the second term is negative and describes the relaxation to equilibrium, $F_{\mathrm{F}+}(k) \to \tanh\left(\frac{\varepsilon_+(k)}{2T}\right)$. This term comes from the process where a right fermion loses momentum by colliding against a left moving phonon, causing it to backscatter and to become a right moving phonon. This process favours the population of fermionic modes with lower energy, thereby leading to relaxation. Here, by neglecting the first term, we consider the scattering time approximation, that amounts to neglecting terms populating

93

higher energy modes and leads to an underestimation for the decay time, τ [13]. In other words, it means that in this approximation fermions need at least a time τ to equilibrate.

We proceed to study the system in a state slightly out of equilibrium. This amounts to writing,

$$F_{F+}(x, k, t) = \tanh\left(\frac{\varepsilon_+(k)}{2T}\right) + f_{F+}(x, k, t), \qquad (3.64)$$

where $f_{F+}(x, k)$ is a small variation from the homogeneous equilibrium distribution, $\tanh\left(\frac{\varepsilon_+(k)}{2T}\right)$. Moreover, since we are considering small momenta, we keep only the lowest momentum term of the decay time in Eq. (3.61), that is,

$$\frac{1}{\tau} = \frac{\pi^5}{128} \frac{T^7 \Gamma_0'^2}{(m^* c^2)^2 \, c^2}. \qquad (3.65)$$

Within these approximations and using the fact that, as seen in Sec. 1.6, right hand sides of kinetic equation kinetic equation (3.63) are identically zero for the equilibrium distribution, $\tanh\left(\frac{\varepsilon_+(k)}{2T}\right)$, the kinetic equation reduces to,

$$[i\partial_t + v(k)\partial_x] \, f_{\mathrm{F}+}(x, k, t) = -\frac{f_{\mathrm{F}+}(x, k, t)}{\tau}.$$

This differential equation is solved by,

$$f_{\mathrm{F}+}(x, k, t) = e^{-|t|/\tau} f_{F+}(x - v(k)t, k, t = 0), \qquad (3.66)$$

where the modulus in the exponent comes from the time-reversed solution.

Now that we know the time evolution of the density of states, Eqs. (3.64) and (3.66), we proceed to the calculation of the dynamical structure factor, Eq. (3.51). First, we note that apart for the static limit, $\omega = 0$, the equilibrium part of the density of states, Eq. (3.64), does not contribute. Second, right and left moving fermions are independent and give the same contribution, but in different regions: right moving fermions contribute to $q > 0$ and left moving fermions to $q < 0$. Then, using decomposition (3.52), the dynamical

structure factor for $q > 0$ becomes,

$$S(q, \omega) = K \int \frac{\mathrm{d}k\,\mathrm{d}k'}{2\pi\,2\pi} \int \mathrm{d}x\mathrm{d}t \, \langle f_{\mathrm{F}+}(x, k, t) f_{\mathrm{F}+}(0, k', 0) \rangle \, e^{-iqx+i\omega t} \,, \qquad (3.67)$$

Since the second term in the average is independent of time and position, the average satisfies the same kinetic equation of $f_{\mathrm{F}+}$, Eq. (3.66), which leads to,

$$\langle f_{\mathrm{F}+}(x, k, t) f_{\mathrm{F}+}(0, k', 0) \rangle = e^{-|t|/\tau} \, \langle f_{\mathrm{F}+}(x - v(k)t, k, t = 0) f_{\mathrm{F}+}(0, k', 0) \rangle \,,$$

Substituting this into the dynamical structure factor, shifting $x \to x + v(k)t$ and integrating over t we find,

$$S(q, \omega) = K \int \frac{\mathrm{d}k\,\mathrm{d}k'}{2\pi\,2\pi} \frac{2\tau^{-1}}{(\tau^{-1})^2 + (\omega - qv(k))} \int \mathrm{d}x \, \langle f_{\mathrm{F}+}(x, k, 0) f_{\mathrm{F}+}(0, k', 0) \rangle \, e^{-iqx} \,. \quad (3.68)$$

What remains to be done is to determine the initial condition, $\langle f_{\mathrm{F}+}(x, k, 0) f_{\mathrm{F}+}(0, k', 0) \rangle$. Given that fermions with different momenta do not interact, only the $k = k'$ component of the average survives,

$$\langle f_{\mathrm{F}+}(x, k, 0) f_{\mathrm{F}+}(0, k', 0) \rangle \propto \langle f_{\mathrm{F}+}(x, k, 0) f_{\mathrm{F}+}(0, k, 0) \rangle \, 2\pi\delta(k - k') \,,$$

where the factor 2π is there because the integration measure in momentum space has 2π at the denominator. Since the range of simultaneous fluctuations is of the order of the particle size and the particles are treated as infinitesimally small, the average is proportional to $\delta(x)$. This locality condition gives,

$$\langle f_{\mathrm{F}+}(x, k, 0) f_{\mathrm{F}+}(0, k', 0) \rangle = 2\pi \, \langle (f_{\mathrm{F}+}(0, k, 0))^2 \rangle \, \delta(k - k')\delta(x) \,.$$

Inserting this expression into Eq. (3.68) and integrating over k' and x, we have,

$$S(q, \omega) = K \int \frac{\mathrm{d}k}{2\pi} \frac{2\tau^{-1}}{(\tau^{-1})^2 + (\omega - qv(k))^2} \, \langle (f_{\mathrm{F}+}(0, k, 0))^2 \rangle \,.$$

Finally, we use the fluctuation-dissipation theorem for the fluctuations of a thermodynamic ensemble of statistically independent particles [56],

$$\left\langle (f(0,k,0))^2 \right\rangle = T \left[\partial_\mu n_{\mathrm{F}}(\varepsilon_+(k) - \mu)\right]_{\mu=0}$$

$$= \frac{1}{4\cosh^2\left(\frac{\varepsilon_+(k)}{2T}\right)}$$

$$\approx \frac{1}{4\cosh^2\left(\frac{ck}{2T}\right)}, \qquad k \ll m^*c,$$

where $n_{\mathrm{F}}(\varepsilon) = (1 - \tanh(\varepsilon/2T))/2$ is the fermionic density of states and μ is the chemical potential, which is zero in our case as we measure the energy from the Fermi surface. Putting everything together, the dynamical structure factor reads,

$$S(q,\omega) = \frac{Km^*}{q} \int \frac{dk}{4\pi} \frac{1}{\cosh^2\left(\frac{ck}{2T}\right)} \frac{m^*/\tau q}{[m^*/\tau q]^2 + [k - m^*(\omega - cq)/q]^2},$$

where we used Eq. (3.54) for $v(k)$. The integrand is the product of an inverse hyperbolic cosine squared, which has the shape of a bell centred at $k = 0$ with width T/c, and a Lorentzian, centred at $k = m^*(\omega - cq)/q$ with width $m^*/\tau q$. A comparison between the widths of $\cosh^{-2}$ and the Lorentzian sets the momentum scale $q_{\mathrm{c}} = m^*c/T\tau$, which we call *collision momentum* for a reason that will be clear soon.

For $q > q_{\mathrm{c}}$, the Lorentzian is narrower than $\cosh^{-2}$ and can be approximated by a delta function,

$$\frac{m^*/\tau q}{[m^*/\tau q]^2 + [k - m^*(\omega - cq)/q]^2} \approx \pi\delta\left(k - \frac{m^*}{q}(\omega - cq)\right).$$

Then, integrating over k, the dynamical structure factor becomes,

$$S(q,\omega) = \frac{Km^*}{4q} \frac{1}{\cosh^2\left(\frac{m^*c}{2Tq}(\omega - cq)\right)}$$

$$= \frac{KT}{2c} \frac{1}{\delta\omega_{\mathrm{F}}(q)} \frac{1}{\cosh^2\left(\frac{\omega - cq}{\delta\omega_{\mathrm{F}}(q)}\right)},$$

(3.69)

96

where we defined the characteristic width,

$$\delta\omega_{\mathrm{F}}(q) = \frac{2T}{m^* c}\, q\,.$$

(3.70)

For a fixed q, the dynamical structure factor, as a function of ω, has the shape of a bell centred around $\omega = cq$ with height $\frac{Km^*}{4q}$ and width $\delta\omega_{\mathrm{F}}(q)$. In absence of interactions between fermions, g_2, $g_4 = 0$, the effective mass, m^*, and the velocity, c, becomes the mass of the original fermions, m, and the Fermi velocity, v_{F}, $K = 1$ and Eq. (3.69) reduces to the dynamical structure factor of free fermions, Eq. (2.8). Since m^* and c are the effective mass and the Fermi velocity of the fermionic quasiparticles, we conclude that Eq. (3.69) describes the dynamics of free fermionic quasiparticles [7].[1] This result is consistent with generalisation of the Bose-Fermi mapping to arbitrary interaction strength [58, 7].

For $q < q_{\mathrm{c}}$, the $\cosh^{-2}$ is narrower that the Lorentzian and can be approximated by a delta function,

$$\frac{1}{\cosh^2\left(\frac{ck}{2T}\right)} \approx \frac{4T}{c}\delta(k)\,.$$

Integrating over k, the dynamical structure factor becomes,

$$S(q,\omega) = \frac{K}{\pi}\frac{T}{c}\frac{\tau^{-1}}{\tau^{-2} + (\omega - cq)^2}\,.$$

(3.71)

In this case, for a fixed q, the Lorentzian, as a function of ω, has constant height $\frac{K}{\pi}\frac{T}{c}\tau$ and constant width τ^{-1}. Both height and width depend on the relaxation time of fermions, τ, which, in turn, follows from the collisions of fermions against phonons. Therefore, the Lorentzian shape of the dynamical structure factor is associated to fermions experiencing the scattering against phonons, contrary to $\cosh^{-2}$ that is associated to the free motion of fermions. Then, the collision momentum, q_{c}, separates a regime where fermions move freely from a regime where they experience collisions against phonons, justifying its name. We conclude that the dynamics of fermions is characterised by two time scales: the collision

---

[1]Width (3.70) first appeared in Ref. [57] without derivation.

time, $1/cq_{\rm c}$, and the relaxation time, τ. This means that, when fermions are weakly perturbed, it will take at least a time $1/cq_{\rm c}$ for them to scatter against phonons and will take at least a time τ to reach equilibrium.

3.6 Phonons dynamics

In this section we study the phononic contribution to the dynamics of the system. To calculate the dynamical structure factor using phonons, we see from partition function (2.56) that the density in terms of phonons is,

$$n(x,t) = \frac{2\sqrt{K}}{\pi} \left(\partial_x \tilde{\chi}^{\rm cl}_+(x,t) + \partial_x \tilde{\chi}^{\rm cl}_-(x,t) \right). \tag{3.72}$$

As in the case of fermions, left and right moving phonons do not interact with each other and phonons moving to the right and to the left contribute respectively to positive and negative momenta in the dynamical structure factor. Then, focusing only on positive momenta, we substitute decomposition (3.72) into Eq. (3.51) and obtain,

$$S(q,\omega) = \frac{4K}{\pi^2} \int_{-\infty}^{\infty} dx \int_{-\infty}^{\infty} {\rm d}t \left\langle \partial_x \tilde{\chi}^{\rm cl}_+(x,t) \partial_x \tilde{\chi}^{\rm cl}_+(0,0) \right\rangle e^{-iqx+i\omega t}, \tag{3.73}$$

To calculate the average of the classical fields we need to know the equation of motion of $\tilde{\chi}^{\rm cl}_+(x,t)$ in the presence of fermions. Without fermions, we saw that the equation of motion is given by Eq. (2.57). In order to see how fermions modify the motion of phonons, we consider the partition function of the full system, with action given by Eq. (3.37), and integrate over the fermionic fields. This leads to additional terms to phononic Lagrangian (3.38), that now reads,

$$L_{{\rm Ph},+} = \int {\rm d}x \left[\frac{1}{2} \tilde{\chi}^{\alpha}_{\eta} \left(\tilde{D}^{-1}_{0,+} - {\rm iIm}\Pi^{\rm R} \right) \tilde{\chi}_{\eta\alpha} - \frac{1}{2} \tilde{\chi}^{\rm q}_+ \Pi^{\rm K} \tilde{\chi}^{\rm q}_+ - \frac{1}{2\pi m^*} (\tilde{\chi}'^{\rm cl}_+)^2 \tilde{\chi}'^{\rm q}_+ \right], \tag{3.74}$$
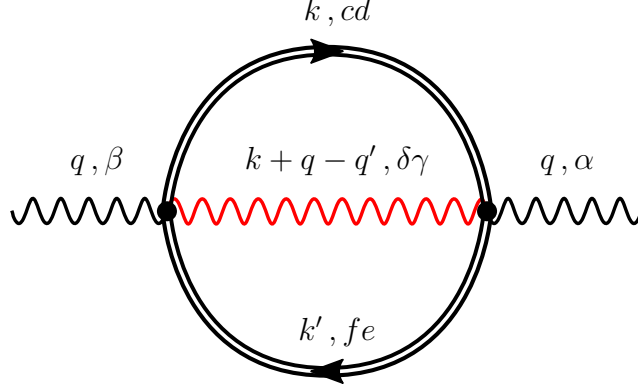
Figure 3.6: Phonon self-energy at second order in perturbation theory.

where Π_+^{R} and Π_+^{K} are the retarded and Keldysh components of the phononic self-energy. Since the real part of the retarded self-energy gives just a small correction to the phonic spectrum, we neglect it in first approximation. We consider only its imaginary part because it is related to dissipation and therefore to the relaxation from a non-equilibrium to an equilibrium state. In the next section, we proceed to calculate the self-energy.

3.6.1 Self-energy and diffusion

As we did for fermions, we consider the phonon self-energy in energy-momentum space at the lowest order in perturbation theory, which is depicted in Fig. 3.6 and reads,

$$
\begin{aligned}
-\mathrm{i}\Pi_{\alpha\beta}(q) &= -\int \frac{d^2k}{(2\pi)^2}\frac{d^2k'}{(2\pi)^2}\, \Gamma_{\alpha\gamma}^{de}\left(k',k;q+k-k',q\right)\mathrm{i}G_+^{ef}(k')\mathrm{i}D_-^{\gamma\delta}(q+k-k') \\
&\qquad\times \Gamma_{\delta\beta}^{fc}\left(k,k';q,q+k-k'\right)\mathrm{i}G_+^{cd}(k) \\
&= -\frac{\mathrm{i}}{(8\pi)^2}\frac{\Gamma_0'^2 c^2}{(m^*)^2}\int \frac{d^2k}{(2\pi)^2}\frac{d^2k'}{(2\pi)^2}\, q^2(q+k-k')^2\left(k+k'\right)^4 \\
&\qquad\times \left[\gamma_{\alpha\gamma}^{de}G_+^{ef}(k')D_-^{\gamma\delta}(q+k-k')\gamma_{\delta\beta}^{fc}G_+^{cd}(k)\right]\,,
\end{aligned}
\tag{3.75}
$$

where the minus sign in the first line is given by the fermionic loop and the factor $1/2$ coming from the second order perturbation theory is cancelled by the factor 2 due to the symmetry by exchange of the vertices. The retarded component is given by,

$$\Pi^R(q) = \Pi_{qcl}(q)$$

$$= \frac{1}{(8\pi)^2} \frac{\Gamma_0'^2 c^2}{(m^*)^2} \int \frac{d^2 q}{(2\pi)^2} \frac{d^2 q'}{(2\pi)^2} q^2 (q+k-k')^2 (k+k')^4$$

$$\times \left[D_-^K(q+k-k') \left(G_+^R(k') G_+^K(k) + G_+^K(k') G_+^A(k) \right) + \right.$$

$$\left. + D_-^R(q+k-k') \left(G_+^K(k') G_+^K(k) - \left(G_+^R(k') - G_+^A(k') \right) \left(G_+^R(k) - G_+^A(k) \right) \right) \right].$$

As we did for fermions, we use representations (3.47) and (3.41) for the Keldysh propagators and, taking the imaginary part of the retarded self-energy, as needed in Lagrangian (3.74), we obtain,

$$2i\text{Im}\Pi^R(q) = \frac{1}{(8\pi)^2} \frac{\Gamma_0'^2 c^2}{(m^*)^2} \int \frac{d^2 k}{(2\pi)^2} \frac{d^2 k'}{(2\pi)^2} d^2 q' q^2 (q')^2 (k+k')^4 \delta^2(q+k-k'-q')$$

$$\times \Delta_{\text{Ph}-}(q') \Delta_{\text{F}+}(k') \Delta_{\text{F}+}(k) \mathcal{F}^R_{\text{Ph}}(q, q'; k, k'),$$

$$(3.76)$$

where the delta function, $\delta^2(...)$, imposes momentum and energy conservation and we defined,

$$\mathcal{F}^R_{\text{Ph}}(k, k'; q, q') = F_{\text{Ph}-}(q') \left(F_{\text{F}+}(k) - F_{\text{F}+}(k') \right) + F_{\text{F}+}(k') F_{\text{F}+}(k) - 1.$$

As before, we imposed the mass shell condition on the external energy since the quantities of interest in which $\text{Im}\Pi^R_+(q)$ appears are always multiplied by $\Delta_{\text{Ph}+}(q) \sim \delta(\omega - cq)$ [13]. Substituting in Eq. (3.76) the explicit values $\Delta_{\text{F}\pm}(k)$ and $\Delta_{\text{Ph}\pm}(q)$ from Eqs. (3.42) and (3.48) and integrating over $d\omega$, $d\omega'$, $d\varepsilon'$, we find,

$$\text{Im}\Pi^R(q) = -\frac{1}{(16\pi)^2} \frac{\Gamma_0'^2 c^2}{(m^*)^2} \int dk dk' dq' \, \delta(c(q+q') + \varepsilon_+(k) - \varepsilon_+(k'))$$

$$\times \delta(q+k-k'-q')$$

$$\times q^2 q' (k+k')^4 \mathcal{F}^R_{\text{Ph}}(q, q'; k, k').$$

Integrating over dq', making the change of variables $k \to (k+k')/2$, $k' \to (k-k')/2$ and integrating over dk', the integral reduces to,

$$\mathrm{Im}\Pi^{\mathrm{R}}(q) =$$

$$= -\frac{1}{(16\pi)^2} \frac{\Gamma_0'^{\,2}}{32\,(m^*)^3} q^3 \int dk\, k^5 \left| \frac{1}{1+\frac{k}{4m^*c}} \right| \left(\frac{1}{1+\frac{k}{4m^*c}} \right)$$

$$\times \mathcal{F}^{\mathrm{R}}_{\mathrm{Ph}} \left(q, +\frac{qk}{4m^*c} \left(\frac{1}{1+\frac{k}{4m^*c}} \right); \frac{1}{2}\left[k - q\left(\frac{1}{1+\frac{k}{4m^*c}} \right) \right], \frac{1}{2}\left[k + q\left(\frac{1}{1+\frac{k}{4m^*c}} \right) \right] \right) .$$

At the lowest order in $k, q \ll m^*c$, we have,

$$\mathrm{Im}\Pi^{\mathrm{R}}(q) = -\frac{1}{512\pi^2} \frac{\Gamma_0'^{\,2}}{(2m^*)^3} q^3 \int dk\, k^5 \mathcal{F}^{\mathrm{R}}_{\mathrm{Ph}} \left(q, \frac{qk}{4m^*c}; \frac{k-q}{2}, \frac{k+q}{2} \right) . \qquad (3.77)$$

Here the second argument of $\mathcal{F}^{\mathrm{R}}_{\mathrm{Ph}}$ represents the momentum of the left-moving boson in the scattering process. As in the case of fermions, discussed at p. 90 and Fig. 3.7, the momentum is parametrically small and can be understood with the help of Fig. 3.7, depicting the momentum and energy conservation for the process in Fig. 3.6. At equilibrium we use the fluctuation-dissipation theorem in the form of Eqs. (3.43) and (3.49), for which we have,

$$\mathcal{F}^{\mathrm{R}}_{\mathrm{Ph}}(q, q'; k, k') = \left[\coth\left(\frac{cq'}{2T} \right) - \coth\left(\frac{c(k'-k)}{2T} \right) \right] \left[\tanh\left(\frac{ck'}{2T} \right) - \tanh\left(\frac{ck}{2T} \right) \right] . \qquad (3.78)$$

In the limit $k, q \ll m^*c$, the terms with the divergent factor $\coth\left(\frac{cq'}{2T} \right)$ dominate as a consequence of the conservation of energy and momentum and, substituting Eq. (3.78) into Eq. (3.77), the expression simplifies to,

$$\mathrm{Im}\Pi^{\mathrm{R}}(q) = -\frac{1}{2\pi^2} \frac{T\Gamma_0'^{\,2}}{256\,(m^*)^2} q^2 \int dk\, k^4 \left[\tanh\left(\frac{c}{2T}\frac{k+q}{2} \right) - \tanh\left(\frac{c}{2T}\frac{k-q}{2} \right) \right] ,$$
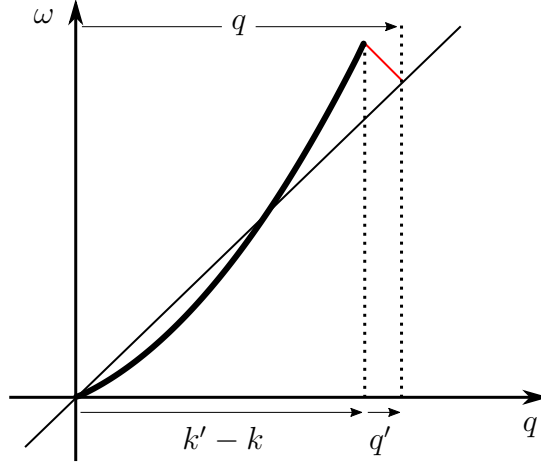
Figure 3.7: Kinematics of the scattering process described by the diagram in Fig. 3.6. The black thick line represents the spectrum of right moving fermions and the black and red thin lines the spectrum of right and left moving phonons. Given the weak non-linearity m^{*-1} of the fermionic spectrum, the momentum q' of the left-moving phonon is parametrically small with respect to q.

which leads to,[2]

$$\text{Im}\Pi^{\text{R}}(q) = -\frac{q^3}{\pi}\left[D + o\left(q^2\right)\right] \ . \tag{3.79}$$

where we defined the *diffusion coefficient*,

$$D = \frac{7\pi^3}{120}\frac{T^5\Gamma_0'^{\,2}}{(m^*c^2)^2} \ . \tag{3.80}$$

As we will see in the rest of this section, this coefficient describes the diffusion of phonons due to the scattering against fermions.

---

[2]Both domains of integration are in the range $|k|, |q| < Tq_0/c$, where q_0 is the momentum cut-off in Fig. 2.6. Since the integrand converges to zero exponentially for $|k|, |q| > Tq_0/c$, the integrals can be well approximated by extending the domain of integration to the entire real axis.

The Keldysh component is given by,

$$\Pi^{\mathrm{K}}(q) = \Pi_{\mathrm{qq}}(q)$$

$$= \frac{1}{(8\pi)^2} \frac{{\Gamma'_0}^2 c^2}{(m^*)^2} \int \frac{\mathrm{d}^2 k}{(2\pi)^2} \frac{\mathrm{d}^2 k'}{(2\pi)^2} q^2 (q+k-k')^2 (k+k')^4$$

$$\times \left[D_{\mp}^{\mathrm{K}}(q+k-k') \left(G_{\pm}^{\mathrm{K}}(k') G_{\pm}^{\mathrm{K}}(k) - \left(G_{\pm}^{\mathrm{R}}(k') - G_{\pm}^{\mathrm{A}}(k') \right) \left(G_{\pm}^{\mathrm{R}}(k) - G_{\pm}^{\mathrm{A}}(k) \right) \right) + \right.$$

$$- G_{\pm}^{\mathrm{K}}(k') \left(\left(D_{\mp}^{\mathrm{R}}(q+k-k') - D_{\mp}^{\mathrm{A}}(q+k-k') \right) \left(G_{\pm}^{\mathrm{R}}(k) - G_{\pm}^{\mathrm{A}}(k) \right) \right) +$$

$$\left. + G_{\pm}^{\mathrm{K}}(k) \left(D_{\mp}^{\mathrm{R}}(q+k-k') - D_{\pm}^{\mathrm{A}}(q+k-k') \right) \left(G_{\pm}^{\mathrm{A}}(k') - G_{\pm}^{\mathrm{R}}(k') \right) \right] ,$$

The calculation proceeds in the same way as for the retarded self-energy, with the difference that $\mathcal{F}_{\mathrm{Ph}}^{\mathrm{R}}$ gets replaced by,

$$\mathcal{F}_{\mathrm{Ph}}^{\mathrm{K}}(k, k'; q, q') = F_{\mathrm{Ph}-}(q') \left(F_{\mathrm{F}+}(k') F_{\mathrm{F}+}(k) - 1 \right) - F_{\mathrm{F}+}(k') + F_{\mathrm{F}+}(k) ,$$

and leads to the result,

$$\Pi^{\mathrm{K}}(q) = -\frac{2}{\pi} \mathrm{i} \left[D + o\left(q^2 \right) \right] q^3 \coth\left(\frac{cq}{2T} \right)$$
$$= \coth\left(\frac{cq}{2T} \right) \left(\Pi^{\mathrm{R}}(q) - \Pi^{\mathrm{A}}(q) \right) , \tag{3.81}$$

consistent with the fluctuation-dissipation theorem for the self-energy, Eq. (1.47). Now that we have calculated the polarisation, we proceed to the calculation of the equations of motions of phonons in the presence of fermions and the dynamical structure factor.

3.6.2 Phonon effective action

As we evaluated the polarisation in momentum-energy space, we take the Fourier transform of action $S_{\mathrm{Ph},+} = \int \mathrm{d}t \, L_{\mathrm{Ph},+}$, where $L_{\mathrm{Ph},+}$ is given by Eq. (3.74), and substitute results (3.79) and (3.81) at the lowest order in q,

$$S_{\mathrm{Ph},+} = \frac{1}{2\pi} \int \frac{\mathrm{d}\omega}{2\pi} \frac{\mathrm{d}q}{2\pi} \left[\tilde{\chi}_\eta^\alpha \left(q(\omega - cq) + \mathrm{i} q^3 D \right) \tilde{\chi}_{\eta\alpha} + \tilde{\chi}_+^{\mathrm{q}} \left(2\mathrm{i} D q^3 \coth\left(\frac{cq}{2T} \right) \right) \tilde{\chi}_+^{\mathrm{q}} \right]$$
$$- \frac{1}{2\pi} \int \mathrm{d}t \mathrm{d}x \, \frac{1}{m^*} (\tilde{\chi}_+^{\prime\mathrm{cl}})^2 \tilde{\chi}_+^{\prime\mathrm{q}} ,$$

Taking the Fourier transform back to position-time space, we have,[3]

$$S_{\text{Ph},+} = \frac{1}{\pi} \int \mathrm{d}t \mathrm{d}x \left\{ -\partial_x \tilde{\chi}_+^{\text{q}} \left((\partial_t + c\partial_x) - D\partial_x^2 \right) \tilde{\chi}_+^{\text{cl}} \right.$$
$$+ \mathrm{i} \frac{D}{2} \left[\frac{2T}{c} (\partial_x \tilde{\chi}_+^{\text{q}})^2 + \frac{\pi T^2}{2} \int \mathrm{d}x' \frac{(\partial_x \tilde{\chi}_+^{\text{q}}(x) - \partial_{x'} \tilde{\chi}_+^{\text{q}}(x'))^2}{\sinh^2 \left[\pi \frac{T}{C} (x - x') \right]} \right]$$
$$\left. - \frac{1}{2m^*} (\tilde{\chi}_+^{\prime\text{cl}})^2 \tilde{\chi}_+^{\prime\text{q}} \right\} ,$$

In the semiclassical limit, the last term in the second line is zero [13] and the remaining quadratic term in the quantum field can be split by means of a Hubbard-Stratonovich transformation in the field ξ,

$$S_{\text{Ph},+} = -\frac{1}{\pi} \int \mathrm{d}t \mathrm{d}x \, \partial_x \tilde{\chi}_+^{\text{q}} \left\{ \left((\partial_t + c\partial_x) - D\partial_x^2 \right) \tilde{\chi}_+^{\text{cl}} - \xi + \frac{1}{2m^*} (\partial_x \tilde{\chi}_+^{\text{cl}})^2 \right\} ,$$

where ξ is a real Gaussian random field with second momentum given by,

$$\langle \xi(x)\xi(x') \rangle = 4\pi \frac{DT}{c} \delta(x - x') . \tag{3.82}$$

Finally, the integration over the quantum field gives the semiclassical equation of motion,

$$(\partial_t + c\partial_x) \tilde{\chi}_+^{\text{cl}} = -\frac{\left(\partial_x \tilde{\chi}_+^{\text{cl}} \right)^2}{2m^*} + D\partial_x^2 \tilde{\chi}_+^{\text{cl}} + \xi . \tag{3.83}$$

This is the equation of motion of phonons in the presence of a thermal bath of fermionic quasiparticles. The left hand side describes the motion of a phonon with velocity c. In the right hand side we have three terms. The first is the nonlinearity of phonons derived in last chapter. The second term, proportional to the second space derivative, represents the diffusion of phonons due to the presence of fermions, justifying the identification of D with the diffusion coefficient made before. The third term represents the noise that phonons experience due to the presence of fermions. Diffusion and noise are related by the fluctuation-dissipation theorem in the form of Eq. (3.82): the diffusion represents the

---

[3]See Ref. [13] for the Fourier transform of the term $\sim (\tilde{\chi}_+^{\text{q}})^2$.

dissipation and the noise represents the fluctuations.

The kinetic equation of phonons, Eq. (3.83), can be identified with the celebrated Kardar-Parisi-Zhang (KPZ) equation for the dynamics of interface growth [59, 60, 61]. Therefore, we connected the low temperature semiclassical dynamics of one-dimensional systems to the Kardar-Parisi-Zhang universality class. The connection between one-dimensional quantum gases and the KPZ equation was first conjectured and verified numerically in Ref. [62] using the Gross-Pitaevskii equation. Examples of processes modelled using the KPZ equation include particle deposition on a surface, turbulent liquid crystals, crystal growth on a thin film, facet boundaries, bacteria colony growth, paper wetting, crack formation and burning fronts.[4] All these processes are said to belong to the KPZ universality class. Recently it was shown that particles forming coffee-rings, through their deposition on the edge of the rings, provide the first easily-tuned example and one of the few direct tests of the KPZ equation [64]. Given our result, one-dimensional atomic gases, having high versatility and experimental control, may represent in the future another easily-tuned direct test of the KPZ equation.

Now we discuss the effect of each term in the KPZ equation, Eq. (3.83), on the kinetics of the chiral phase, $\tilde{\chi}_+^{\mathrm{cl}}$, with the help of Fig. 3.8. Starting from the left hand side, the second term leads the chiral phase to drift to the right with velocity c. On the right hand side, the first term tells us that $\tilde{\chi}_+^{\mathrm{cl}}$ increases in the regions where the curvature is higher. This term being slope dependent, the time evolution of $\tilde{\chi}_+^{\mathrm{cl}}$ at some position x depends on the values in its vicinity, adding the attribute of locality to the KPZ equation. The second term on the right hand side provides diffusion, leading to a smoothening of peaks and wells. The third term provides noise, randomly and locally increasing or decreasing the value of $\tilde{\chi}_+^{\mathrm{cl}}$.

The KPZ equation governs the dynamics of the right moving chiral field, $\tilde{\chi}_+^{\mathrm{cl}}$. The same equation, with a minus sign in front of c, governs the dynamics of the left moving chiral field, $\tilde{\chi}_-^{\mathrm{cl}}$. As is seen from partition function (2.56), the dynamics of the density is

---

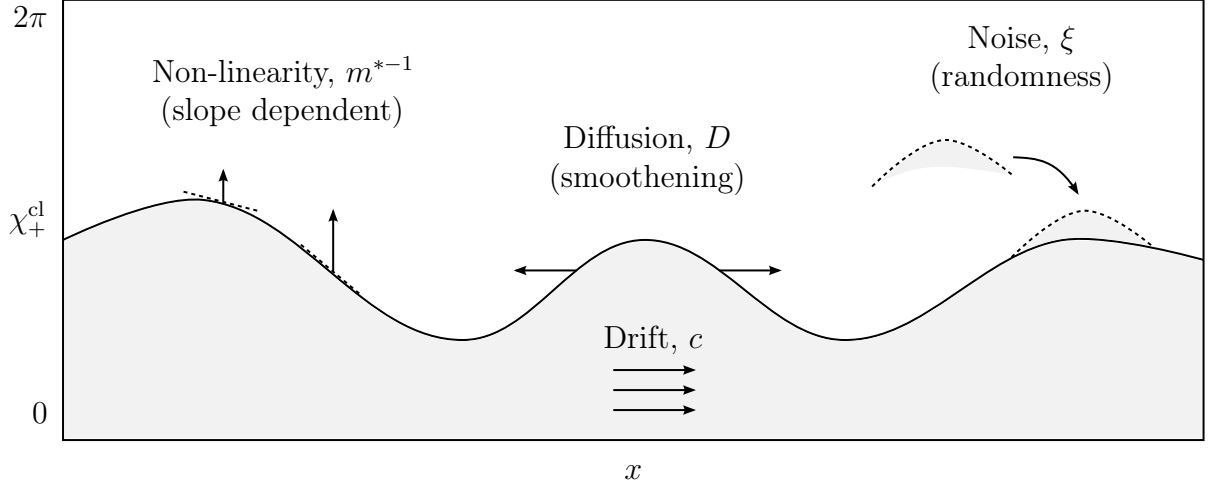[4]See Ref. [63] and references therein.

Figure 3.8: Cartoon explaining the effect of each term in the KPZ equation, Eq. (3.83). Note that the slope of $\tilde{\chi}^{\mathrm{cl}}_+$ has been exaggerated in order to better understand its kinetics. The arrows show the time evolution of $\tilde{\chi}^{\mathrm{cl}}_+$ due to the various terms in the KPZ equation.

proportional to the gradient of $\tilde{\chi}^{\mathrm{cl}}_+ + \tilde{\chi}^{\mathrm{cl}}_-$. Therefore, the important quantity for the study of density-density correlations is the slope of $\tilde{\chi}^{\mathrm{cl}}_+$ and $\tilde{\chi}^{\mathrm{cl}}_-$, as can be also seen from Eq. (3.73).

Now the we know the time evolution of $\tilde{\chi}^{\mathrm{cl}}_+$, we can calculate the dynamical structure factor, Eq. (3.73). The dynamical structure factor of a system obeying the KPZ equation was obtained in Ref. [65]. Since the derivation is laborious, we omit it here and give just the result. The dynamical structure factor was found in terms of the universal function $\mathring{f}(s)$, called polynuclear function, describing the scaling limit of the polynuclear growth model, a model for layer-by-layer growth through deposition from ambient atmosphere. The equation satisfied by the polynuclear function, $\mathring{f}(s)$, has only been solved numerical and leads to a function with the shape of a bell centred at $s = 0$ and with unitary width and height. In terms of this function, the dynamical structure factor reads,

$$S(q, \omega) = \frac{T}{c} \frac{K}{2\pi} \frac{1}{\delta\omega_{\mathrm{Ph}}(q)} \mathring{f}\left(\frac{\omega - cq}{\delta\omega_{\mathrm{Ph}}(q)}\right) , \tag{3.84}$$

where,

$$\delta\omega_{\mathrm{Ph}}(q) = \sqrt{\frac{2T}{m^{*2}c}} \, q^{\frac{3}{2}} . \tag{3.85}$$

106

Given the unitary width and height of the polynuclear function, the dynamical structure factor is centred at $\omega = cq$, has width $\delta\omega_{\mathrm{Ph}}(q) \sim q^{\frac{3}{2}}$ and height $\frac{T}{c}\frac{K}{2\pi}\frac{1}{\delta\omega_{\mathrm{Ph}}(q)}$.

It is interesting to note that the dynamical structure factor does not depend on D, characterising diffusion and noise and, therefore, on the relaxation mechanism. This is a consequence of $\mathring{f}(s)$ being a universal function in the scaling limit, that is, valid in the limit of very large distances or small momenta. With this in mind, we study the dynamical structure factor of KPZ equation (3.83) without either the non-linearity or the diffusion and noise. We start from the equation without non-linear term. Then, KPZ equation (3.83) reduces to,

$$\left(\partial_t + c\partial_x - D\partial_x^2\right)\tilde{\chi}_+^{\mathrm{cl}} = \xi \,.$$

We Fourier transform it, find the expression of $\tilde{\chi}_+^{\mathrm{cl}}$ in terms of ξ, substitute it in Eq. (3.73) and evaluate the average with respect to ξ using Eq. (3.82) to find that the dynamical structure factor is proportional to a Lorentzian with width $\sim DTq^2$.

We turn to the KPZ equation without diffusion and noise,

$$\left[\partial_t + \left(c + \frac{\partial_x \tilde{\chi}_+^{\mathrm{cl}}}{2m^*}\right)\partial_x\right]\tilde{\chi}_+^{\mathrm{cl}} = 0 \,, \tag{3.86}$$

First, to have an equation for the density of right movers, $\rho_+ \sim \partial_x \tilde{\chi}_+^{\mathrm{cl}} = \tilde{\chi}_+'^{\mathrm{cl}}$, we differentiate Eq. (3.86) by ∂_x,

$$\left[\partial_t + \left(c + \frac{1}{m^*}\tilde{\chi}_+'^{\mathrm{cl}}\right)\partial_x\right]\tilde{\chi}_+'^{\mathrm{cl}} = 0 \,. \tag{3.87}$$

From this equation, we see that the non-linearity can be restated in terms of a sound velocity dependent on phononic fluctuations of the liquid. Indeed, the presence of a phonon changes the density and velocity of the background liquid as $n \to n + \rho$ and $0 \to 0 + v$, as shown in Fig. 3.2. Then, the sound velocity in presence of a phonon is,

$$\begin{aligned} c(n) \to \quad & c(n + \rho) + v \\ \approx \ & c(n) + \partial_n c(n)\rho + v \\ \approx \ & c(n) + \frac{1}{m^*}\tilde{\chi}_+' \,, \end{aligned} \tag{3.88}$$

where in the second line we expanded to the first order in small density fluctuations, ρ, and in the third line we used Eq. (3.22) together with Eq. (C.6) and we neglected the left chiral field, $\tilde{\chi}_-$, for a reason explained later. Using Eq. (3.88), we interpret Eq. (3.87) as the equation of a phonon, $\tilde{\chi}'^{\mathrm{cl}}_+$ outside the square brackets, traveling on a region of the liquid where another phonon is present, $\tilde{\chi}'^{\mathrm{cl}}_+$ inside the brackets. In this way, the first phonon experiences a static background liquid plus the small variations due to the second phonon: the first phonon travels over the second phonon and, as a consequence, travels with a modified sound velocity. In light of this interplay of two phonons, we neglected $\tilde{\chi}'_-$ in the last line of Eq. (3.88) because the overlapping time for two phonons moving in different directions, $\sim c^{-1}$, is much shorter than for two moving in the same direction, $\sim m^*$.

Now we derive the width of the dynamical structure factor due to the non-linearity, m^{*-1}, following the argument of Refs. [66, 67]. If the non-linearity is not present, than Eq. (3.87) tells that all phonons move with the same velocity, which means that only excitations with momentum q and energy ω, satisfying $\omega = cq$, can be created. Consequently, the dynamical structure factor is non-zero only on the line $\omega = cq$. The presence of the non-linearity smears this line to an extent $\delta\omega(q) = \delta c(q)\, q$, where $\delta c(q)$ is the deviation of the velocity fluctuations at a certain point and time due to phonons with wavelength larger than q^{-1}. Only phonons larger than q^{-1} contribute to the fluctuations of a phonon with wavelength q^{-1} because it experiences a modified velocity only when traveling over a larger phonon and the effect of smaller phonons is averaged out. Then, using Eq. (3.88), the square of the velocity fluctuations is,

$$\delta c^2(q) = \frac{1}{m^{*2}}\langle|\partial_x \tilde{\chi}^{\mathrm{cl}}_+(x,t)|^2\rangle = \frac{1}{m^{*2}}\int_{-q}^{q}\frac{\mathrm{d}q'}{2\pi}\pi q'\coth\left(\frac{cq'}{2T}\right)\approx\frac{2T}{m^{*2}c}\,q\,,\qquad(3.89)$$

where in the second equality we took the Fourier transform and used the Keldysh propagator for $\langle|\partial_x \tilde{\chi}^{\mathrm{cl}}_+(x,t)|^2\rangle$, Eqs. (3.41) and (3.43), and in the third equality we considered just the

first term of the asymptotic expansion of coth at small momenta, since $q < T/c$. Using Eq. (3.89), we find the width,

$$\delta\omega(q) = \delta c(q)\, q = \sqrt{\frac{2T}{m^{*2}c}}\, q^{\frac{3}{2}}$$

that coincides with the characteristic width of the KPZ equation, Eq. (3.85).

From the widths of the KPZ equation without non-linear term or without diffusion and noise it becomes clear that the second one, that scales like $\sim q^{3/2}$, dominates over the first one, that scales like $\sim q^2$, at small momenta. Therefore, as KPZ equation (3.84) is valid in the scaling limit, namely at small momenta, there is no contribution from dissipation and noise. From a different point of view, smaller momenta are related to processes closer to equilibrium, so that dissipation and noise, characterising the equilibration process, play a marginal role. So, it seems that fermions do not influence the dynamics of phonons. However, they control the region of validity of the phononic contribution to the dynamical structure factor: after a time τ fermions reach equilibrium and they do not contribute anymore, leaving the dynamics to phonons. Then, phonons contribute to the dynamics for times longer than τ or energies smaller than τ^{-1}. This is consistent with the fact that the height of the phonon contribution to the dynamical structure factor, Eq. (3.84), scales like $\sim q^{-3/2}$, dominating at small momenta over the constant height of the fermion contribution, Eq. (3.71), in the collisional regime. In the next section we will see that τ^{-1} is very small, justifying the scaling limit approximation. Now that we have both fermionic and phononic contributions to the dynamical structure factor, in the next section we put them together to build the whole picture.

3.7 Dynamical Structure Factor at small temperatures

In this section we put together the results found in this chapter in the graphical form of Fig. 3.9. We build the picture from right to left, starting from higher and proceeding towards lower momenta. When a weak density perturbation is applied to the system, before time
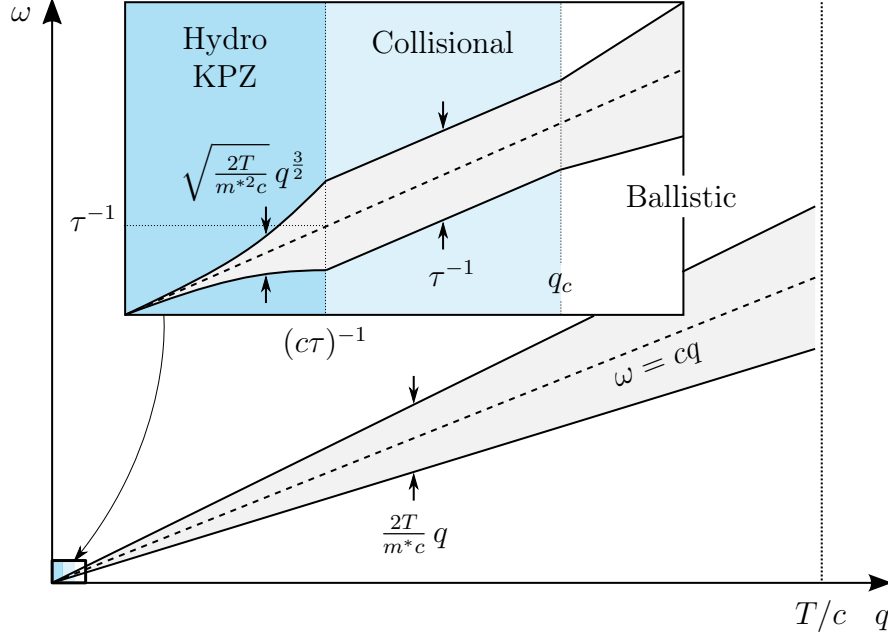
Figure 3.9: Dynamical structure factor as a function of momentum q and energy ω. The grey areas represent qualitatively the widths of the bell-shaped distributions at fixed q as a function of ω. At momenta lower than T/c and energies lower than T, there are three regimes distinguished by the colours: from right to left we have ballistic fermionic quasiparticles (Ballistic), fermionic quasiparticles colliding against phonons (Collisional) and non-linear phonons on a thermal bath of fermionic quasiparticles (Hydro KPZ).

T^{-1} the dynamics is dominated by quantum effects. The dynamics at these short times is reviewed in Ref. [7]. In this work we studied the thermal dynamics of one-dimensional systems, characterising times larger than T^{-1}: after a time T^{-1}, the density perturbation propagates trough the systems by means of effective thermal excitations.

The excitations that dominate the dynamics at shorter times after T^{-1} are free fermionic quasiparticles with effective mass m^* moving with average velocity c. These fermions propagate ballistically until a time $1/cq_c$, when they start to collide against phonons. We call the regime *ballistic* between times T^{-1} and $1/cq_c$. In this regime, corresponding to energies $cq_c < \omega < T$ and momenta $q_c < q < T/c$, the dynamical structure factor is given by Eq. (3.69) and is characterised by width (3.70), linear in q. The ballistic regime is represented in white colour in Fig. 3.9.

At times longer than $1/cq_c$ the fermionic quasiparticles start to collide with phonons until they reach equilibrium after a time τ, defining the *collisional* regime. In this regime,

corresponding to energies $\tau^{-1} < \omega < cq_c$ and momenta $(c\tau)^{-1} < q < q_c$, the dynamical structure factor is given by Eq. (3.71) and has a constant width τ^{-1}, as shown in the light blue region in Fig. 3.9.

Finally, after time τ, fermions equilibrate and the dynamics is given by non-linear phonons in the thermal bath of fermions, defining a *hydrodynamical KPZ* regime. In this regime, corresponding to energies $0 < \omega < \tau^{-1}$ and momenta $0 < q < (c\tau)^{-1}$, the dynamical structure factor is given by Eq. (3.84) and has a width given by Eq. (3.85) and proportional to $q^{3/2}$, as shown in the blue region in Fig. 3.9. As we saw in the previous section, this width arise from a two-phonon semiclassical dynamics.

The most important quantity characterising the dynamics in Fig. 3.9 is the relaxation time of fermions, τ, given by Eq. (3.65), because it controls the boundary between the regions where the dynamics is due to phonons or fermions. Since τ^{-1} is proportional to the seventh power of temperature, at small temperatures it is very small, meaning that the greatest part of thermal dynamics is dominated by fermionic quasiparticles. Besides, τ^{-1} is proportional to the inverse square of the effective mass, m^{*-2}, and as a consequence to the inverse square of the mass of the original particles, m^{-2}. Then, in the case where the original particles are fermions with linear spectrum, $m^{-1} \to 0$, the relaxation time becomes infinite, meaning that the thermal dynamics is govern just by depletons. But for fermions with linear spectrum the width of the dynamical structure factor, Eq. (3.70), tends to zero. This is consistent with the fact that fermions with linear spectrum can be exactly mapped into non-interacting phonons, that, as previously seen in this chapter, leads to the support of the dynamical structure factor being given by the single line, $\omega = cq$, with no width. So, as expected, fermions with linear spectrum and non-interacting phonons give the same result. Lastly, τ^{-1} is proportional to the square of the backscattering parameter, $\Gamma_0'^2$. The backscattering parameter, Γ_0', characterises the rate of backscattering between fermions and phonons. Since both fermions and phonons represent excitations of the original system, if we start with an integrable model, the excitations do not interact with each others, leading to $\Gamma_0' = 0$. These integrable models include models solvable by Bethe ansatz, such

as the Lieb-Liniger and Yang-Yang models describing bosons with contact interaction at zero and finite temperature [42, 68, 69]. It is instructive to evaluate the explicit value of Γ'_0 for a system of bosons with contact repulsion, described by Lagrangian (2.42), with the addition of a weak three-body interaction, $-\frac{\alpha}{6}(\bar{\varphi}\varphi)^3$, that breaks the integrability of the system. First we check the integrable case, $\alpha = 0$, for which we should find $\Gamma'_0 = 0$. Substituting the mean-field chemical potential, $\mu(n)$, and sound velocity, $c(n)$, Eqs. (2.43) and (2.47), into Eq. (3.33) and using Eq. (C.6), we find,

$$\Gamma'_0 = \frac{1}{16mc^2n} \, . \tag{3.90}$$

Contrary to our expectations, this parameter is not zero. This, however, is a spurious artefact of the mean-field approximation for the chemical potential, $\mu(n)$, in Eq. (2.43) [70, 71]. In the non-integrable case, Eqs. (2.43) and (2.47) become,

$$\mu(n, \alpha) = gn + \frac{\alpha}{2}n^2 \, ,$$
$$c(n, \alpha) = \sqrt{\frac{gn + \alpha n^2}{m}} \approx \sqrt{\frac{gn}{m}} \left(1 + \frac{\alpha n}{2g}\right) \, .$$

Using these expression and subtracting the spurious mean-field offset, Eq. (3.90), we obtain,

$$\Gamma'_0 \approx -\frac{1}{48} \frac{\alpha n}{m^2 c^4} \, .$$

up to the first order in α. Using this value of the backscattering parameter, we estimate the relaxation time, τ, for the experiment of Ref. [28]. Using $\alpha = 12 \ln(4/3)\hbar a^2 \omega_\perp$ [72, 73], where a is the scattering length and $\omega_\perp$ is the frequency of transverse confinement used to create a one-dimensional system, we can recast Eq. (3.65) into dimensionless form,

$$\frac{\hbar}{\tau mc^2} = \frac{A}{K^3} \left(\frac{mc^2}{\hbar\omega_\perp}\right)^2 \left(\frac{k_B T}{mc^2}\right)^7 \, ,$$

where the numerical factor $A = 9\pi^7 \left(\ln(4/3)\right)^2 / 2^{15} \simeq 0.07$ and we reintroduced the Planck and Boltzmann constants. For the experiment in Ref. [28], $K \sim 10$, $mc^2/\hbar \sim 5.5$ kHz and

$\omega_\perp \sim 66$ kHz, which results in τ of the order of tens of seconds even for $k_B T/mc^2 = 1$. Because of the T^7 dependence, decreasing the temperature will result in even longer relaxation times. Since for these experimental parameters we have $\tau \approx 1/cq_\mathrm{c}$, the collisional regime would require times of the order of τ, making the fermionic ballistic result the only one likely to be observed. In conclusion, we have shown that the hydrodynamic description of one-dimensional bosons is only valid for times longer than τ. The latter diverges as one approaches the integrable point, and a non-hydrodynamic behaviour due to fermionic quasiparticles prevails.

3.8 Weakly-interacting bosons

In the previous section we saw the importance of the ballistic regime in the thermal dynamics of one-dimensional systems. However, we have not discussed the limitations imposed to weakly interacting bosons by the small momentum approximation on the fermionic quasiparticle spectrum mentioned in Sec. 2.3,

$$q \ll p_\mathrm{G} = \frac{3}{\sqrt{K}}\, mc \,,$$

where p_G is the Ginzburg momentum [46, 47, 74]. This section constitutes the last original part of this work. The Ginzburg momentum is found by comparing the value of the momentum for which the quadratic spectrum,

$$\varepsilon(p) = cp + \frac{p^2}{2m^*} \,, \quad p \ll p_\mathrm{G} \,,$$

crosses over to the Bogoliubov spectrum,

$$\varepsilon(p) = cp\sqrt{1 + \frac{p^2}{4m^2c^2}} \approx cp + \frac{p^3}{8m^2c} \,, \quad p \gg p_\mathrm{G} \,.$$

The two energies match at momentum,

$$p_{\mathrm{G}} = 4 \left(\frac{m}{m^*} \right) mc = \frac{3}{\sqrt{K}} mc \, ,$$

where we used Eq. (2.55) for the value of the effective mass.

Since $K \gg 1$ for weakly interacting bosons, the region of validity of the fermionic quasiparticle description in Fig. 3.9 is very limited in the momentum axis. Therefore, for the complementary region,

$$p_{\mathrm{G}} = \frac{3}{\sqrt{K}} mc \ll q \ll \frac{T}{c} \, , \tag{3.91}$$

we need a different approach. Since we are dealing with weakly interacting gases, we can use a semiclassical approach. The validity of the semiclassical approximation relies on having a macroscopic number of particles in a healing length, $n\xi = \frac{1}{2}\sqrt{\frac{n}{mg}} \sim K \gg 1$, the same requirement seen in Sec. 3.8 for the validity of the mean-field theory [29]. For weakly interacting bosons we have $mg \ll n$ and the condition $n\xi \gg 1$ is satisfied. We use a semiclassical approach by dividing the one-dimensional systems in regions of length Δx such that,

$$\xi < \Delta x < q^{-1} \, .$$

as shown in Fig. 3.10. We refer to this approximation as local density approximation. This is because each region of length Δx is uncorrelated from the others since they are further apart than the correlation length, ξ. Moreover, we know that in each region of length Δx there are enough particles to use the semiclassical description and that the regions are small enough compared to variation of the external field probing the response to a perturbation with momentum q.

Within the local density approximation we calculate the dynamical structure factor,

$$S(q,\omega) = \int \mathrm{d}x \mathrm{d}t \, \langle \rho(x,t)\rho(0,0) \rangle \, e^{-i(qx-\omega t)} \, , \tag{3.92}$$

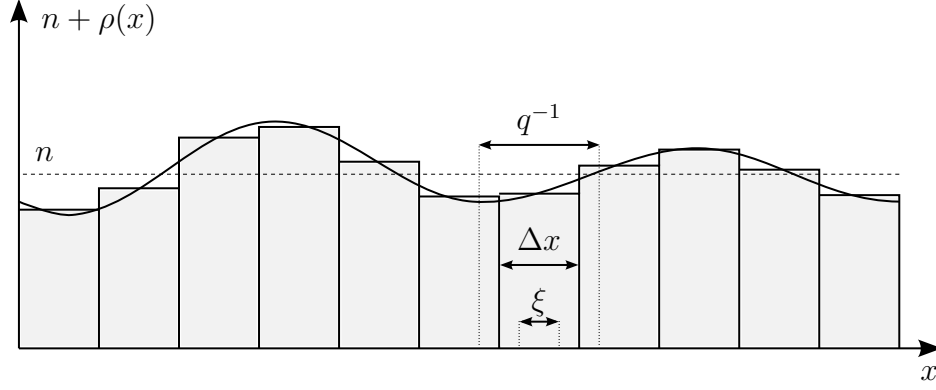where $\rho(x)$ is the density fluctuation over the homogeneous value, n, and the integral is

Figure 3.10: Local Density approximation. $\rho(x)$ is the density fluctuation at position x over the homogeneous value, n.

understood as a sum over the different regions of length Δx, $\int \mathrm{d}x \approx \Delta x \sum$. Now we use the result derived previously for which for times shorter τ, independent density excitations move ballistically,

$$\left(\partial_t + v(k)\partial_x\right) f(x, k, t) = 0 \tag{3.93}$$

where $f(x, k, t)$ is the density of states with rapidity, k, at position x and time t, satisfying the condition,

$$\rho(x, t) = \int \mathrm{d}k\, f(x, k, t)\,. \tag{3.94}$$

Here we decomposed the density in term of the rapidities or pseudo-momenta of the Lieb-Liniger model of bosons with contact repulsive interactions [42, 68]. We choose these rapidities because they label independent excitations that we need for the ballistic regime. In the case of weakly interacting bosons, these excitations with different rapidities take the place of the fermionic quasi-particles with different momenta given by Eq. (3.91). We will come back to these excitations later. Substituting decomposition (3.94) into Eq. (3.92) and using the solution of Eq. (3.93),

$$f(x, k, t) = f(x - v(k)t, k, t = 0)\,,$$

we have,

$$S(q, \omega) = \int \mathrm{d}k \int \mathrm{d}x\mathrm{d}t\, \langle f(x - v(k)t, k, 0)\rho(0, 0)\rangle\, e^{-i(qx - \omega t)}\,.$$

115

Making the shift $x \rightarrow x + vt$ and integrating over time, we find,

$$S(q, \omega) = 2\pi \int \mathrm{d}k \, \delta(\omega - v(k)q) \int \mathrm{d}x \, \langle f(x, k, 0)\rho(0, 0) \rangle \, e^{-iqx} \,.$$

Now we use the local density approximation to evaluate the last integral,

$$S(q, \omega) \approx 2\pi \int \mathrm{d}k \, \delta(\omega - v(k)q) \, \Delta x \sum_i \langle f(x_i, k, 0)\rho(x_0 = 0, 0) \rangle \, e^{-iqx_i} \,, \qquad (3.95)$$

where the index i labels the regions of length Δx. First we note that, since the regions are uncorrelated, the average is,

$$\langle f(x_0 = 0, k, 0)\rho(x_0 = 0, 0) \rangle \, \delta_{i,0} \,.$$

Substituting this expression into Eq. (3.95) and summing over i, we find,

$$S(q, \omega) = 2\pi \int \mathrm{d}k \delta(\omega - v(k)q) \, \langle f(0, k, 0)(\Delta x \rho(0, 0)) \rangle \,,$$

where $\Delta x \rho(0, 0)$ is the total number of particles in the region Δx. Since each region Δx contains a macroscopic number of particles, we use thermodynamics to evaluate the average. To use thermodynamics, we assume a weak density perturbation such that each region can be considered in thermodynamical equilibrium. Then, we use the fluctuation-dissipation theorem [56],

$$\langle f(0, k, 0)(\Delta x \rho(0, 0)) \rangle = T \partial_\mu \bar{f}(k) \,, \qquad (3.96)$$

where $\bar{f}(k)$ is the equilibrium density of states with rapidity k and is independent of space because we are considering a small perturbation over a homogenous system. Then, we have,

$$S(q, \omega) = \frac{2\pi T}{q} b \left(\frac{\omega}{q} \right) \,.$$

where we defined the velocity distribution,

$$b(v) = \int dk\, f_\mu(k)\delta(v - v(k)), \quad f_\mu(k) = \partial_\mu \bar{f}(k).$$ (3.97)

Thus, we found that the dynamical structure factor of weakly interacting bosons in the semiclassical approximation has hight proportional to q^{-1} and shape given by the thermodynamical velocity distribution, $b(v = \omega/q)$, that depends just on the ratio between energy and momentum ω/q. This result is similar to the case of fermionic-quasiparticles, Eq. (3.69), where the height is proportional to q^{-1} and the shape is given by a $\cosh^{-2}$ distribution dependent only on the ratio ω/q. To complete the study, in the following part of the section we examine the velocity distribution, $b(v)$.

3.8.1 Velocity distribution

To evaluate the velocity distribution, Eq. (3.97), we employ the Yang-Yang model, describing the thermodynamics of the Lieb-Liniger model of bosons with a repulsive contact interaction [69]. The Hamiltonian of the Lieb-Liniger model in terms of first quantisation is given by [42, 68],[5]

$$\hat{H} = -\frac{\hbar^2}{2m}\sum_{i=1}^{N}\partial_{x_i}^2 + g\sum_{i>j}\delta(x_i - x_j).$$

The thermodynamics of this model was solved exactly by Yang and Yang using the Bethe ansatz, leading to the integral equation for the spectrum [69],

$$\varepsilon(k) = -\mu + \frac{k^2}{2m} - \frac{T}{\pi}\int_{-\infty}^{\infty} dq\, \frac{mg}{(mg)^2 + (k-q)^2}\, \log\left(1 + e^{\varepsilon(q)/T}\right)$$ (3.98)

---

[5]Note that the relation with the parameters in the original paper by Lieb-Liniger is obtained by the substitutions $g \to c/m$ and $H \to H/2m$.

where k and q are rapidities. The density of states in terms of the rapidities is found using the relation,[6]

$$\bar{f}(k) = -\frac{\partial_\mu \varepsilon(k)}{2\pi \left(1 + e^{\varepsilon(k)/T}\right)}, \qquad (3.99)$$

which leads to the equation,

$$\bar{f}(k)\left(1 + e^{\varepsilon(k)/T}\right) = \frac{1}{2\pi} + \frac{1}{\pi}\int_{-\infty}^{\infty} dq \, \frac{mg}{(mg)^2 + (k-q)^2} \, \bar{f}(q) \qquad (3.100)$$

Differentiating with respect to the chemical potential, μ, and using Eq. (3.99), we derive the integral equation for $\partial_\mu \bar{f}(k) = f_\mu(k)$ in Eq. (3.97),

$$f_\mu(k) = \frac{2\pi}{T}\varrho(k)^2 e^{\varepsilon(k)/T} + \frac{1}{1 + e^{\varepsilon(k)/T}}\frac{1}{\pi}\int_{-\infty}^{\infty} dq \, \frac{mg}{(mg)^2 + (k-q)^2} \, f_\mu(q). \qquad (3.101)$$

To evaluate $b(v)$ using Eq. (3.97) we also need the velocity of the excitations, $v(k)$, as a function of the rapidity, k, given by,

$$v(k) = \frac{\partial E(k)}{\partial p(k)} = \frac{\partial E(k)}{\partial k}\left(\frac{\partial p(k)}{\partial k}\right)^{-1}, \qquad (3.102)$$

where $E(k)$ and $p(k)$ are the energy and momentum of an excitation with rapidity k. As we will see later, $f_\mu(k)$, depends strongly on the temperature in the small temperature limit, $T \ll \mu$, so that we can neglect the small temperature corrections to the velocity [75]. Therefore, for the calculation of $v(k)$ we use the zero temperature limit, $T \to 0$, of Eqs. (3.98) and (3.100) for the spectrum and density of states,

$$\varepsilon(k) = -\mu + \frac{k^2}{2m} + \frac{1}{\pi}\int_{-k_0}^{k_0} dq \, \frac{mg}{(mg)^2 + (k-q)^2} \, \varepsilon(q),$$

and,

$$\bar{f}(k) = \frac{1}{2\pi} + \frac{1}{\pi}\int_{-k_0}^{k_0} dq \, \frac{mg}{(mg)^2 + (k-q)^2} \, \bar{f}(q), \qquad k^2 < k_0^2.$$

---

[6]Here, $\bar{f}(k)$ correspond to $\rho(k)$ in Ref. [69].

118

where k_0 is the rapidity such that $\varepsilon(k_0) = 0$ at zero temperature. The energy, $E(k)$, is related to the spectrum $\varepsilon(k)$ as [68, 76],

$$E(k) = \begin{cases} \varepsilon(0) - \varepsilon(k), & |k| \leq k_0 \\ \varepsilon(k) - \varepsilon(0), & |k| > k_0, \end{cases} \tag{3.103}$$

and the momentum, $p(k)$, is related to the density of states, $\bar{f}(k)$, as [68, 76],

$$p(k) = \begin{cases} k - \pi n + 2 \int_{-k_0}^{k_0} dq \, \text{arctanh}\left(\frac{q-k}{mg}\right) \bar{f}(q), & |k| \leq k_0, \\ -k + \int_{-k_0}^{k_0} dq \left[\pi - 2 \, \text{arctanh}\left(\frac{q-k}{mg}\right) \bar{f}(q)\right], & |k| > k_0, \end{cases} \tag{3.104}$$

Since $E(k)$ and $p(k)$ are even functions of k, we focus only on positive rapidities. The solutions of the spectrum and density of states equations in the weakly interacting limit, $g \to 0$, is found in Appendix D and reads,

$$\varepsilon(k) = \begin{cases} -\frac{1}{6m^2 g}\left(k_0^2 - k^2\right)^{\frac{3}{2}}, & k \leq k_0 \\ \frac{1}{2m} k \sqrt{k^2 - k_0^2}, & k > k_0. \end{cases} \tag{3.105}$$

and,

$$\bar{f}(k) = \begin{cases} \frac{1}{2\pi m g} \sqrt{k_0^2 - k^2}, & k \leq k_0 \\ 0, & k > k_0. \end{cases} \tag{3.106}$$

where,

$$\begin{aligned} k_0 &= 2\sqrt{mgn} = 2mc, \\ \mu &= \frac{k_0^2}{4m}. \end{aligned} \tag{3.107}$$

Using Eqs. (3.105) and (3.106) into Eqs. (3.103) and (3.104) we find [76],

$$E(k) = \begin{cases} \frac{1}{6m^2 g}\left(k_0^2 - k^2\right)^{\frac{3}{2}}, & k \leq k_0 \\ \frac{1}{2m}|k|\sqrt{k^2 - k_0^2}, & k > k_0. \end{cases}$$

and,

$$p(k) = \begin{cases} 2n \left(\arccos \frac{k}{k_0} - \frac{k}{k_0} \sqrt{1 - \frac{k^2}{k_0^2}} \right) , & |k| \le k_0 , \\ \sqrt{k^2 - k_0^2} , & |k| > k_0 , \end{cases}$$

Using these expressions for the energy and momentum of excitations in Eq. (3.102), we find the relation between the velocity and the rapidity,

$$v(k) = \begin{cases} \frac{k}{2m} , & k \le k_0 \\ \frac{1}{2m} \left(\frac{2k^2 - k_0^2}{k} \right) = \frac{k}{m} - \frac{k_0^2}{2m} \frac{1}{k} , & k > k_0 . \end{cases}$$

Inverting the relation we find,

$$k(v) = \begin{cases} 2mv , & v \le c \\ \frac{m}{2} v (1 + \sqrt{1 + 8(c/v)^2}) , & v > c . \end{cases}$$

This expression for the velocity is continuous but not differentiable at $v = c$. This is due to solutions (3.105) and (3.106) being more accurate further away from $v = c$. However, using Eqs. (3.104) and (3.100) it can be shown that at zero temperature the corrections are exponentially small in the weakly interacting limit. Using this relation in Eq. (3.97), we have,

$$b(v) = |\partial_v k(v)| \, f_\mu(k(v))$$

$$\approx \begin{cases} 2m \, f_\mu(2mv) , & v \le c \\ \left[\frac{m}{2} v \left(1 + \frac{1}{\sqrt{1 + 8(c/v)^2}} \right) \right] f_\mu \left(\frac{m}{2} v (1 + \sqrt{1 + 8(c/v)^2}) \right) , & v > c , \end{cases}$$

The non-differentiability of $k(v)$ at $v = c$ manifests itself in a discontinuity for $b(v)$ at $v = c$. However this is just an artefact of the approximate analytical solution for $k(v)$.

What remains to be done is to evaluate $f_\mu(k)$ using Eq. (3.101). As Eq. (3.101) cannot be solved analytically, we resort to a numerical evaluation. To do so, it is convenient to use dimensionless quantities: $k = k_0 x$, $q = k_0 y$, $\nu = 2m\mu/k_0^2$, $\lambda = mg/k_0$, $e(x) = 2m\varepsilon(k_0 x)/k_0^2$,
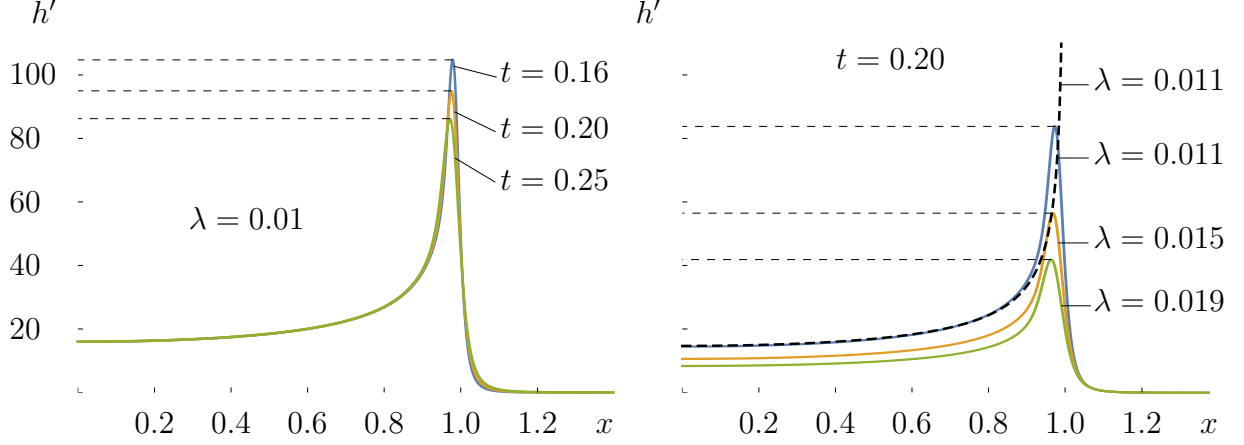
Figure 3.11: Numerical solution of $h'(x)$ from Eqs. (3.108) for different values of t and λ satisfying condition (3.109). The dashed line is the approximate analytical solution for $t = 0$, Eq. (3.111). The numerics was implemented in Wolfram *Mathematica*®.

$t = 2mT/k_0^2$, $h(x) = \bar{f}(k_0 x)$ and $h'(x) = k_0^2 f_\mu(k_0 x)/2m$. We rescaled the quantities using the zero temperature "Fermi rapidity" k_0 because we are in the limit $T \ll \mu$. In terms of these dimensionless quantities, Eqs. (3.98), (3.100) and (3.101) become,

$$e(x) = -\nu + x^2 - \tfrac{t}{\pi} \int_{-\infty}^{\infty} dy\, \tfrac{\lambda}{\lambda^2 + (x-y)^2} \log\left(1 + e^{e(y)/t}\right)$$

$$\downarrow$$

$$2\pi h(x)\left(1 + e^{e(x)/t}\right) = 1 + 2 \int_{-\infty}^{\infty} dy\, \tfrac{\lambda}{\lambda^2 + (x-y)^2} h(y) \tag{3.108}$$

$$\downarrow$$

$$h'(x) = \tfrac{2\pi}{t} h(x)^2 e^{e(x)/t} + \tfrac{1}{1 + e^{e(x)/t}} \tfrac{1}{\pi} \int_{-\infty}^{\infty} dy\, \tfrac{\lambda}{\lambda^2 + (x-y)^2} h'(y)\,.$$

Here the arrows indicate the order in which the equations have to be solved numerically because the equation for $h(x)$ depends on $e(x)$ and the equation for $h'(x)$ depends on $e(x)$ and $h(x)$. We need to solve these equations in the parameter range,

$$cp_{\mathrm{G}} = \frac{3}{\sqrt{K}}\mu < T < \mu\,,$$

which in dimensionless form becomes,

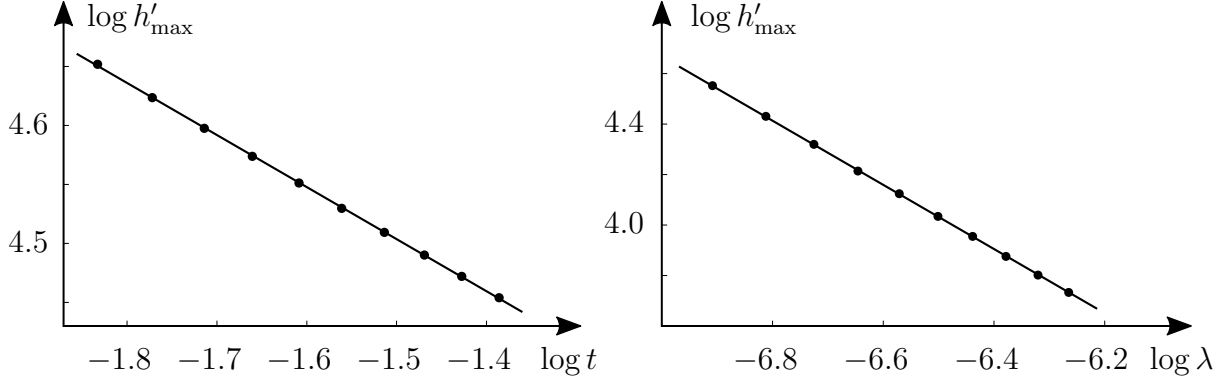$$1.6\,\sqrt{\lambda} \lesssim 2t < 1\,, \tag{3.109}$$

121

Figure 3.12: Dependence of the height of the peak, $h'_{\max}$, in Fig. (3.11) on t and λ. The plots are logarithmic in both axis. The linear interpolation of the left and right data plots give $\log h'_{\max} = 3.84 - 0.44 \log t$ and $\log h'_{\max} = -4.23 - 1.27 \log \lambda$. This means that $h'_{\max}(t, \lambda) \sim t^{-0.44} \lambda^{-1.27}$ in the parameter range given by Eq. (3.109). The fits were obtained using Wolfram *Mathematica*®.

where we used the identities $\lambda K = \pi/2$ and $\nu = 1/2$ for weakly interacting bosons. The numerical solution of $h'(x)$ is plotted in Fig. 3.11 for different values of t and λ satisfying condition (3.109). $h'(x)$ has a peak at $x \approx 1$, corresponding to $k \approx k_0 = 2mc$, and a non-zero region for $x < 1$. An asymptotic analysis of Eqs. (3.108) shows that for $x \gg 1$ the function has a Gaussian decay, $h'(x) \sim e^{-x^2}$. The left plot in Fig. 3.11 shows $h'(x)$ at fixed λ as for different temperatures, t. The temperature just modifies the peak at $x \approx 1$ and as the temperature becomes smaller the peak becomes higher. Therefore, for $2t \ll 1$ or $T \ll \mu$, the temperature affects just a region close to the peak. This is supported by the calculation of $f_\mu(k)$ at zero temperature, in the weakly interacting limit. Indeed, differentiating Eq. (3.106) with respect to μ and using Eq. (3.107) for the relation between μ and k_0, we have,

$$f_\mu(k) = \begin{cases} \frac{1}{\pi g} \frac{1}{\sqrt{k_0^2 - k^2}}, & k \le k_0 \\ 0, & k > k_0, \end{cases} \tag{3.110}$$

which in dimensionless form becomes,

$$h'(x) = \begin{cases} \frac{1}{2\pi\lambda} \frac{1}{\sqrt{1-x^2}}, & x \le 1 \\ 0, & x > 1. \end{cases} \tag{3.111}$$

122

This function, plotted as the dashed line in Fig. 3.11, fits the numerical solution outside a region of width $(T/c)^\alpha$ around the peak at $k \approx k_0$ or a region of width t^α around the peak at $x \approx 1$. However, we were not able to evaluate the exponent $\alpha > 0$ due to the widths of the peaks being too close together. The right plot in Fig. 3.11 shows $h'(x)$ at fixed t for different interaction strengths, λ. The non-zero region for $x < 1$ scales as $\sim \lambda^{-1}$ as can be shown by comparing the plot with Eq. (3.111) and the peak increases faster than $\sim \lambda^{-1}$ as λ decreases. The numerical solution allowed us to determine the dependence of the height of the peak, $h'_{\max}$, on t and λ. The dependence of $h'_{\max}$ on t and λ is shown in Fig. 3.12 and reads $h'_{\max}(t, \lambda) \sim t^{-0.44} \lambda^{-1.27}$. The power-law dependence may not be close to a simple fraction due to the chosen values of t and λ in the numerical simulation: due to a dramatic increase of the computational time, we were not able to choose smaller values of λ in order for condition (3.109) to be well satisfied. Therefore, the exponents of t and λ may not be close to a simple fraction because they are not far enough from the cross-over values, $1.6\sqrt{\lambda} \approx 2t = 1$. Apart from this limitation, the exponents of t and λ seem to suggest that $h'_{\max}(t, \lambda) \sim t^{-1/2} \lambda^{-5/4}$. The dependence on temperature can be explained by looking at the power-law divergence of $h'(x)$ at zero temperature at $x \approx 1$ in Eq. (3.111), $h'(x) \sim x^{-1/2}$. As can be seen in Fig. 3.11-left, by comparing the blue and dashed lines, the effect of the temperature seems to smooth out the divergence, replacing x with t. In other words, in Eq. (3.110), close to $k \approx k_0$, the rapidity, k, in the divergence, $f_\mu(k) \sim k^{-1/2}$, is replaced by the thermal momentum, T/c, such that $f_\mu(k \approx k_0) \sim T^{-1/2}$. The dependence on lambda instead can be split in two contributions: one coming from Eq. (3.111) at zero temperature, $\sim \lambda^{-1}$, and one coming from the smoothening of the peak, $\sim \lambda^{-1/4}$. Then, in terms of the interaction, g, the peak scales like, $f_\mu(k \approx k_0) \sim g^{-5/4}$.

We showed that for weakly interacting bosons, the dynamical structure factor for $p_G \ll q \ll T/c$,

$$ S(q, \omega) \sim \frac{1}{q} b\left(\frac{\omega}{q}\right), $$

has the same ballistic scaling obtained with fermionic quasiparticles, Eq. (3.69). They both have a peak at $\omega \approx cq$, their height scales like q^{-1} and the rest of the expression is only

123

a function of the combination ω/q. Since $b(\omega/q)$ depends on ω/q, the width of the both peaks scales linearly in q. The main difference from the case of fermionic quasiparticles is the non-zero region for $\omega < cq$, corresponding to $x < 1$ in Fig. 3.11. We also note that the profile of the dynamical structure factor just derived seems to be the extension of that found numerically in Ref. [77] in the opposite limit, $T/c < p_{\mathrm{G}}$, using the the integral equations from the Bethe ansatz solution.

Conclusions

In this thesis we explored the world of non-equilibrium one-dimensional quantum systems, in particular their thermal dynamics. We started with a pedagogical derivation of the non-equilibrium formalism of many-body quantum field theory using the Keldysh technique. The Keldysh formulation has been successfully improved over the years, moving from its initial operator form to the functional integral form. However, the derivation of the non-equilibrium functional integral was still based on the discretised time. In this work we developed a continuum approach, which results in a simpler derivation that leads to new insights on the relation between the classical and quantum fields of the non-equilibrium formalism.[7] The approach is set in the framework of differential equations, where the boundary conditions account for the initial distribution. Using the boundary conditions, we showed how a state with a smaller quantum field is more classical and we connected the classical field, the quantum field and the occupation of a state in a single equation. This equation shows that, consistently with statistical quantum mechanics, for a higher occupation of a state, the amplitude of the quantum field is smaller, corresponding to a more classical state. Finally, we generalised the continuum formalism to arbitrary non-interacting density matrices, suggesting possible applications to the quench dynamics of free effective theories.

Using the non-equilibrium quantum field theory developed in the first chapter, in the second chapter we gave a self-contained pedagogical presentation of the physics of one-dimensional quantum systems. This presentation constitutes the first original part of

---

[7]See Ref. [2] in the Publications section at the beginning of this thesis.

the second chapter.[8] We started with the derivation of the Tomonaga-Luttinger liquid for a system of interacting fermions. First, we considered the linear spectrum approximation, that amounts to neglecting the spectrum curvature. This is a good approximation at low energies, where there are mainly small particle-hole excitations around the two Fermi points. As a correction to this approximation, we calculated the first non-linear contribution arising from the spectrum curvature, corresponding to the interaction between three phonons. We checked the result obtained within the Keldysh formalism with a more rigorous approach based on the Matsubara formalism developed in Appendix B. Within the Matsubara formalism we evaluated the low-energy asymptotic contribution of the three- and four-phonon interactions to the action and some properties of the five-phonon interaction. With these results we conjectured the asymptotic curvature and temperature dependence of n-phonon interaction terms. The study of the curvature corrections within the Keldysh and Matsubara formalisms constitutes the second original part of the second chapter.[8] Then, we moved to interacting bosonic particles. We derived bosonization in the weak and strong interaction limits. In the weak interaction limit, we used the standard mean-field approach to derive the effective phononic action. In the strong interacting limit we decoupled the interaction term with a Hubbard-Stratonovich transformation and showed how a system of bosons with infinite repulsive interaction can be restated as a system of free fermions. Finally, we used the relation between non-linear phonons and interacting fermions to refermionise the system, that is, to derive an approximate theory of fermionic quasiparticles. The contents of the second chapter culminated in a map between fermionic and bosonic particles and bosonic and fermionic excitations, that is, phonons and fermionic quasiparticles. In particular, we noticed that the description of one-dimensional quantum systems in term of phonons and fermionic quasiparticles should be equivalent. However, studying the dynamical structure factor we saw that the equivalence applies only to static and zero-temperature dynamical properties and leads to different results for thermal dynamical properties, raising an apparent paradox.

---

[8]See Ref. [4] in the Publications section at the beginning of this thesis.

To solve the paradox, in the third chapter we studied the thermal dynamics of one-dimensional quantum systems. The third chapter represents the main contribution to this thesis.[9] We approached the study by observing that phonons and fermionic quasiparticles correspond respectively to excitations with long and short wavelengths. This observation allowed us to treat them on different grounds and construct a theory in which both excitations are present. To derive the interaction between phonons and fermionic quasiparticles, we used the depleton approach developed in Ref. [50] for the description of an impurity and the depletion cloud that the impurity induces in the liquid. The depleton approach was particularly useful in our case as we associated the depletion cloud localised around the impurity to the short-wavelength excitations of the system and used a massless impurity just to define the position and momentum of the excitations. We integrated over the depletion cloud in the partition function to define the effective, dressed, point-like impurity, because the fermionic quasiparticles derived in the second chapter are point-like excitations. Therefore, we obtained an effective theory of interacting phonons and fermionic quasiparticles. Within this theory, we proceeded with the calculation of the dynamical structure factor at low temperatures. As we are dealing with low temperatures and low energies, we considered small density variations for the density-density correlations in the dynamical structure factor. In this way, we found three regimes for the thermal dynamics of one-dimensional quantum systems. At higher energies or shorter times we have a ballistic regime, in which the dynamics are dominated by the free motion of fermionic quasiparticles. At lower energies or longer times we have a collisional regime, in which the fermionic quasiparticles experience collisions with phonons. Finally, at the lowest energies and longest times, we have a hydrodynamical regime, where the dynamics are governed by long wave-length non-linear phonons experiencing collisions with fermions. We found that the chiral phase fields described by the phonons satisfy the Kardar-Parisi-Zhang equation, thereby linking the low-energy thermal dynamics of one-dimensional quantum systems to the universality class of the dynamics of surface growth. This result could provide the base

---

[9]See Ref. [1] in the Publications section at the beginning of this thesis.

for future experimental tests of the Kardar-Parisi-Zhang dynamics. The most important result of this work is the determination of the time, τ, that separates the regime dominated by fermionic quasiparticles from the regime dominated by phonons. The time separating the regime of free and colliding fermions is of the same order of τ, meaning that the regime of colliding fermions is short with respect to the other two. Time τ is the relaxation time of fermionic quasiparticles: the dynamics is govern by fermionic quasiparticles until they relax to an equilibrium state after time τ, leaving the dynamics to phonons. There are three important parameters on which τ depends: temperature, particle mass and backscattering parameter. τ is inversely proportional to the seventh power of temperature, meaning that at low temperatures τ is an extremely long time. τ is proportional to the quasiparticle mass, which implies that in the case of linear fermions, τ is infinite. Finally, τ depends on the scattering rate between phonons and fermionic quasiparticles. As phonons and fermionic quasiparticles represent excitations of the system, for integrable models where all excitations are non-interacting, there is no scattering and τ is infinite. Therefore, one needs a term that breaks the integrability of the system, such as a density cubed interaction in the case of bosonic particles. All these dependences suggest that τ is a very long time compared to other time scales characterising a one-dimensional system. Indeed, calculating the value of τ for a typical cold atom experiment with interacting bosons, we saw that τ is too long to be experimentally reached yet, meaning that the regime of ballistic fermionic quasiparticles is the only one likely to be observed.

The approach based on phonons and fermionic quasiparticles has a limited range of validity in energy and momentum for weakly interacting bosons. The limitation arises because the spectrum of weakly interacting bosons is not quadratic for momenta greater than the Ginzburg momentum, p_{G}, and, therefore, cannot be mapped to the quadratic spectrum of fermionic quasiparticles. To derive the dynamical structure factor of weakly interacting bosons we used a semiclassical approach based on a local density approximation. As a result we saw that the dynamical structure factor of weakly interacting bosons has the same ballistic scaling as the one obtained using fermionic quasiparticles. As a consequence

128

the ballistic regime can be extended to momenta greater than p_{G}.[10]

We conclude by proposing future research directions originating from this work. In our approach we used the impurity defining the depleton just as a tool to define the position of an excitation. However, the extension to the case of real impurities is straightforward. This allows us to extend this treatment, for example, to two-component one-dimensional quantum gases with a majority atomic species, modelling the atoms of the majority and minority species, respectively, as phonons of the host gas and dilute depletons. Other interesting directions include the study of mixtures where the minority species have different statistics, such as in Bose-Fermi and Fermi-Fermi mixtures or the addition of spin degrees of freedom, that would lead to the study of spin-wave dynamics in quantum gases with impurities.

---

[10]See Ref. [3] in the Publications section at the beginning of this thesis.

Appendix A

Hubbard-Stratonovich transformation with boundary conditions

Hubbard-Stratonovich transformation for the complex bosonic field, $\theta^\alpha(t)$,

$$
\begin{aligned}
Z[\theta] &= e^{\int_{t_i}^{t_f} dt\, \bar{\theta}^\alpha(t)\Sigma^{\alpha\beta}(t,t')\theta^\beta(t')} \\
&= \frac{1}{\det\left[\Sigma^{-1}\right]} \int \mathcal{D}[\bar{\phi},\phi] e^{-\int_{t_i}^{t_f} dt\, \bar{\phi}^\alpha(t)\left[\sigma_1\Sigma^{-1}\sigma_1\right]^{\alpha\beta}(t,t')\phi^\beta(t')+\bar{\theta}^\alpha(t)\sigma_1^{\alpha\beta}\phi^\beta(t)+\bar{\phi}^\alpha(t)\sigma_1^{\alpha\beta}\theta^\beta(t)} \\
&= \frac{1}{1+\bar{n}} \int_{\phi^{\mathrm{q}}(t_i)=-\frac{\phi^{\mathrm{cl}}(t_i)}{1+2\bar{n}}}^{\phi^{\mathrm{q}}(t_f)=0} \mathcal{D}[\bar{\phi},\phi] e^{-\int_{t_i}^{t_f} dt\, \bar{\phi}^\alpha(t)\left[\Sigma^{-1}\right]^{\alpha\beta}(t,t')\phi^\beta(t')+\bar{\theta}^\alpha(t)\sigma_1^{\alpha\beta}\phi^\beta(t)+\bar{\phi}^\alpha(t)\sigma_1^{\alpha\beta}\theta^\beta(t)} .
\end{aligned}
$$

Hubbard-Stratonovich transformation for the real bosonic field, $X^\alpha(t)$,

$$
\begin{aligned}
Z[\theta] &= e^{\frac{1}{2}\int_{t_i}^{t_f} dt\, X^\alpha(t)\Sigma^{\alpha\beta}(t,t')X^\beta(t')} \\
&= \frac{1}{\sqrt{\det\left[\Sigma^{-1}\right]}} \int \mathcal{D}[\bar{Y},Y] e^{-\frac{1}{2}\int_{t_i}^{t_f} dt\, \bar{Y}^\alpha(t)\left[\sigma_1\Sigma^{-1}\sigma_1\right]^{\alpha\beta}(t,t')Y^\beta(t')+X^\alpha(t)\sigma_1^{\alpha\beta}Y^\beta(t)} \\
&= \frac{1}{\sqrt{1+\bar{n}}} \int_{Y^{\mathrm{q}}(t_i)=-\frac{Y^{\mathrm{cl}}(t_i)}{1+2\bar{n}}}^{Y^{\mathrm{q}}(t_f)=0} \mathcal{D}[\bar{Y},Y] e^{-\frac{1}{2}\int_{t_i}^{t_f} dt\, \bar{Y}^\alpha(t)\left[\Sigma^{-1}\right]^{\alpha\beta}(t,t')Y^\beta(t')+X^\alpha(t)\sigma_1^{\alpha\beta}Y^\beta(t)} .
\end{aligned}
$$

Hubbard-Stratonovich transformation for the Grassmann field, $\xi^\alpha(t)$,

$$Z[\theta] = e^{\frac{1}{2}\int_{t_i}^{t_f} dt\, \xi^a(t)\Sigma^{ab}(t,t')\xi^b(t')}$$

$$= \det\left[\Sigma^{-1}\right]\int \mathcal{D}[\bar{\varsigma},\varsigma]e^{-\int_{t_i}^{t_f} dt\, \bar{\varsigma}^a(t)\left[\Sigma^{-1}\right]^{ab}(t,t')\varsigma^b(t')+\bar{\xi}^a(t)\varsigma^a(t)+\bar{\varsigma}^a(t)\xi^a(t)}$$

$$= (1-\bar{n})\int_{\varsigma_1(t_i)=-(1-2\bar{n})\varsigma_2(t_i)}^{\varsigma_2(t_f)=0} \mathcal{D}[\bar{\varsigma},\varsigma]e^{-\int_{t_i}^{t_f} dt\, \bar{\varsigma}^a(t)\left[\Sigma^{-1}\right]^{ab}(t,t')\varsigma^b(t')+\bar{\xi}^a(t)\varsigma^a(t)+\bar{\varsigma}^a(t)\xi^a(t)}\,.$$

Appendix B

n-loop reduction formula

In this section we derive a reduction formula for the symmetrised fermionic n-loop by adapting the zero temperature derivation of Refs. [78, 79] to finite temperatures, T, using the Matsubara formalism. The fermionic n-loop is shown in Fig. B.1 and is defined as (compare it with the analogous expression (2.23) in the Keldysh formalism),

$$\Gamma_n(Q_1, \ldots, Q_{n-1}) = I_n(P_1, \ldots, P_n) = -\frac{1}{\beta} \sum_{E_\ell} \int \frac{\mathrm{d}k}{2\pi} G(K + P_1) \ldots G(K + P_n) \, ,$$

where $Q_j = (\omega_j, q_j)$ are phononic momentum and Matsubara energy variables and $P_j = (\epsilon_j, p_j) = Q_1 + \ldots + Q_j$ and $K = (E_\ell, k)$ are fermionic ones. The Matsubara Green's function is defined as,

$$G(K) = \frac{1}{\mathrm{i}E_\ell - \varepsilon(k)} \, ,$$

and $\varepsilon(k) = v_\mathrm{F} k + k^2/2m$ is the right mover spectrum. Here we limit the study to right movers as the results for left movers are symmetric. The sum over fermionic energies $E_\ell = \pi \mathrm{i}(2\ell + 1)T$ is easily evaluated by means of the residue theorem and yields,

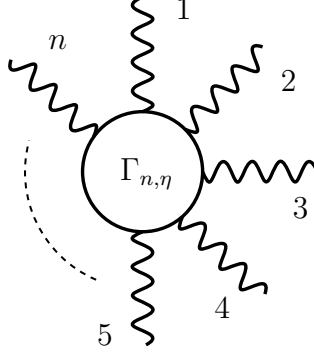$$I_n(P_1, \ldots, P_n) = \int \frac{\mathrm{d}k}{2\pi} \sum_{i=1}^{n} n_i \prod_{\substack{j=1 \\ j \neq i}}^{n} \frac{1}{f_{ji}(k)} \, ,$$

Figure B.1: n-loop.

where,

$$n_i = n_{\mathrm{F}}(-\mathrm{i}\epsilon_i + \varepsilon(k + p_i))\,,$$

is the occupation factor of a state with momentum p_i and energy ϵ_i and,

$$f_{ij}(k) = (\mathrm{i}\epsilon_i - \varepsilon(k + p_i)) - (\mathrm{i}\epsilon_j - \varepsilon(k + p_j))$$

$$= (\mathrm{i}\epsilon_i - \varepsilon(p_i)) - (\mathrm{i}\epsilon_j - \varepsilon(p_j)) - \frac{p_i - p_j}{m}k\,.$$

The n-loop can be rewritten as,

$$I_n(P_1, \ldots, P_n) = \int \frac{\mathrm{d}k}{2\pi} \sum_{i=1}^{n} n_i \prod_{\substack{j=1 \\ j \neq i}}^{n} \left(\frac{m}{p_{ij}}\right) \prod_{\substack{j=1 \\ j \neq i}}^{n} \left(\frac{1}{k - \Delta_{ij}}\right)\,, \tag{B.1}$$

where $p_{ij} = p_i - p_j$ and,

$$\Delta_{ij} = \frac{m}{p_{ij}}[(\mathrm{i}\epsilon_i - \varepsilon(p_i)) - (\mathrm{i}\epsilon_j - \varepsilon(p_j))]\,.$$

134

The last product in the n-loop (B.1) can be expressed as a sum using a partial fraction expansion,

$$\prod_{\substack{j=1 \\ j\neq i}}^{n}\left(\frac{1}{k-\Delta_{ij}}\right) = \sum_{\substack{j=1 \\ j\neq i}}^{n}\left[\frac{1}{k-\Delta_{ij}}\prod_{\substack{n=1 \\ n\neq i,j}}^{n}\left(\frac{1}{\Delta_{ij}-\Delta_{in}}\right)\right].$$

Then, the n-loop (B.1) becomes,

$$I_n(P_1,\ldots,P_n) = \sum_{\substack{i,j=1 \\ i\neq j}}^{n}\left(\frac{m}{p_{ij}}\int\frac{\mathrm{d}k}{2\pi}\frac{n_i}{k-\Delta_{ij}}\right)\prod_{\substack{n=1 \\ n\neq i,j}}^{n}\left(\frac{1}{f_{ij}^n}\right),$$

where,

$$f_{ij}^n = \frac{p_{in}}{m}(\Delta_{ij}-\Delta_{in}) = \mathrm{i}\frac{p_{jn}\epsilon_{in}-p_{in}\epsilon_{jn}}{p_{ij}} + \frac{p_{in}p_{jn}}{2m}$$

$$= \frac{1}{p_{ij}}\left[p_{jl}(\tilde{\varepsilon}_i - \frac{p_i^2}{2m}) - p_{il}(\tilde{\varepsilon}_j - \frac{p_j^2}{2m}) + p_{ij}(\tilde{\varepsilon}_l - \frac{p_l^2}{2m})\right].$$

Using the symmetries $f_{ij}^n = f_{ji}^n$ and $\Delta_{ij} = \Delta_{ji}$, we expressed the sum using the difference of occupation factors,

$$I_n(P_1,\ldots,P_n) = \sum_{\substack{i,j=1 \\ i>j}}^{n}\left(\frac{m}{p_{ij}}\int\frac{\mathrm{d}k}{2\pi}\frac{n_i-n_j}{k-\Delta_{ij}}\right)\prod_{\substack{n=1 \\ n\neq i,j}}^{n}\left(\frac{1}{f_{ij}^n}\right).$$

The term in the first parenthesis coincides with the two-loop,

$$\begin{aligned}I_2(P_i,P_j) &= -\frac{1}{\beta}\sum_{E_\ell}\int\frac{\mathrm{d}k}{2\pi}G(K+P_i)G(K+P_j) \\ &= \frac{m}{p_{ij}}\int\frac{\mathrm{d}k}{2\pi}\frac{n_i-n_j}{k-\Delta_{ij}},\end{aligned} \tag{B.2}$$

shown in Fig. B.2. Making the shift $K \to K - P_j$, we obtain,

$$I_2(P_i,P_j) = -\frac{1}{\beta}\sum_{E_\ell}\int\frac{\mathrm{d}k}{2\pi}G(K+P_i-P_j)G(K) = I_2(P_i-P_j,0) \equiv I_2(P_i-P_j).$$

The two-loop depends only on the differences $p_{ij} = p_i - p_j$ and $\epsilon_{ij} = \epsilon_i - \epsilon_j$ as a consequence of energy and momentum conservations. Finally, the reduction formula becomes,

$$I_n(P_1, \ldots, P_n) = \sum_{\substack{i,j=1 \\ i>j}}^{n} I_2(P_{ij}) \prod_{\substack{n=1 \\ n \neq i,j}}^{n} \left(\frac{1}{f_{ij}^n} \right) . \tag{B.3}$$

B.1 Two-loop

We rewrite the two-loop (B.2) as,

$$I_2(P_i, P_j) = -\frac{m}{4\pi p_{ij}} \int_{-\infty}^{\infty} dk \frac{\tanh \left(\frac{\varepsilon(k+p_i)}{2T} \right) - \tanh \left(\frac{\varepsilon(k+p_j)}{2T} \right)}{k - \Delta_{ij}} ,$$

In this form, a shift of the variable k cannot be taken separately for the two hyperbolic tangents, as only their difference is convergent at $k \to \pm\infty$. To allow the shift to be taken for the two terms separately, we integrate by parts,

$$I_2(P_i, P_j) = \frac{m}{8\pi T p_{ij}} \int dk \log (k - \Delta_{ij}) \left[\frac{v_{\mathrm{F}} + (k + p_i)/m}{\cosh^2 \left(\frac{\varepsilon(k+p_i)}{2T} \right)} - \frac{v_{\mathrm{F}} + (k + p_j)/m}{\cosh^2 \left(\frac{\varepsilon(k+p_j)}{2T} \right)} \right] .$$

Now the two terms converge separately and we make the shifts $k \to k - p_i$ in the first one and $k \to k - p_j$ in the second one to obtain,

$$\begin{aligned} I_2(P_{ij}) &= \frac{m}{8\pi T p_{ij}} \int dk \log \left(\frac{k - p_i - \Delta_{ij}}{k - p_j - \Delta_{ij}} \right) \frac{v_{\mathrm{F}} + k/m}{\cosh^2 \left(\frac{\varepsilon(k)}{2T} \right)} \\ &= \frac{m}{8\pi T p_{ij}} \int dk \log \left[\frac{\tilde{\epsilon}_{ij} - \frac{p_{ij}}{m} \left(k - \frac{p_{ij}}{2} \right)}{\tilde{\epsilon}_{ij} - \frac{p_{ij}}{m} \left(k + \frac{p_{ij}}{2} \right)} \right] \frac{v_{\mathrm{F}} + k/m}{\cosh^2 \left(\frac{v_{\mathrm{F}} k + k^2/2m}{2T} \right)} , \end{aligned} \tag{B.4}$$

where we defined $\tilde{\epsilon}_{ij} = i\epsilon_{ij} - v_{\mathrm{F}} p_{ij}$, where the double index from now on denotes the difference, for example $\tilde{\epsilon}_{ij} = \tilde{\epsilon}_i - \tilde{\epsilon}_j$. At zero temperature,

$$\lim_{T \to 0} \frac{1}{4T \cosh^2 \left(\frac{v_{\mathrm{F}} k + k^2/2m}{2T} \right)} = \delta \left(v_{\mathrm{F}} k + \frac{k^2}{2m} \right) .$$
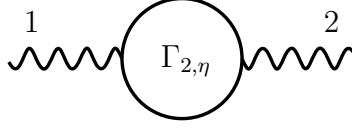
Figure B.2: Two-loop.

The zeros of the argument of the delta function are at $k = 0$ and $k = -2mv_{\mathrm{F}} = -2k_F$, but only the first zero is in the integration interval, $|k| < k_0$ (k_0 is the momentum cut-off around the Fermi point, see Chap. 2). Integrating over k, the two-loop simplifies to,

$$I_{2,0}(P_{ij}) = \frac{m}{2\pi p_{ij}} \log \left[\frac{\tilde{\epsilon}_{ij} + \frac{p_{ij}^2}{2m}}{\tilde{\epsilon}_{ij} - \frac{p_{ij}^2}{2m}} \right].$$

Noting that I_2 is even in m, an expansion in powers of m^{-1} at zero temperature reads,

$$I_{2,0}(P_{ij}) = \frac{m}{\pi p_{ij}} \sum_{\substack{n=1 \\ n \text{ odd}}}^{\infty} \frac{1}{n} \left(\frac{p_{ij}^2}{2m\tilde{\epsilon}_{ij}} \right)^n = \frac{1}{2\pi} \frac{p_{ij}}{\tilde{\epsilon}_{ij}} + \frac{1}{24\pi m^2} \frac{p_{ij}^5}{\tilde{\epsilon}_{ij}^3} + \mathcal{O}(m^{-4})$$

The dynamical condition for the convergence of the series is $p_{ij}^2 \ll m\tilde{\epsilon}_{ij}$. Instead, in the static limit, $\epsilon_i \to 0$, we have $\tilde{\epsilon}_{ij} \to -cp_{ij}$ and the condition for convergence becomes $|p_{ij}| = |q_i + \ldots + q_{j-1}| \ll mv_{\mathrm{F}} = k_{\mathrm{F}}$, which means that the phononic momenta must be small compared to the Fermi momentum, as seen in Chap. 2. At finite temperatures, the two-loop gets an additional term dependent on T in the second term of the expansion in m^{-1},

$$I_2(P_{ij}) = \frac{1}{2\pi} \frac{p_{ij}}{\tilde{\epsilon}_{ij}} + \frac{1}{24\pi m^2} \frac{p_{ij}^2}{\tilde{\epsilon}_{ij}^3} \left[p_{ij}^3 + 2\pi^2 \frac{T^2}{c^3} (2cp_{ij} - \tilde{\epsilon}_{ij}) \right] + \mathcal{O}(m^{-4}).$$

Note that we did not expand in T.

B.2 Three-loop and four-loop

The three-loop, the first in Fig. B.3, is given in terms of q_i and ω_i, by,

$$
\begin{aligned}
\Gamma_3(Q_1, Q_2) &= I_3(P_1 = 0, P_2 = Q_1, P_3 = Q_1 + Q_2) \\
&= \frac{q_1 I_2(Q_1) + q_2 I_2(Q_2) - (q_1 + q_2) I_2(Q_1 + Q_2)}{\mathrm{i}(q_1 \epsilon_2 - q_2 \epsilon_1) + q_1 q_2 (q_1 + q_2)/2m} .
\end{aligned}
$$

n-loops are symmetric by exchange of external legs. Therefore, we symmetrise by taking the circular permutations of Q_1, Q_2 and Q_3, which amount to summing $\Gamma_3(Q_1, Q_2)$ and $\Gamma_3(Q_2, Q_1)$. The symmetric part of the three loop is,

$$
\begin{aligned}
\widetilde{\Gamma}_3(Q_1, Q_2) &= \Gamma_3(Q_1, Q_2) + \Gamma_3(Q_2, Q_1) \\
&= -\frac{q_1 q_2 (q_1 + q_2)}{2m} \frac{q_1 I_2(Q_1) + q_2 I_2(Q_2) - (q_1 + q_2) I_2(Q_1 + Q_2)}{(q_1 \epsilon_2 - q_2 \epsilon_1)^2 + (q_1 q_2 (q_1 + q_2)/2m)^2} .
\end{aligned}
$$

An $m^{-1} \to 0$ power expansion reads,

$$
\begin{aligned}
\widetilde{\Gamma}_3(Q_1, Q_2) &= \frac{1}{4\pi m} \frac{q_1 q_2 q_3}{\tilde{\omega}_1 \tilde{\omega}_2 \tilde{\omega}_3} \\
&+ \frac{1}{8\pi m^3} q_1 q_2 q_3 \left\{ \frac{1}{(q_2 \tilde{\omega}_1 - q_1 \tilde{\omega}_2)^2} \left[\frac{1}{2} \frac{q_1^2 q_2^2 q_3^2}{\tilde{\omega}_1 \tilde{\omega}_2 \tilde{\omega}_3} - \frac{1}{3} \left(\frac{q_1^6}{\tilde{\omega}_1^3} + \frac{q_2^6}{\tilde{\omega}_2^3} + \frac{q_3^6}{\tilde{\omega}_3^3} \right) \right. \right. \\
&\left. - \frac{4}{3} \pi^2 \frac{T^2}{c^2} \left(\frac{q_1^4}{\tilde{\omega}_1^3} + \frac{q_2^4}{\tilde{\omega}_2^3} + \frac{q_3^4}{\tilde{\omega}_3^3} \right) \right] - \frac{2}{3} \pi^2 \frac{T^2}{c^3} \frac{q_1 \tilde{\omega}_2 \tilde{\omega}_3 + \tilde{\omega}_1 q_2 \tilde{\omega}_3 + \tilde{\omega}_1 \tilde{\omega}_2 q_3}{\tilde{\omega}_1^2 \tilde{\omega}_2^2 \tilde{\omega}_3^2} \right\} \\
&+ \mathcal{O}(m^{-5}) ,
\end{aligned}
$$

where $\tilde{\omega}_i = \mathrm{i}\omega_i - v_\mathrm{F} q_i$ and $Q_3 = -Q_1 - Q_2$. We note that at the first order in m^{-1}, the three-loop does not depend on temperature. Moreover, there is no term independent of m, which leads to $\lim_{m^{-1} \to 0} \widetilde{\Gamma}_3 = 0$, consistent with the Dzyaloshinski-Larking theorem (see page 47). Similarly, the symmetrised four-loop, the second in Fig. B.3, is,

$$
\widetilde{\Gamma}_4(Q_1, Q_2, Q_3) = \frac{1}{4\pi m^2} \frac{q_1 q_2 q_3 q_4}{\tilde{\omega}_1 \tilde{\omega}_2 \tilde{\omega}_3 \tilde{\omega}_4} \left[\frac{q_1 + q_2}{\tilde{\omega}_1 + \tilde{\omega}_2} + \frac{q_1 + q_3}{\tilde{\omega}_1 + \tilde{\omega}_3} + \frac{q_2 + q_3}{\tilde{\omega}_2 + \tilde{\omega}_3} \right] + \mathcal{O}(m^{-4}) .
$$

As for the three-loop, at the first order in m^{-1}, the three-loop does not depend on temperature and it is consistent with the Dzyaloshinski-Larking theorem, $\lim_{m^{-1} \to 0} \widetilde{\Gamma}_4 = 0$.

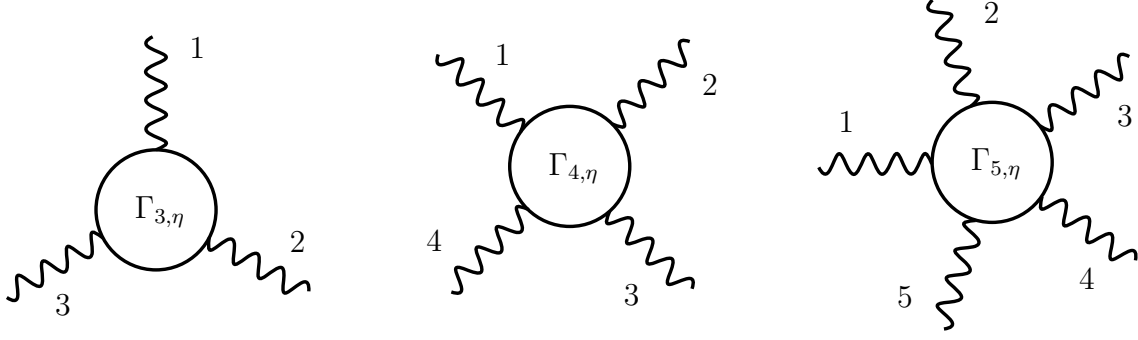Figure B.3: Three-loop, four-loop and five-loop.

However, $\widetilde{\Gamma}_4 = \mathcal{O}(m^{-2})$ goes to zero faster than $\widetilde{\Gamma}_3 = \mathcal{O}(m^{-1})$ for $m^{-1} \to 0$. Moreover, it can be checked that the five-loop, the third in Fig. B.3, is $\widetilde{\Gamma}_5 = \mathcal{O}(m^{-3})$ for $m^{-1} \to 0$ and at the lowest order, m^{-3}, $\widetilde{\Gamma}_5$ does not depend on temperature.[1] This suggests the following n-loop conjecture:

1. $\widetilde{\Gamma}_n = \mathcal{O}(m^{-(n-2)})$ for $m^{-1} \to 0$;

2. $\widetilde{\Gamma}_n$ does not depend on temperature at the lowest order in m^{-1}, that is, $m^{-(n-2)}$.

Moreover, this conjecture is supported by a dimensional analysis of the n-loop: if momenta and energies are rescaled by mv_F and mv_F^2 and made dimensionless, the n-loop (B.3) behaves as $\widetilde{\Gamma}_n \sim (mv_\mathrm{F}^2)^{-(n-2)}$. Within this conjecture, successive terms of the series (2.22), given by fermionic loops with an increasing number of phononic external legs as in Fig. 2.5, are smaller and smaller in the spectrum curvature or closer to the Fermi points, justifying the dropping of loops with more than three legs, as we did in Chap. 2.

---

[1]The symmetrisation was done numerically and took too long for loops with more than five legs.

Appendix C

Backscattering amplitude

The backscattering amplitude $\Gamma(P) = \Gamma_{+-}(P) = \Gamma_{-+}(P)$, corresponds to the off-diagonal terms of the inverse of matrix 3.28. In Ref. [50] it is shown that, using Eqs. (3.7), (3.6) and (3.13), the backscattering parameter takes the form,

$$\Gamma(P) = -\frac{1}{c} \left(\Phi \frac{\partial N_0(P,n)}{\partial P} - N \frac{\partial \Phi_0(P,n)}{\partial P} + \frac{\partial N_0(P,n)}{\partial n} \right) , \qquad \text{(C.1)}$$

where $N_0(P,n)$ and $\Phi_0(P,n)$ are the equilibrium values defined by Eqs. (3.16) and we omit the dependence of $\Gamma(P)$ on n. For small momenta, $P \ll m^*c$, we may expand $\Gamma(P)$ in Taylor series around $P = 0$ and consider only the first two terms.

$$\Gamma(P) \approx \Gamma_0 + \Gamma_0' P.$$

To determine the coefficients Γ_0 and Γ_0', we expand N_0 and Φ_0 in Taylor series, as well,

$$N_0(P,n) = N_0(n) + N_0'(n)P + N_0''(n)P^2 + \dots ,$$

$$\Phi_0(P,n) = \Phi_0(n) + \Phi_0'(n)P + \Phi_0''(n)P^2 + \dots ,$$

and substituting them in Eq. (C.1) we obtain,

$$\Gamma_0 = -\frac{1}{c}\left(\Phi_0(n)N_0'(n) - N_0(n)\Phi_0'(n) + \frac{\partial N_0(n)}{\partial n}\right), \qquad (C.2)$$

and

$$\Gamma_0' = -\frac{1}{c}\left(2\Phi_0(n)N_0''(n) - 2N_0(n)\Phi_0''(n) + \frac{\partial N_0'(n)}{\partial n}\right). \qquad (C.3)$$

The equilibrium values $N_0(P,n)$ and $\Phi_0(P,n)$ are obtained by inverting Eqs. (3.16),

$$N_0(P,n) = \frac{1}{m}\frac{V_0(P,n)P + n\partial_n E(P,n)}{c^2 - V_0^2(P,n)},$$

$$\Phi_0(P,n) = \frac{P}{n} + \frac{m}{n}V_0(P,n)N_0(P,n). \qquad (C.4)$$

For the values of $V_0(P,n)$ and $\partial_n E(P,n)$ we use the quadratic dispersion of fermionic quasiparticles, Eq. (3.17),

$$V_0(P,n) = c + \frac{P}{m^*},$$

$$\partial_n E(P) = \frac{\partial c}{\partial n}P - \frac{P^2}{2m^{*2}}\frac{\partial m^*}{\partial n},$$

and for the lowest order coefficients in Eqs. (C.4) we find,

$$N_0(n) = -\frac{m^*}{2m}\left(1 + \frac{n}{c}\frac{\partial c}{\partial n}\right) = -\sqrt{K},$$

$$\Phi_0(n) = -\frac{m^*c}{2n}\left(1 + \frac{n}{c}\frac{\partial c}{\partial n}\right) = -\frac{\pi}{\sqrt{K}}. \qquad (C.5)$$

Here used the expression for effective mass m^* in terms of n, c and K,

$$\frac{1}{m^*} = \frac{c}{K}\frac{\partial}{\partial\mu}(c\sqrt{K}) = \frac{1}{2m\sqrt{\frac{\pi n}{mc}}}\left(1 + \frac{n}{c}\frac{\partial c}{\partial n}\right), \qquad (C.6)$$

obtained by performing a transformation to the effective chiral fields, $\tilde{\chi}_\pm$, in hydrodynamic Hamiltonian (2.1) and using the mean field relation $e_0'[n] = \mu$ (See also Refs. [80, 7]). In the last term we used the thermodynamic relation $K = \pi n/mc$. For the first order

coefficients in Eqs. (C.4) we find,

$$
\begin{aligned}
N_0' &= \frac{1}{4mc}\left(\frac{n}{m^*}\frac{\partial m^*}{\partial n} - \left(1 - \frac{n}{c}\frac{\partial c}{\partial n}\right)\right), \\
\Phi_0' &= \frac{1}{4n}\left(\frac{n}{m^*}\frac{\partial m^*}{\partial n} + \left(1 - \frac{n}{c}\frac{\partial c}{\partial n}\right)\right).
\end{aligned}
\tag{C.7}
$$

Substituting Eqs. (C.5) and (C.7) in Eq. (C.2), the expression for Γ_0 simplifies to,

$$
\Gamma_0 = -\frac{m^*}{4mcn}\left(1 - \left(\frac{n}{c}\frac{\partial c}{\partial n}\right)^2\right) - \frac{1}{c}\partial_n N_0.
$$

Using Eqs. (C.5) and (C.6), we have,

$$
\partial_n N_0 = -\partial_n K = -\partial_n\sqrt{\frac{\pi n}{mc}} = \sqrt{\frac{\pi}{mnc}}\left(1 - \frac{n}{c}\frac{\partial c}{\partial n}\right),
$$

which, together with Eq. (C.6), leads to Γ_0 vanishing identically,

$$
\Gamma_0 = 0.
$$

Substituting Eqs. (C.5) and (C.7) in Eq. (C.3), the expression for Γ_0' simplifies to,

$$
\begin{aligned}
\Gamma_0' &= -\frac{1}{nc}\left(\left(1 + \frac{n}{c}\frac{\partial c}{\partial n}\right) + n\frac{\partial}{\partial n}\right)N_0' \\
&= -\frac{1}{4nc}\left(\left(1 + \frac{n}{c}\frac{\partial c}{\partial n}\right) + n\frac{\partial}{\partial n}\right)\left[\frac{1}{mc}\left(\frac{n}{m^*}\frac{\partial m^*}{\partial n} - \left(1 - \frac{n}{c}\frac{\partial c}{\partial n}\right)\right)\right],
\end{aligned}
\tag{C.8}
$$

where we used the relation,

$$
\Phi_0''(n) = \frac{mc}{n}N_0''(n) + \frac{m}{m^*n}N_0'(n).
$$

Appendix D

Solutions of the Lieb-Liniger equations in the weakly interacting limit

In this section we solve the integral equations for spectrum and density of states of the Lieb-Liniger model in the weakly interacting limit, $g \to 0$. At zero temperature, Eqs. (3.98) and (3.100) reduce to,

$$\varepsilon(k) = -\mu + \frac{k^2}{2m} + \frac{1}{\pi} \int_{-k_0}^{k_0} \mathrm{d}q \, \frac{mg}{(mg)^2 + (k-q)^2} \varepsilon(q) \,, \tag{D.1}$$

and,

$$\bar{f}(k) = \frac{1}{2\pi} + \frac{1}{\pi} \int_{-k_0}^{k_0} \mathrm{d}q \, \frac{mg}{(mg)^2 + (k-q)^2} \, \bar{f}(q) \,, \qquad k^2 \leq k_0^2 \,, \tag{D.2}$$

with $\varrho(k) = 0$ for $k^2 > k_0^2$. In the weakly interacting limit we can approximate the Lorentzian kernel of the integral equations,

$$\frac{1}{\pi} \frac{mg}{(mg)^2 + k^2} \simeq \delta(k) + \frac{mg}{\pi} \mathrm{P} \frac{1}{k^2} \,,$$

where P denotes the principal value operator. In this limit, the two integral equations reduce to,

$$\fint_{-k_0}^{k_0} \frac{\varepsilon(q)}{(q-k)^2} dq = \frac{1}{mg} \left(\mu - \frac{k^2}{2m} \right) \,,$$

and,

$$\fint_{-k_0}^{k_0} \frac{\bar{f}(q)}{(q-k)^2} dq = -\frac{1}{2mg},$$

where $\fint$ is a principle value integral. Integrating both sides by k we have,

$$\fint_{-k_0}^{k_0} \frac{\varepsilon(q)}{q-k} dq = \frac{1}{mg}\left(\mu k - \frac{k^3}{6m}\right), \tag{D.3}$$

and,

$$\fint_{-k_0}^{k_0} \frac{\bar{f}(q)}{q-k} dq = -\frac{k}{2mg}, \tag{D.4}$$

where the integration constant is zero as $\varepsilon(k)$ and $\bar{f}(k)$ are even functions, so that the right hand sides must be odd. These two equations are Cauchy or singular integral equations and can be solved with the methods described in Refs. [81, 82]. We start from the equation of the density of states, as it is simpler.

D.1 Density of states

Cauchy integral equation (D.4) can be solved by considering the respective Riemann problem. By defining the quantity,

$$w(z) = \int_{-k_0}^{k_0} \frac{\bar{f}(q)}{q-z} \, \mathrm{d}q,$$

where z is a complex variable. $w(z)$ has a branch cut for $-k_0 \leq z \leq k_0$. In terms of $w(z)$, the principal value integral in Eq. (D.4) is,

$$2\fint_{-k_0}^{k_0} \frac{\bar{f}(q)}{q-k} dq = w_+(k) + w_-(k) = -\frac{k}{mg}, \quad |k| \leq k_0 \tag{D.5}$$

where $w_\pm(k) = w(z \to k \pm \mathrm{i}0^+)$ are the values above and below the branch cut and we used the Plemelj formula [81].

$$\frac{1}{k \pm \mathrm{i}0} = \mathrm{P}\frac{1}{k} \mp \pi \mathrm{i}\delta(k). \tag{D.6}$$

Then, the density of states is obtained by,

$$\bar{f}(k) = \frac{w_+(k) - w_-(k)}{2\pi \mathrm{i}}, \tag{D.7}$$

where we used the Plemelj formula, Eq. (D.6), again. The solution is the sum of a general solution proportional to $(k_0^2 - k^2)^{-1/2}$ and a particular solution. To start we need one solution of the homogenous part of Eq. (D.5), $w_+(k) + w_-(k) = 0$. We choose the solution $A(z) = \sqrt{z^2 - 1}$ and divide Eq. (D.5) by $A_+(k) = A(z \to k + \mathrm{i}0^+)$,

$$\frac{w_+(k)}{A_+(k)} - \frac{w_-(k)}{A_-(k)} = -\frac{k}{mg}\frac{1}{A_+(k)},$$

where we used the fact that $A_+(k) = -A_-(k)$. Splitting the right hand side in two equal parts and using the relation between A_+ and A_- we find,

$$\frac{w_+(k) + k/2mg}{A_+(k)} = \frac{w_-(k) + k/2mg}{A_-(k)} \equiv S(k),$$

where in the last equality we defined $S(z)$. $S(z)$ is a single valued function with possible poles at $k = \pm k_0$ and infinity. At infinity $S(z) \sim 1/2mg + O(1/z^2)$, so $S(z) = 1/2mg + S_{k_0}(z)$, where $S_{k_0}(z)$ contains only poles at $z = \pm k_0$. Therefore,

$$w(z) = \sqrt{z^2 - k_0^2}\left(\frac{1}{2mg} + S_{k_0}(z)\right) - \frac{z}{2mg}.$$

Since $w(z)$ has to be integrable in the interval between $-k_0$ and k_0, $S_{k_0}(z)$ can only have first order poles at these points and,

$$w(z) = \sqrt{z^2 - k_0^2}\left(\frac{1}{2mg} + \frac{a}{z - k_0} + \frac{b}{z + k_0}\right) - \frac{z}{2mg}.$$

As seen before $S(z)$ at infinity does not behave as $1/z$, therefore $b = -a$ and,

$$w(z) = \frac{1}{2mg}\left(\sqrt{z^2 - k_0^2} - z\right) + \frac{2a}{\sqrt{z^2 - k_0^2}}.$$

Eq. (D.7) then gives,

$$\bar{f}(k) = \frac{1}{2\pi mg}\sqrt{k_0^2 - k^2} + \frac{B}{\sqrt{k_0^2 - k^2}},$$

where B is a constant. From Eq. (D.2) we know that $\bar{f}(\pm k_0)$ is finite, therefore $B = 0$. Finally

$$\bar{f}(k) = \frac{1}{2\pi mg}\sqrt{k_0^2 - k^2}.$$

Integrating $\bar{f}(k)$ over all the real axis gives the density of the system, n, which provides the relation $k_0 = 2\sqrt{mgn}$.

D.2   Spectrum

Now we consider Cauchy integral equation (D.3). The only difference with respect to the previous case is the inhomogeneous term. With the same procedure we used before we find,

$$S(z) \equiv \frac{1}{A_+(k)}\left[w(z) - \frac{\pi}{mg}(2m\mu z - \frac{z^3}{3})\right] \sim \frac{\pi}{mg}\left(-2m\mu + \frac{k_0^2}{6}\right) + \frac{\pi}{3mg}z^2 + O\left(z^{-2}\right),$$

where,

$$w(z) = \int_{-k_0}^{k_0} \frac{\varepsilon(q)}{q - z}\,\mathrm{d}q.$$

Then,

$$S(z) = \frac{\pi}{mg}\left(-2m\mu + \frac{k_0^2}{6}\right) + \frac{\pi}{3mg}z^2 + \frac{2ak_0}{z^2 - k_0^2},$$

where the last terms contains the only two poles that make $w(z)$ integrable. Inverting the equation in order to have $w(z)$ and using Eq. (D.7) gives,

$$2m\varepsilon(k) = \frac{1}{3mg}\sqrt{k_0^2 - k^2}\left(-6m\mu + \frac{k_0^2}{2} + k^2\right) + \frac{B}{\sqrt{k_0^2 - k^2}},$$

148

where B is a constant. By requiring $\varepsilon(k_0) = 0$, the constant B must be zero. Moreover, since k_0 is a function of μ, using Eq. (3.99) at zero temperature,

$$\partial_\mu \varepsilon(k) = -2\pi \bar{f}(k) \,,$$

we find $\mu = k_0^2/4m$. The final result is,

$$\varepsilon(k) = -\frac{1}{6m^2 g} \left(k_0^2 - k^2 \right)^{\frac{3}{2}} \,.$$

The expression just found holds for $|k| \le k_0$. Outside this region there is no branch cut and the spectrum is given by,

$$2m\varepsilon(k) = -2m\mu + k^2 + \frac{c}{\pi} \partial_k w(k), \quad |k| > k_0 \,.$$

This leads to the expression for the spectrum in the whole real line,

$$\varepsilon(k) = \begin{cases} -\frac{1}{6m^2 g} \left(k_0^2 - k^2 \right)^{\frac{3}{2}} \,, & |k| \le k_0 \\[2mm] \frac{1}{2m} |k| \sqrt{k^2 - k_0^2} \,, & |k| > k_0 \,. \end{cases}$$

Bibliography

[1] T. Giamarchi. *Quantum Physics in One Dimension*. International Series of Monographs on Physics. Oxford University Press, USA, 2004.

[2] S.-I. Tomonaga. Remarks on Bloch's Method of Sound Waves applied to Many-Fermion Problems. *Progress of Theoretical Physics*, 5(4):544–569, 1950.

[3] J. M. Luttinger. An Exactly Soluble Model of a Many-Fermion System. *Journal of Mathematical Physics*, 4(9):1154–1162, 1963.

[4] D. C. Mattis and E. H. Lieb. Exact Solution of a Many-Fermion System and Its Associated Boson Field. *Journal of Mathematical Physics*, 6(2):304–312, 1965.

[5] F. D. M. Haldane. 'Luttinger liquid theory' of one-dimensional quantum fluids. I. Properties of the Luttinger model and their extension to the general 1D interacting spinless Fermi gas. *Journal of Physics C: Solid State Physics*, 14(19):2585, 1981.

[6] F. D. M. Haldane. Effective Harmonic-Fluid Approach to Low-Energy Properties of One-Dimensional Quantum Fluids. *Phys. Rev. Lett.*, 47:1840–1843, 1981.

[7] A. Imambekov, T. L. Schmidt, and L. I. Glazman. One-dimensional quantum liquids: Beyond the Luttinger liquid paradigm. *Rev. Mod. Phys.*, 84:1253–1306, 2012.

[8] J. Hu, T. W. Odom, and C. M. Lieber. Chemistry and Physics in One Dimension: Synthesis and Properties of Nanowires and Nanotubes. *Accounts of Chemical Research*, 32(5):435–445, 1999.

[9] M. Monthioux and V. L. Kuznetsov. Who should be given the credit for the discovery of carbon nanotubes? *Carbon*, 44(9):1621–1623, 2006.

[10] A. M. Chang. Chiral luttinger liquids at the fractional quantum hall edge. *Reviews of Modern Physics*, 75(4):1449–1505, 2003.

[11] X.-W. Guan, M. T. Batchelor, and C. Lee. Fermi gases in one dimension: From Bethe ansatz to experiments. *Reviews of Modern Physics*, 85(4):1633–1691, 2013.

[12] V. V. Deshpande, M. Bockrath, L. I. Glazman, and A. Yacoby. Electron liquids and solids in one dimension. *Nature*, 464(7286):209–216, 2010.

[13] A. Kamenev. *Field Theory of Non-Equilibrium Systems*. Cambridge University Press, 2011.

[14] A. Altland and B.D. Simons. *Condensed Matter Field Theory*. Cambridge University Press, 2010.

[15] I. V. Yurkevich. Bosonisation as the Hubbard Stratonovich Transformation. In I.V. Lerner, B.L. Althsuler, and V.I. Fal'ko, editors, *Strongly Correlated Fermions and Bosons in Low-Dimensional Disordered Systems*, NATO science series: Mathematics, physics, and chemistry. Springer, 2002.

[16] P. Kopietz. *Bosonization of Interacting Fermions in Arbitrary Dimensions*. Bosonization of Interacting Fermions in Arbitrary Dimensions. Springer Berlin Heidelberg, 1997.

[17] J. Schwinger. The Special Canonical Group. *Proceedings of the National Academy of Sciences*, 46(10):1401–1415, 1960.

[18] J. Schwinger. Brownian Motion of a Quantum Oscillator. *Journal of Mathematical Physics*, 2(3):407–432, 1961.

[19] L.P. Kadanoff and G. Baym. *Quantum Statistical Mechanics: Green's Function Methods in Equilibrium and Nonequilibrium Problems.* Frontiers in physics. Benjamin, 1962.

[20] L. V. Keldysh. Diagram Technique for Nonequilibrium Processes. *Sov. Phys. JETP*, 20:1018, 1965.

[21] A. Kamenev. Course 3 Many-body theory of non-equilibrium systems. In H. Bouchiat, Y. Gefen, S. Guéron, G. Montambaux, and J. Dalibard, editors, *Nanophysics: Coherence and Transport École d'été de Physique des Houches Session LXXXI*, volume 81 of *Les Houches*, pages 177 – 246. Elsevier, 2005.

[22] A.L. Fetter and J.D. Walecka. *Quantum Theory of Many-Particle Systems.* Dover Books on Physics. Dover Publications, 2003.

[23] M. Gell-Mann and F. Low. Bound States in Quantum Field Theory. *Phys. Rev.*, 84:350–354, 1951.

[24] A.I. Larkin and Yu. N. Ovchinnikov. Nonlinear conductivity of superconductors in the mixed state. *Sov. Phys. JETP*, 41:960, 1975.

[25] V. N. Popov. *Functional Integrals and Collective Excitations.* Cambridge Monographs on Mathematical Physics. Cambridge University Press, 1991.

[26] P. Nozieres and D. Pines. *Theory Of Quantum Liquids.* Advanced Books Classics Series. Westview Press, 1999.

[27] J. Stenger, S. Inouye, A. P. Chikkatur, D. M. Stamper-Kurn, D. E. Pritchard, and W. Ketterle. Bragg Spectroscopy of a Bose-Einstein Condensate. *Phys. Rev. Lett.*, 82:4569–4573, 1999.

[28] N. Fabbri, D. Clément, L. Fallani, C. Fort, and M. Inguscio. Momentum-resolved study of an array of one-dimensional strongly phase-fluctuating Bose gases. *Phys. Rev. A*, 83:031604, 2011.

[29] L. Pitaevskii and S. Stringari. *Bose-Einstein Condensation.* International Series of Monographs on Physics. Oxford University Press, USA, 2003.

[30] H. C. Fogedby. Correlation functions for the Tomonaga model. *Journal of Physics C: Solid State Physics*, 9(20):3757, 1976.

[31] D. K. K. Lee and Y. Chen. Functional bosonisation of the Tomonaga-Luttinger model. *Journal of Physics A: Mathematical and General*, 21(22):4155, 1988.

[32] A. Grishin, I. V. Yurkevich, and I. V. Lerner. Functional integral bosonization for an impurity in a Luttinger liquid. *Phys. Rev. B*, 69:165108, 2004.

[33] I. V. Lerner and I. V. Yurkevich. Seminar 1 Impurity in the tomonaga-luttinger model: A functional integral approach. In S. Guéron G. Montambaux H. Bouchiat, Y. Gefen and J. Dalibard, editors, *Nanophysics: Coherence and Transport École d'été de Physique des Houches Session LXXXI*, volume 81 of *Les Houches*, pages 109 – 127. Elsevier, 2005.

[34] D. B. Gutman, Y. Gefen, and A. D. Mirlin. Bosonization of one-dimensional fermions out of equilibrium. *Phys. Rev. B*, 81:085436, 2010.

[35] J. M. Luttinger and J. C. Ward. Ground-State Energy of a Many-Fermion System. II. *Phys. Rev.*, 118:1417–1427, 1960.

[36] J. M. Luttinger. Fermi Surface and Some Simple Equilibrium Properties of a System of Interacting Fermions. *Phys. Rev.*, 119:1153–1163, 1960.

[37] A. M. Tsvelik. *Quantum Field Theory in Condensed Matter Physics.* Cambridge University Press, 2003.

[38] I. E. Dzyaloshinskii and A. I. Larkin. Correlation functions for a one-dimensional Fermi system with long-range interaction (Tomonaga model). *Sov. Phys. JETP*, 38:202, 1974.

[39] J. Zinn-Justin. *Quantum Field Theory and Critical Phenomena.* International series of monographs on physics. Clarendon Press, 2002.

[40] F. Dalfovo, S. Giorgini, L. P. Pitaevskii, and S. Stringari. Theory of Bose-Einstein condensation in trapped gases. *Rev. Mod. Phys.*, 71:463–512, 1999.

[41] M. Girardeau. Relationship between Systems of Impenetrable Bosons and Fermions in One Dimension. *J. Math. Phys.*, 1(6):516, 1960.

[42] E. H. Lieb and W. Liniger. Exact Analysis of an Interacting Bose Gas. I. The General Solution and the Ground State. *Phys. Rev.*, 130(4):1605, 1963.

[43] A. V. Rozhkov. Fermionic quasiparticle representation of Tomonaga-Luttinger Hamiltonian. *Eur. Phys. J. B*, 47(2):193–206, 2005.

[44] A. V. Rozhkov. Density-density propagator for one-dimensional interacting spinless fermions with nonlinear dispersion and calculation of the Coulomb drag resistivity. *Phys. Rev. B*, 77(12):1–5, 2008.

[45] J. von Delft and H. Schoeller. Bosonization for beginners — refermionization for experts. *Annalen der Physik*, 7(4):225–305, 1998.

[46] M. Pustilnik and K. A. Matveev. Low-energy excitations of a one-dimensional Bose gas with weak contact repulsion. *Phys. Rev. B*, 89:100504, 2014.

[47] Z. Ristivojevic. Excitation Spectrum of the Lieb-Liniger Model. *Phys. Rev. Lett.*, 113:015301, 2014.

[48] A. F. Andreev. The hydrodynamics of two- and one-dimensional liquids. *Sov. Phys. JETP*, 51:1038–1042, 1980.

[49] K. V. Samokhin. Lifetime of excitations in a clean Luttinger liquid. *J. Phys. Cond. Mat.*, 10:533–538, 1998.

[50] M. Schecter, D. M. Gangardt, and A. Kamenev. Dynamics and Bloch oscillations of mobile impurities in one-dimensional quantum liquids. *Ann. Phys.*, 327(3):639 – 670, 2012.

[51] D. M. Gangardt and A. Kamenev. Quantum Decay of Dark Solitons. *Phys. Rev. Lett.*, 104(19):190402, 2010.

[52] D. C. Wadkin-Snaith and D. M. Gangardt. Quantum Gray Solitons in Confining Potentials. *Phys. Rev. Lett.*, 108:085301, 2012.

[53] D. M. Gangardt and A. Kamenev. Bloch Oscillations in a One-Dimensional Spinor Gas. *Phys. Rev. Lett.*, 102(7):70402, 2009.

[54] M. Khodas, M. Pustilnik, A. Kamenev, and L. Glazman. Fermi-Luttinger liquid: Spectral function of interacting one-dimensional fermions. *Physical Review B*, 76(15):155402, 2007.

[55] K. A. Matveev and A. Furusaki. Decay of Fermionic Quasiparticles in One-Dimensional Quantum Liquids. *Phys. Rev. Lett.*, 111:256401, 2013.

[56] L.D. Landau and E.M. Lifshitz. *Statistical Physics, Part 1*. Number v. 5. Elsevier Science, 1996.

[57] M. Pustilnik, E. G. Mishchenko, L. I. Glazman, and A. V. Andreev. Coulomb Drag by Small Momentum Transfer between Quantum Wires. *Phys. Rev. Lett.*, 91(12):126805, 2003.

[58] T. Cheon and T. Shigehara. Fermion-Boson Duality of One-Dimensional Quantum Particles with Generalized Contact Interactions. *Phys. Rev. Lett.*, 82(12):2536, 1999.

[59] M. Kardar, G. Parisi, and Y.-C. Zhang. Dynamic Scaling of Growing Interfaces. *Phys. Rev. Lett.*, 56(1):889, 1986.

[60] T. Kriecherbauer and J. Krug. A pedestrian's view on interacting particle systems, KPZ universality and random matrices. *J. Phys. A*, 43(40):403001, 2010.

[61] T. Sasamoto and H. Spohn. The $1 + 1$-dimensional Kardar–Parisi–Zhang equation and its universality class. *J. Stat. Mech.*, (11):P11013, 2010.

[62] M. Kulkarni and A. Lamacraft. Finite-temperature dynamical structure factor of the one-dimensional Bose gas: From the Gross-Pitaevskii equation to the Kardar-Parisi-Zhang universality class of dynamical critical phenomena. *Phys. Rev. A*, 88(2):021603, 2013.

[63] I. Corwin. The Kardar-Parisi-Zhang equation and universality class. *ArXiv e-prints*, 2011.

[64] P. J. Yunker, M. A. Lohr, T. Still, A. Borodin, D. J. Durian, and A. G. Yodh. Effects of Particle Shape on Growth Dynamics at Edges of Evaporating Drops of Colloidal Suspensions. *Phys. Rev. Lett.*, 110:035501, 2013.

[65] M. Prähofer and H. Spohn. Exact Scaling Functions for One-Dimensional Stationary KPZ Growth. *J. Stat. Phys*, 115:255–279, 2004.

[66] I. E. Mazets and J. Schmiedmayer. Dephasing in two decoupled one-dimensional Bose-Einstein condensates and the subexponential decay of the interwell coherence. 68(3):335–339, 2009.

[67] H.-P. Stimming, N. J. Mauser, J. Schmiedmayer, and I. E. Mazets. Dephasing in coherently split quasicondensates. *Phys. Rev. A*, 83:023618, 2011.

[68] E. H. Lieb. Exact Analysis of an Interacting Bose Gas. II. The Excitation Spectrum. *Phys. Rev.*, 130(4):1616, 1963.

[69] C. N. Yang and C. P. Yang. Thermodynamics of a One-Dimensional System of Bosons with Repulsive Delta-Function Interaction. *Journal of Mathematical Physics*, 10(7):1115–1122, 1969.

[70] A. S. Campbell. Mobile impurities in one-dimensional quantum liquids. *PhD Thesis*, 2013.

[71] A. S. Campbell, D. M. Gangardt, and K. V. Kheruntsyan. Sudden Expansion of a One-Dimensional Bose Gas from Power-Law Traps. *Physical Review Letters*, 114(12):125302, 2015.

[72] I. E. Mazets, T. Schumm, and J. Schmiedmayer. Breakdown of Integrability in a Quasi-1D Ultracold Bosonic Gas. *Phys. Rev. Lett.*, 100(21):210403, 2008.

[73] S. Tan, M. Pustilnik, and L. I. Glazman. Relaxation of a High-Energy Quasiparticle in a One-Dimensional Bose Gas. *Physical Review Letters*, 105(9):090404, 2010.

[74] P. P. Kulish, S. V. Manakov, and L. D. Faddeev. Comparison of the exact quantum and quasiclassical results for a nonlinear Schrödinger equation. *Theor. Math. Phys.*, 28(1):615–620, 1976.

[75] N. A. Slavnov. Asymptotic expansions for correlation functions of one-dimensional bosons. 174(1):109–121, 2013.

[76] D. M. Gangardt. Dispersion of Type I and Type II Excitations of the Lieb-Liniger Model. *(Unpublished)*.

[77] M. Panfil and J.-S. Caux. Finite-temperature correlations in the Lieb-Liniger one-dimensional Bose gas. *Physical Review A*, 89(3):033605, 2014.

[78] A. Neumayr and W. Metzner. Fermion loops, loop cancellation, and density correlations in two-dimensional Fermi systems. *Phys. Rev. B*, 58:15449–15459, 1998.

[79] A. Neumayr and W. Metzner. Reduction Formula for Fermion Loops and Density Correlations of the 1D Fermi Gas. *Journal of Statistical Physics*, 96(3-4):613–626, 1999.

[80] R. Pereira, J. Sirker, J.-S. Caux, R. Hagemans, J. Maillet, S. White, and I. Affleck. Dynamical Spin Structure Factor for the Anisotropic Spin-1/2 Heisenberg Chain. *Phys. Rev. Lett.*, 96(25):257202, 2006.

[81] A.C. Pipkin. *A Course on Integral Equations.* Texts in Applied Mathematics. Springer, 1991.

[82] V. E. Korepin, N. M. Bogoliubov, and A. G. Izergin. *Quantum Inverse Scattering Method and Correlation Functions.* Cambridge Monographs on Mathematical Physics. Cambridge University Press, 1997.